



# Current Distribution Inference from MSE Coherence Imaging using Bayesian Tomography

(Assesment of IMSE capabilities for Tokamaks and  
Stellarators - ASDEX Upgrade and W7X)

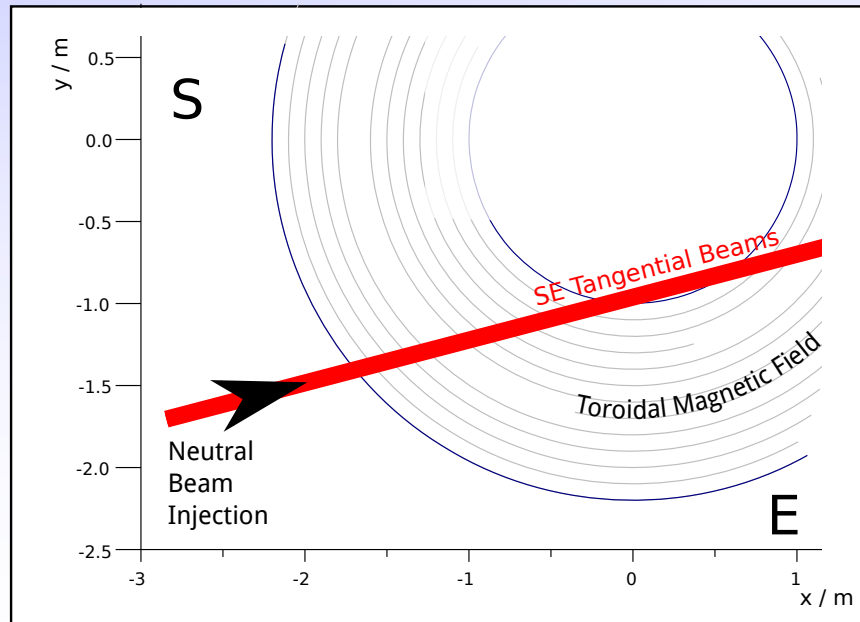
O. P. Ford,<sup>1</sup> J. Howard,<sup>2</sup> J. Svensson,<sup>1</sup> R. Wolf<sup>1</sup>

1: Max-Planck Institut für Plasmaphysik, Greifswald, Germany

2: Plasma Research Laboratory, Australian National University, Canberra

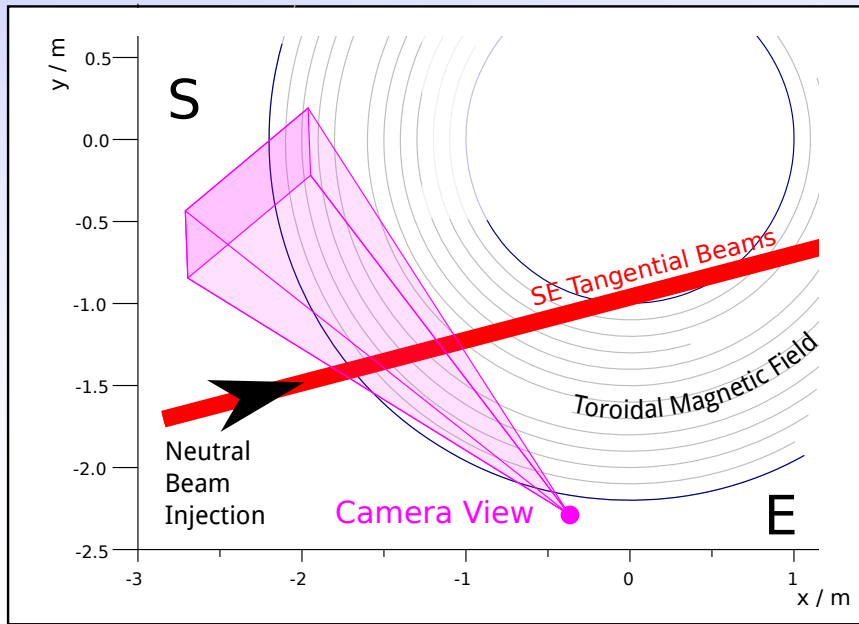
- Imaging MSE.
  - Introduction
  - Forward Model
- ASDEX Upgrade Instrument.
  - 2D measurements under Axisymmetry.
  - Current Tomography.
- W7X Instrument.
  - Capability Analysis
  - Bayesian Inference using Function Parameterisation.

## Introduction - Motional Stark Effect

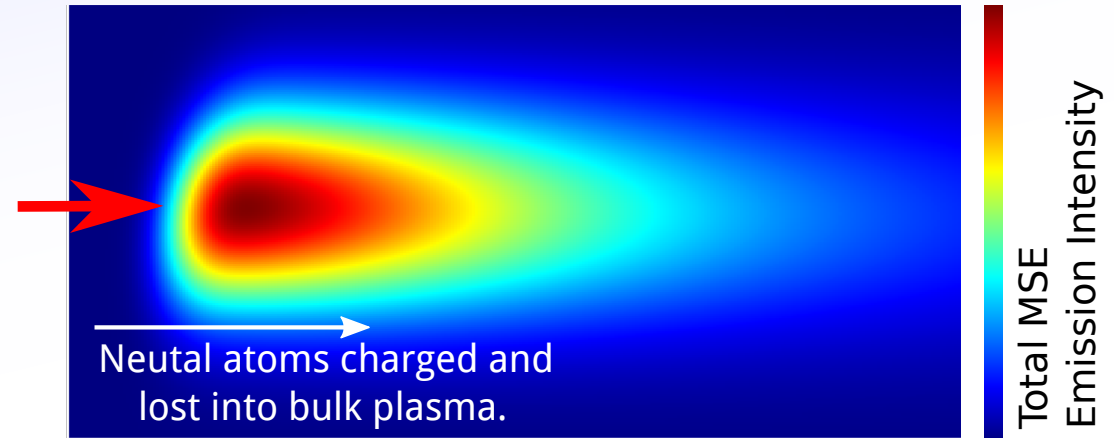


Neutral beam atoms injected into plasma.  
Excited by plasma, then emit  $H\alpha/D\alpha$  radiation.

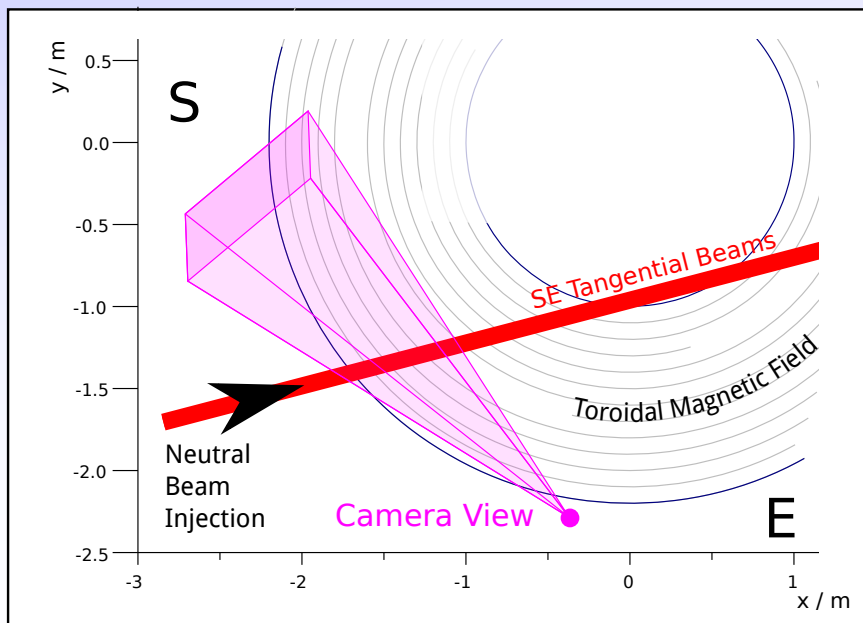
# Introduction - Motional Stark Effect



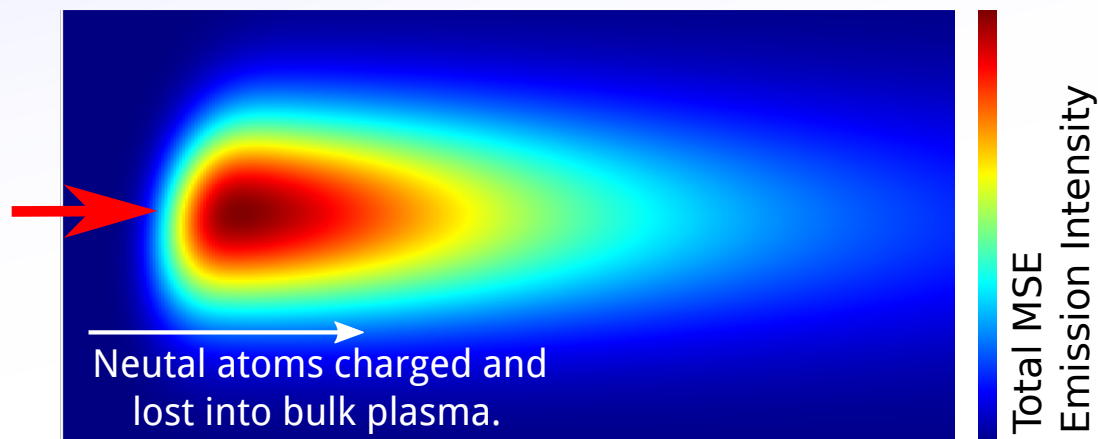
Neutral beam atoms injected into plasma.  
Excited by plasma, then emit  $H\alpha/D\alpha$  radiation.



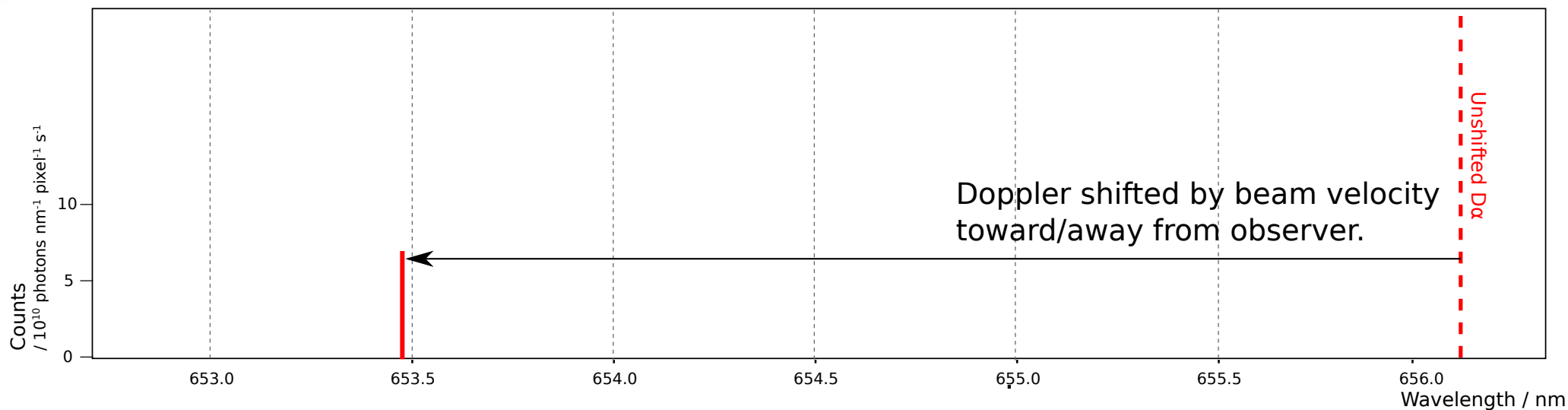
# Introduction - Motional Stark Effect



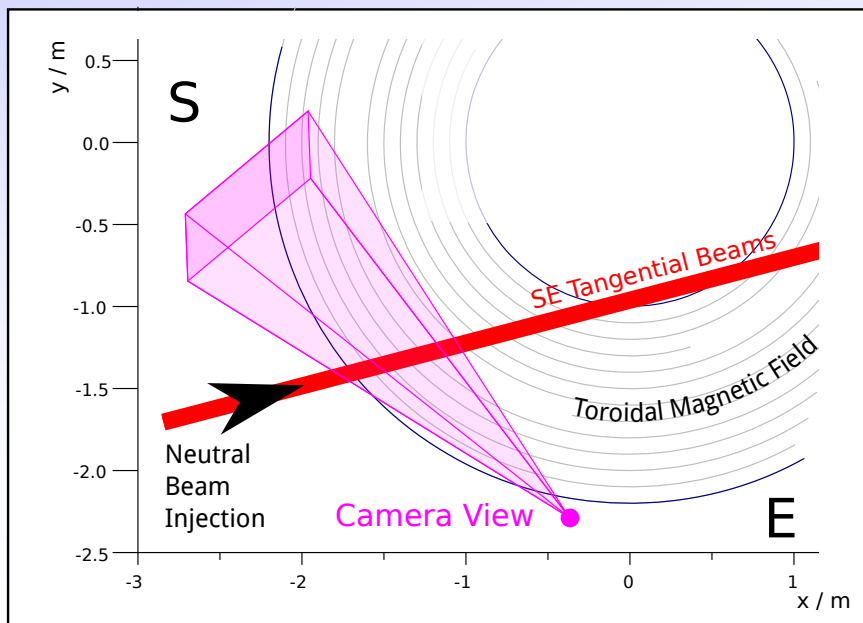
Neutral beam atoms injected into plasma.  
Excited by plasma, then emit H $\alpha$ /D $\alpha$  radiation.



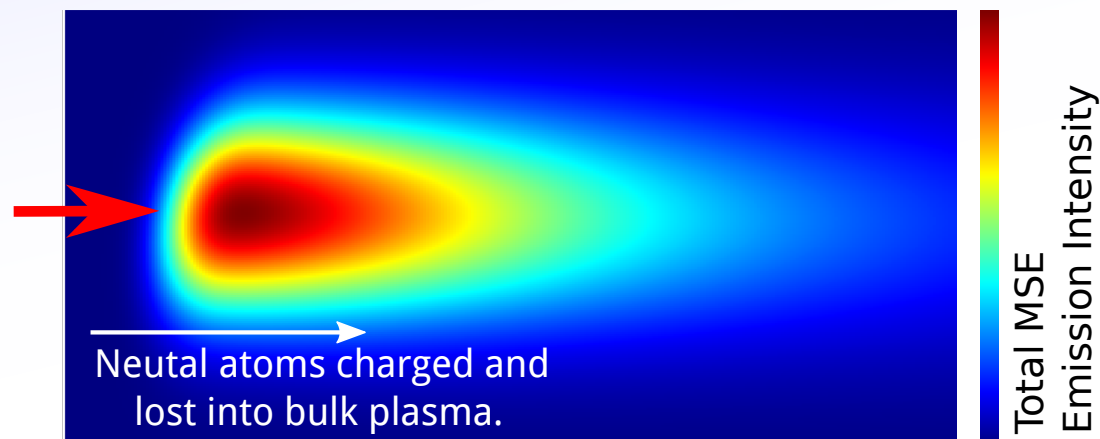
Spectrum from a single pixel:



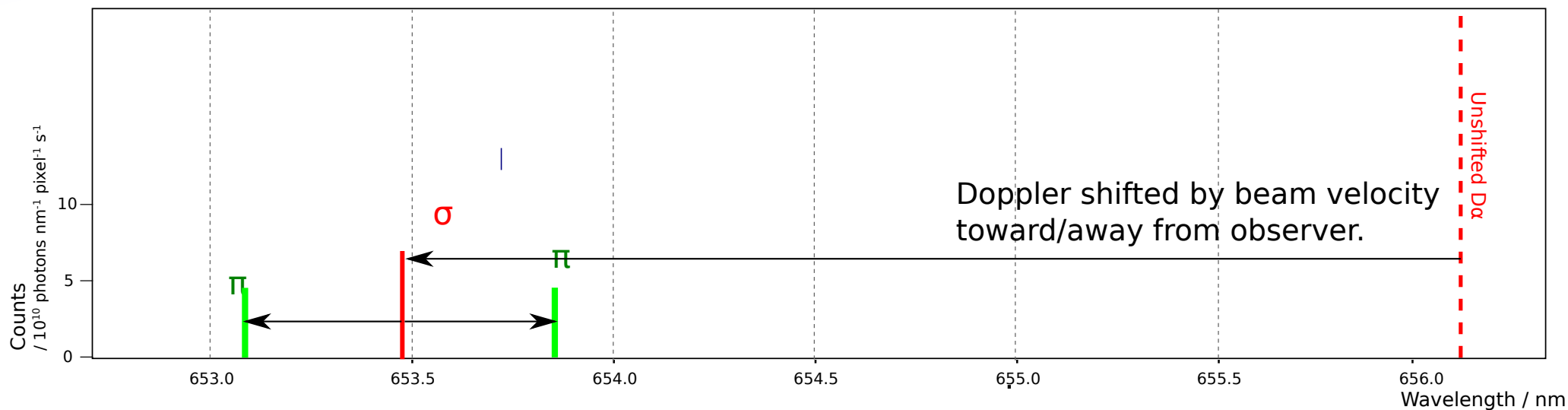
# Introduction - Motional Stark Effect



Neutral beam atoms injected into plasma.  
Excited by plasma, then emit H $\alpha$ /D $\alpha$  radiation.



Spectrum from a single pixel:



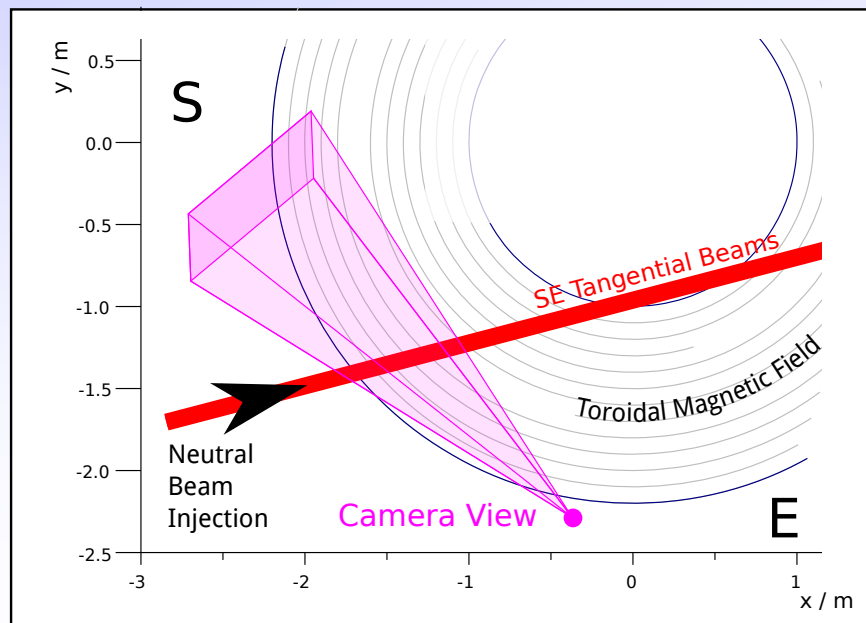
Stark split by electric field in rest frame of atom:

$$\mathbf{E} = \mathbf{v} \times \mathbf{B}$$

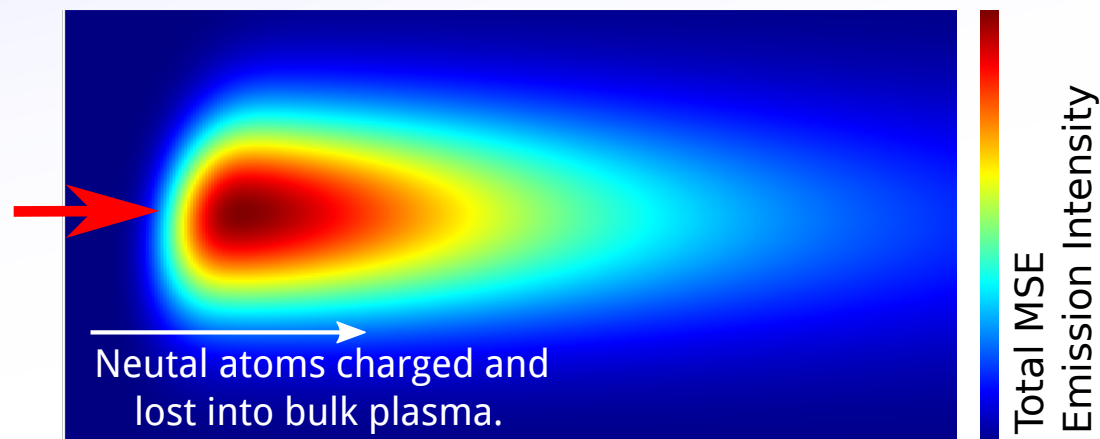
Roughly:  $\pi$  polarised parallel to E.

$\sigma$  polarised perp' to E.

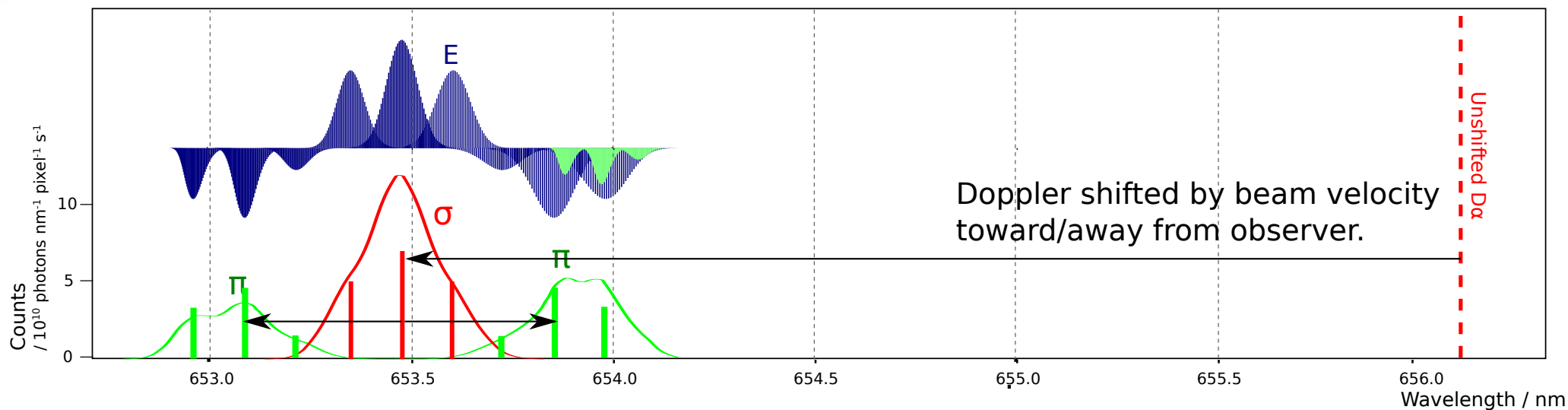
# Introduction - Motional Stark Effect



Neutral beam atoms injected into plasma.  
Excited by plasma, then emit H $\alpha$ /D $\alpha$  radiation.



Spectrum from a single pixel:



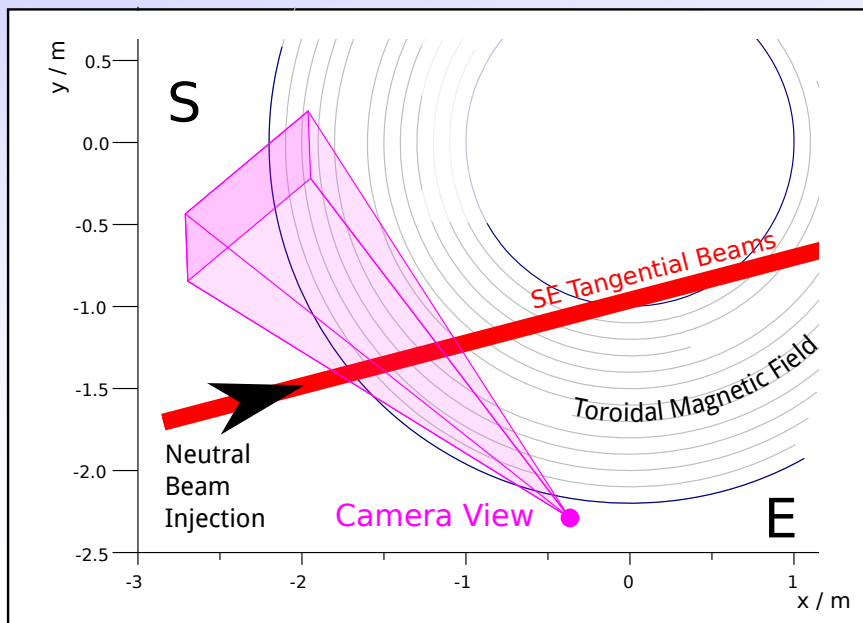
Stark split by electric field in rest frame of atom:

$$\mathbf{E} = \mathbf{v} \times \mathbf{B}$$

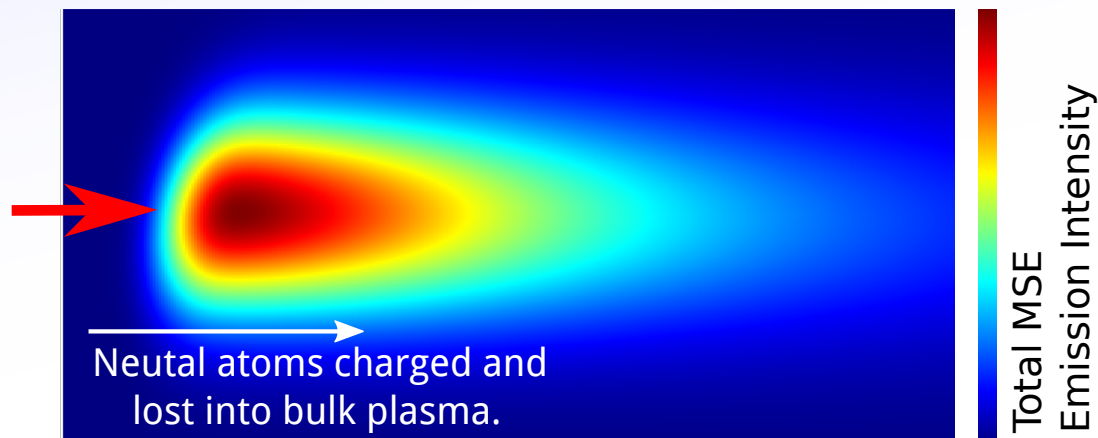
Roughly:  $\pi$  polarised parallel to  $\mathbf{E}$ .

$\sigma$  polarised perp' to  $\mathbf{E}$ .

# Introduction - Motional Stark Effect



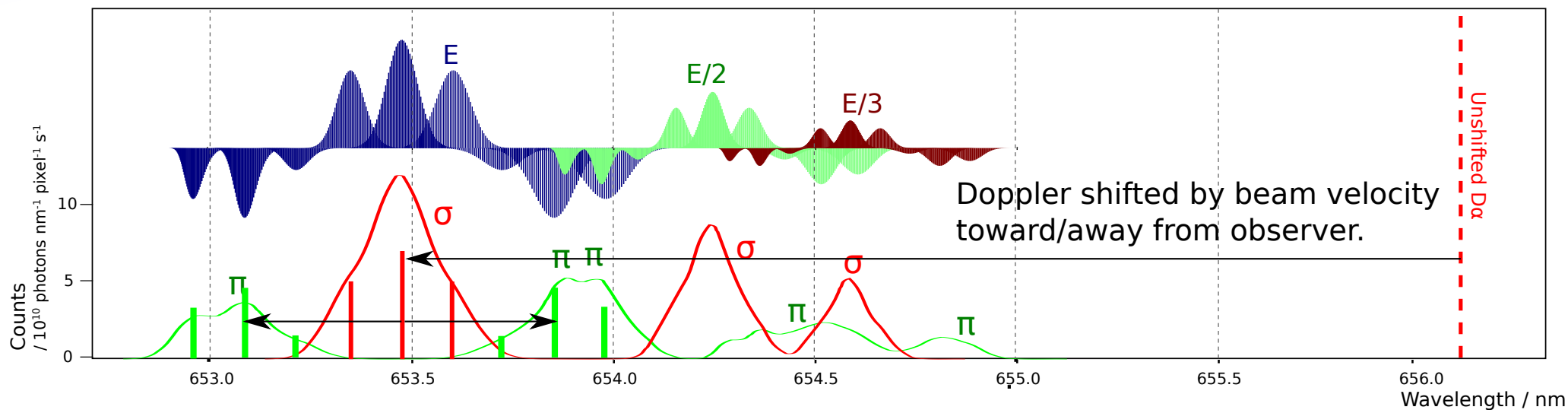
Neutral beam atoms injected into plasma.  
Excited by plasma, then emit H $\alpha$ /D $\alpha$  radiation.



Complications:

Energy components, Doppler broadening,  
Beam divergence, Line integration etc.

Spectrum from a single pixel:



Stark split by electric field in rest frame of atom:

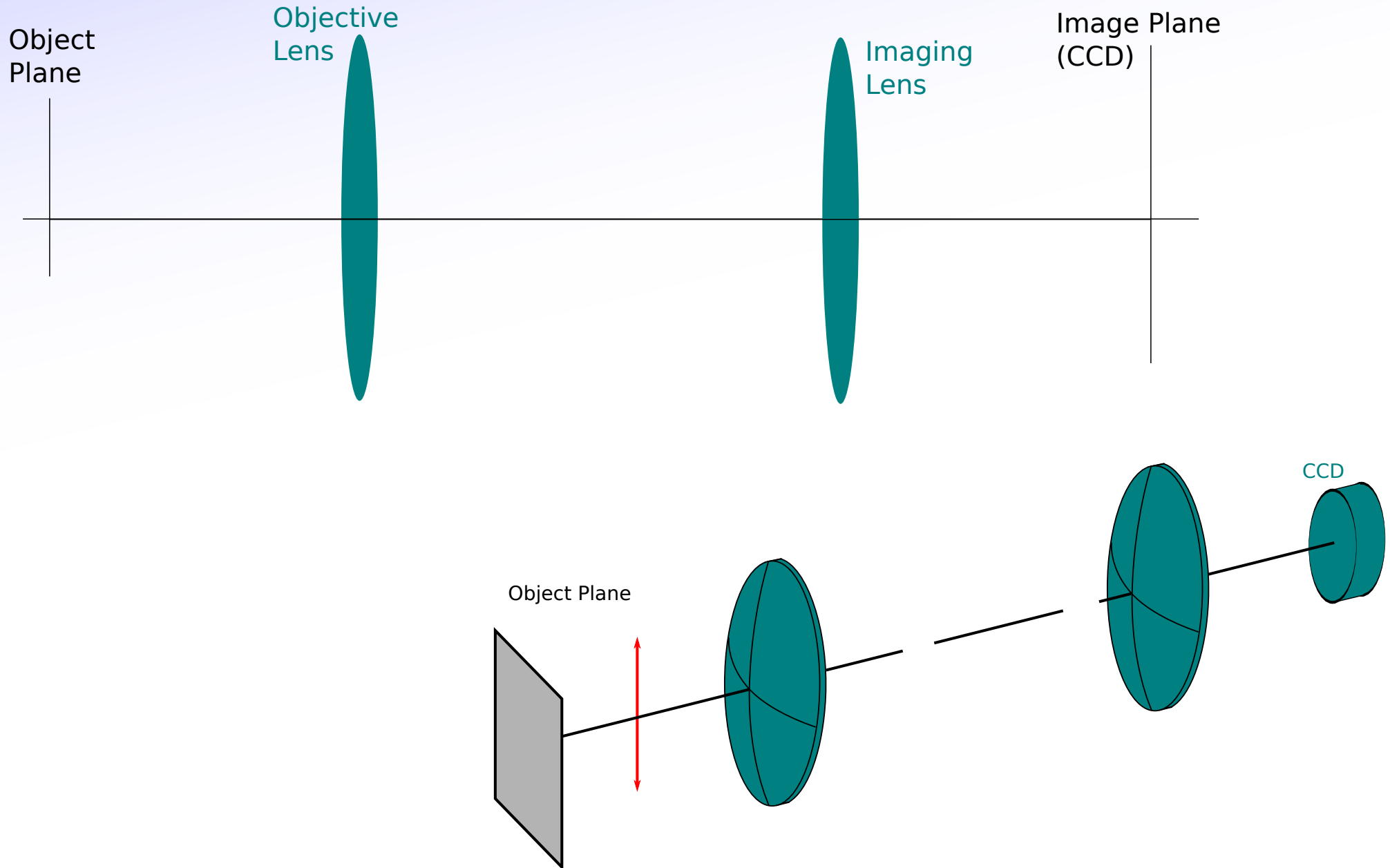
$$\mathbf{E} = \mathbf{v} \times \mathbf{B}$$

Roughly:  $\pi$  polarised parallel to  $\mathbf{E}$ .

$\sigma$  polarised perp' to  $\mathbf{E}$ .

# Savart Plates

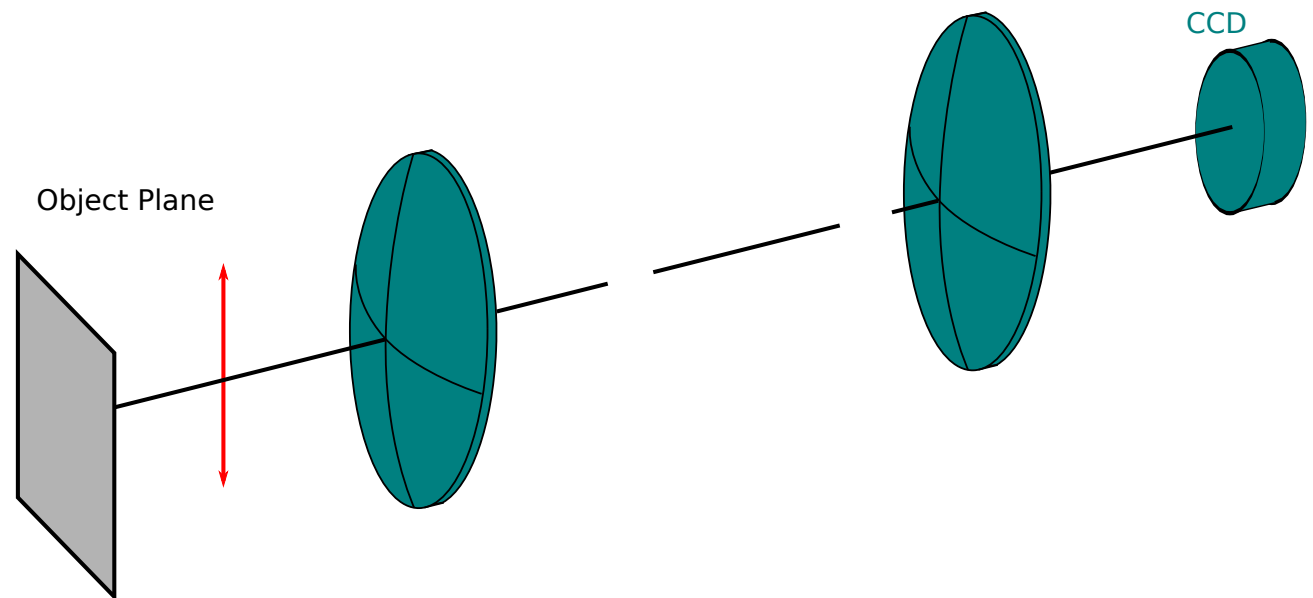
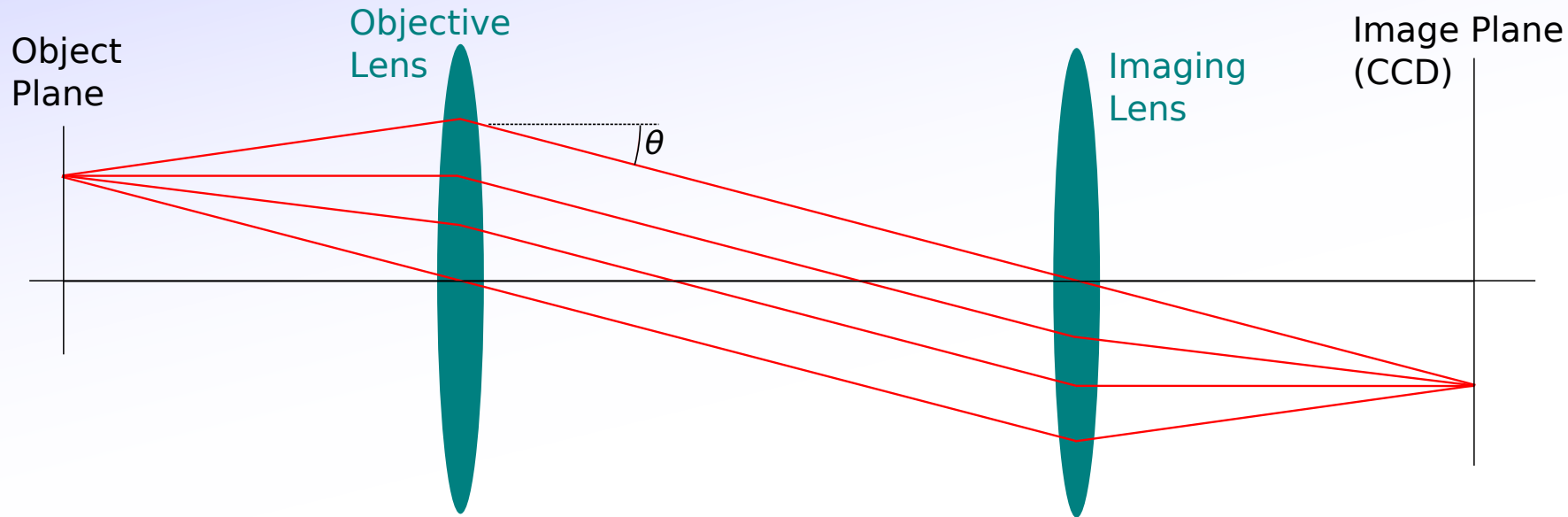
Savart Plate: Angle dependent phase shift --> Interference pattern accross image.





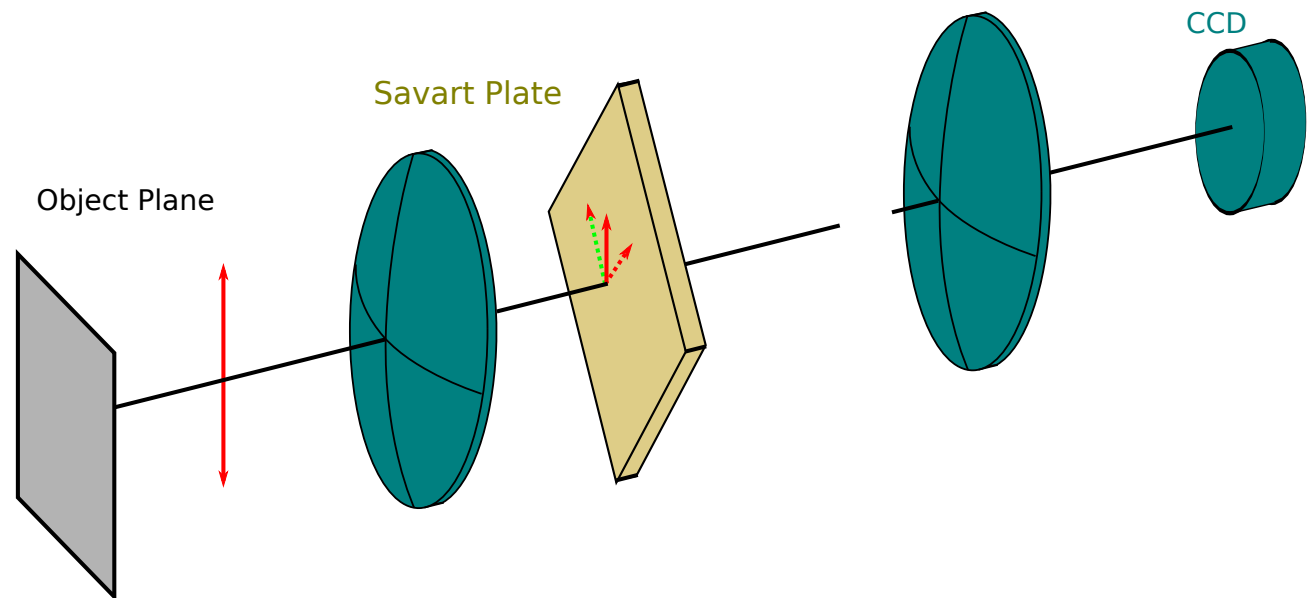
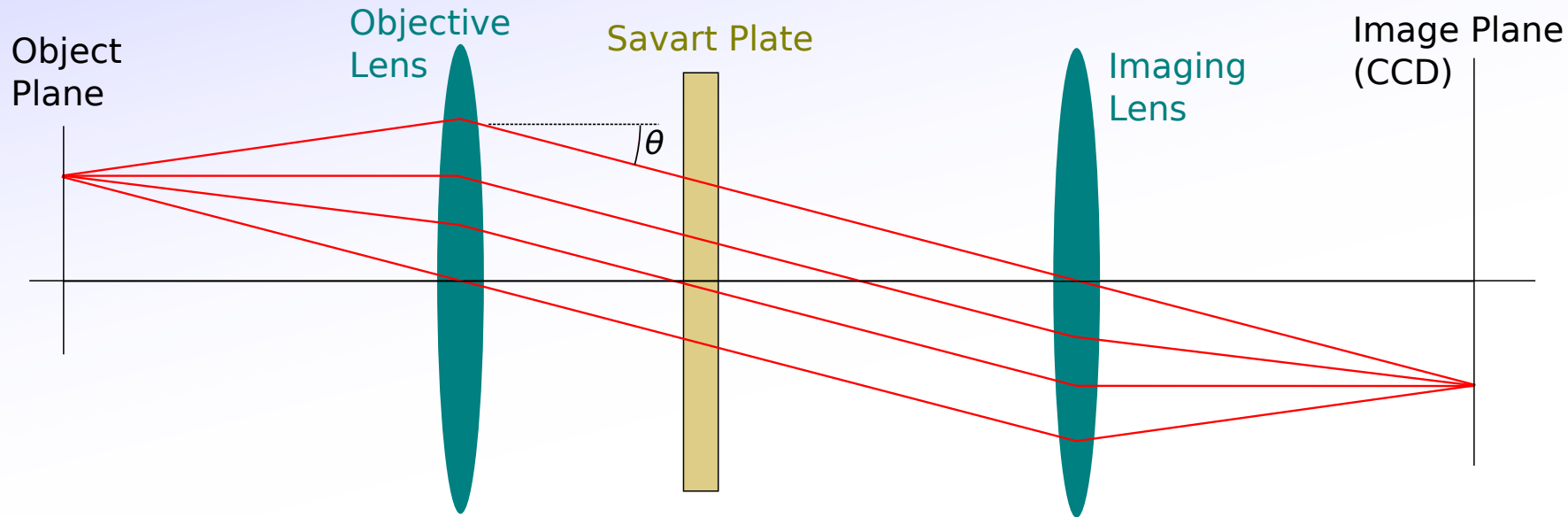
# Savart Plates

Savart Plate: Angle dependent phase shift --> Interference pattern accross image.



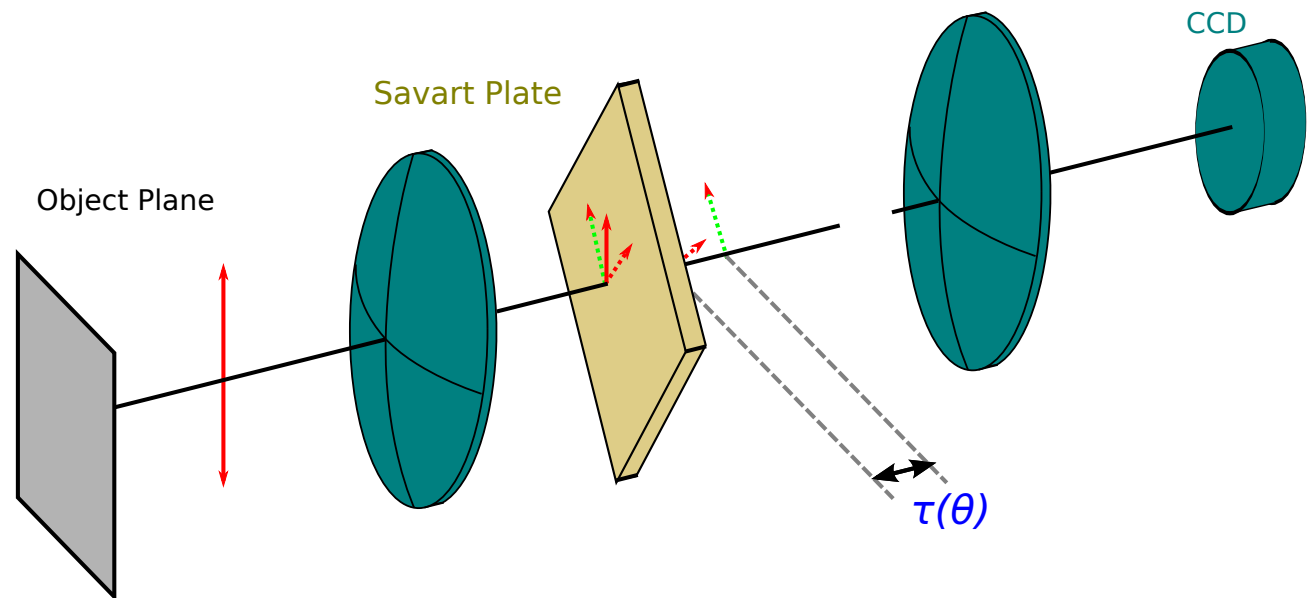
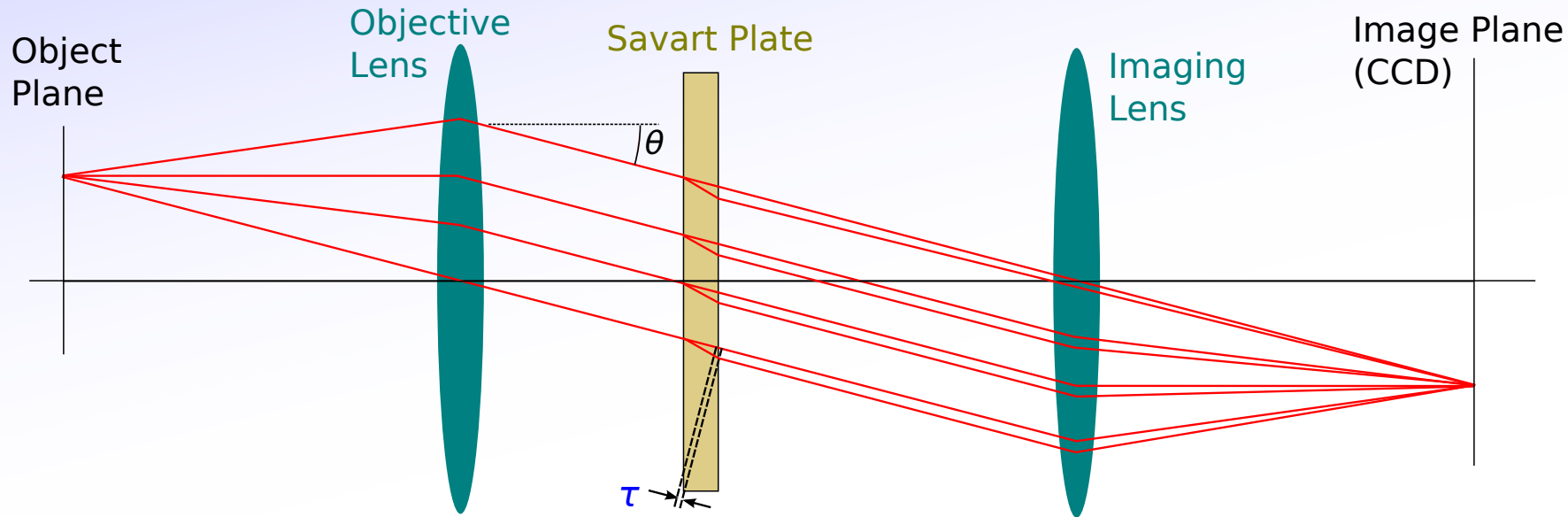
# Savart Plates

Savart Plate: Angle dependent phase shift --> Interference pattern across image.



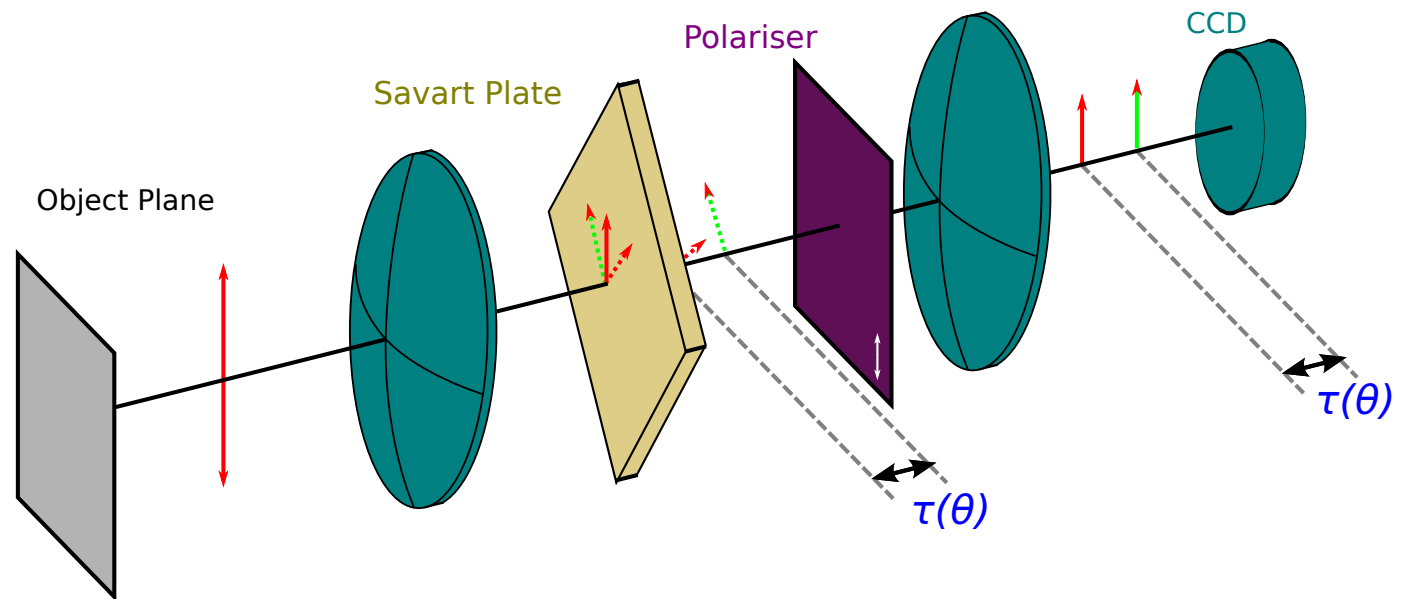
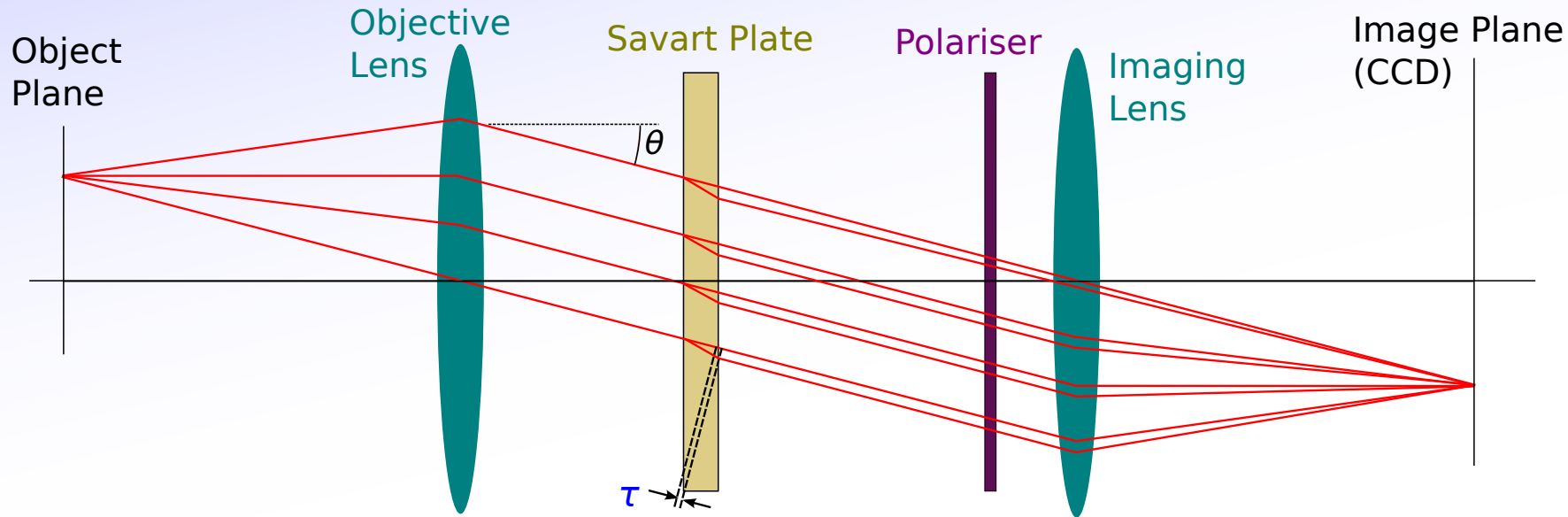
# Savart Plates

Savart Plate: Angle dependent phase shift --> Interference pattern across image.



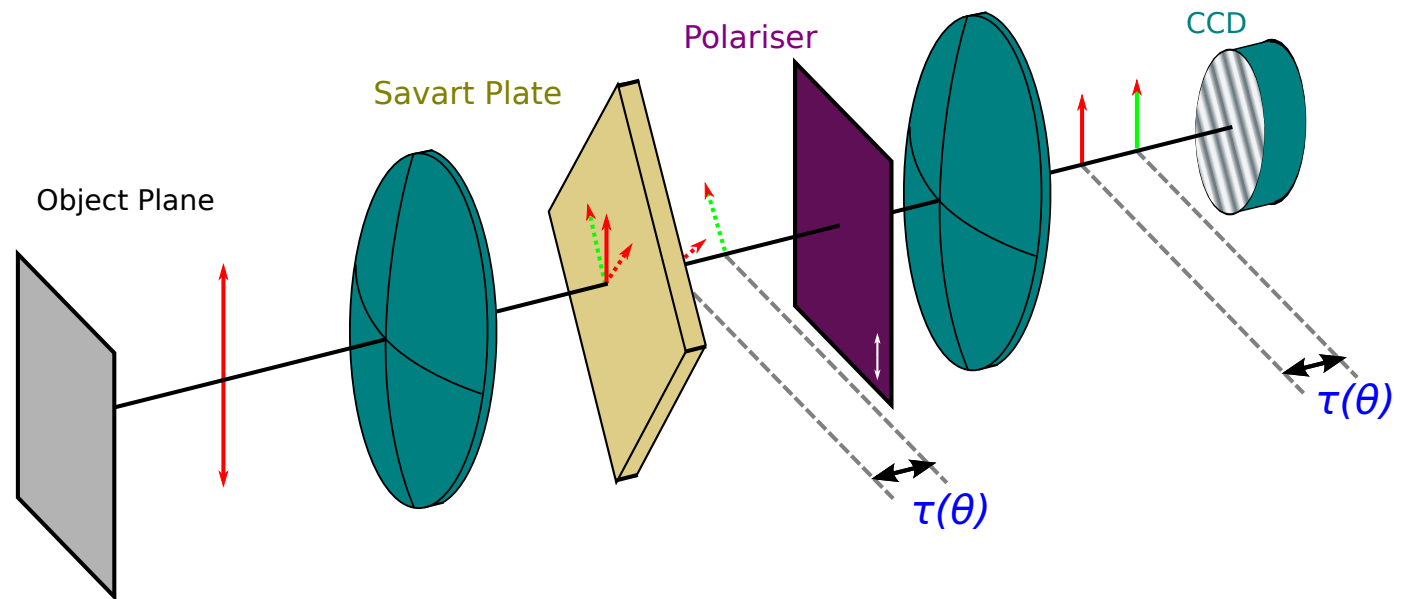
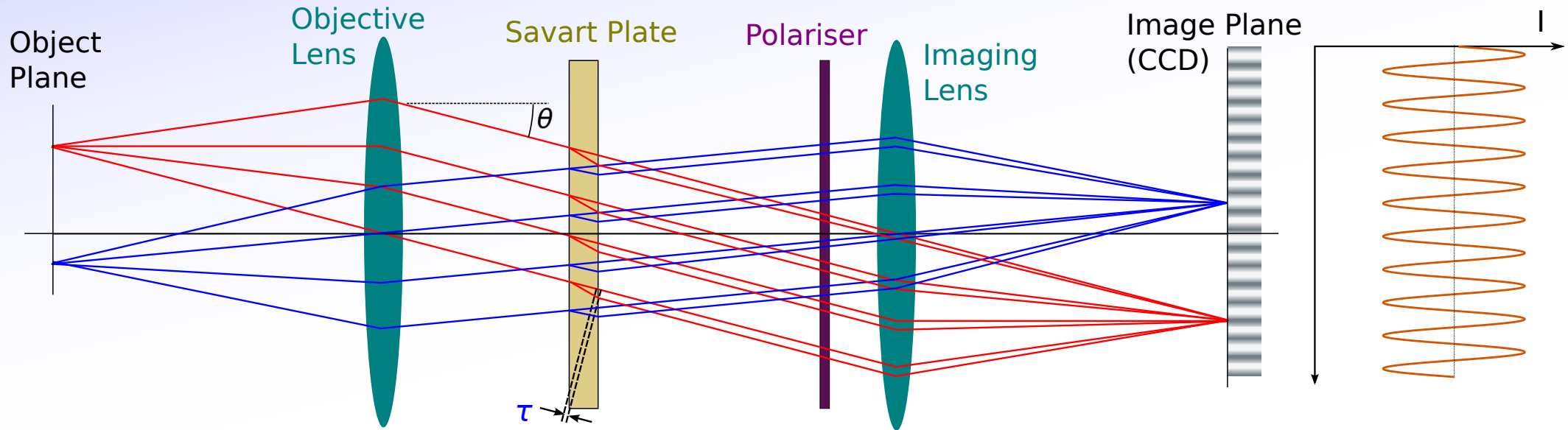
# Savart Plates

Savart Plate: Angle dependent phase shift --> Interference pattern accross image.



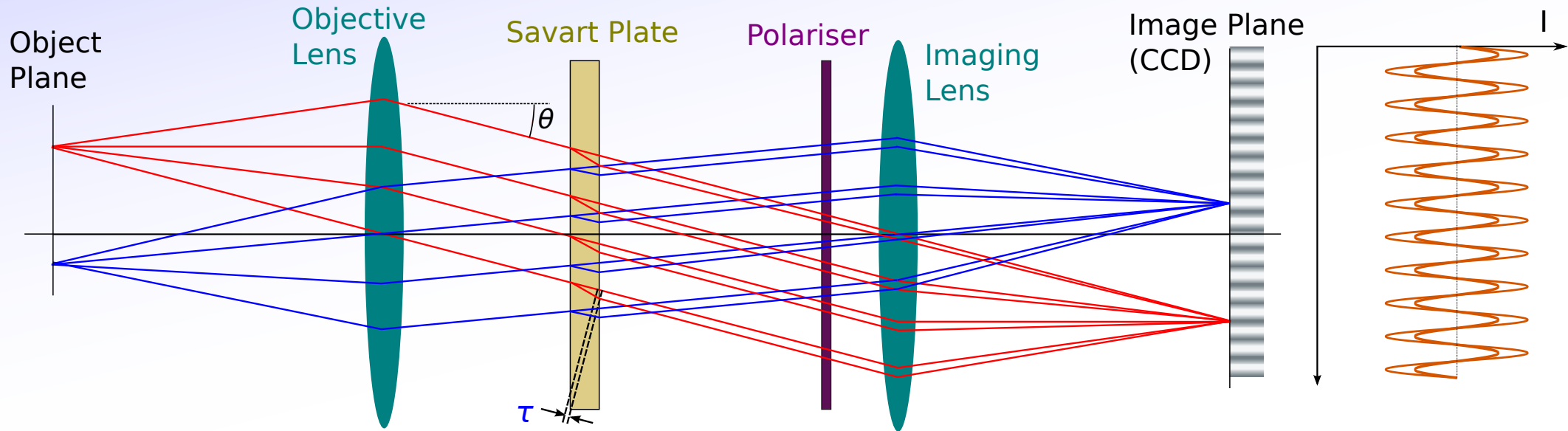
# Savart Plates

Savart Plate: Angle dependent phase shift --> Interference pattern across image.



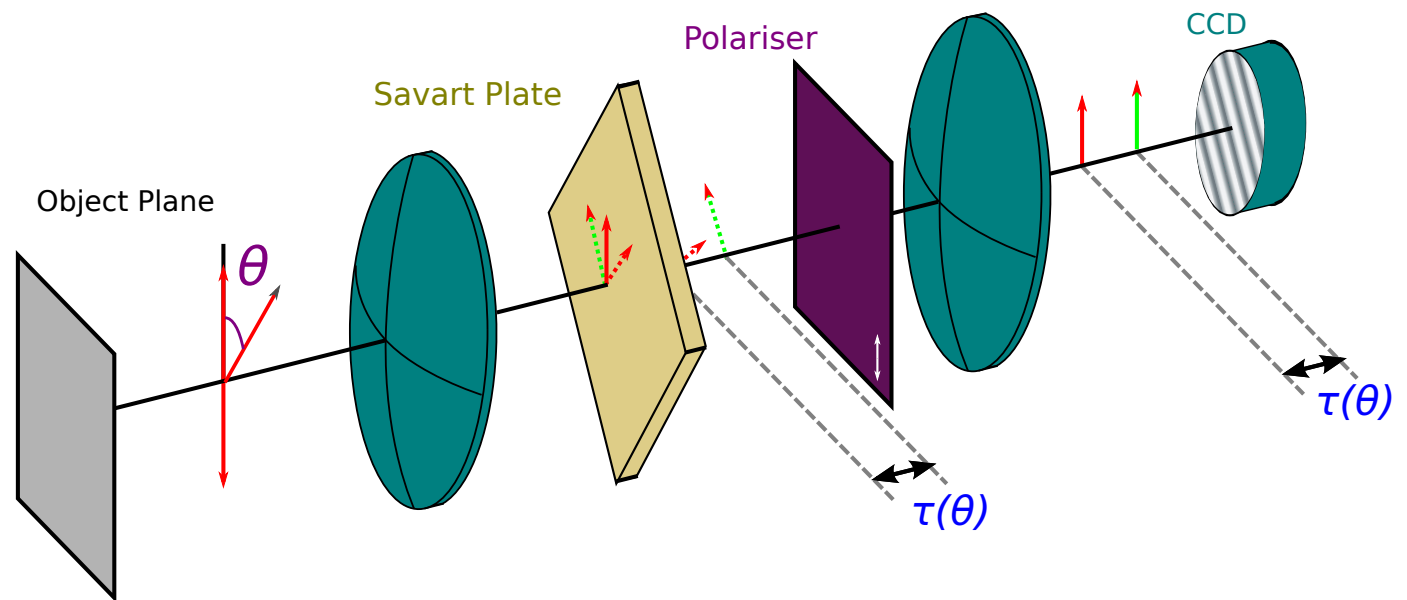
# Savart Plates

Savart Plate: Angle dependent phase shift --> Interference pattern accross image.



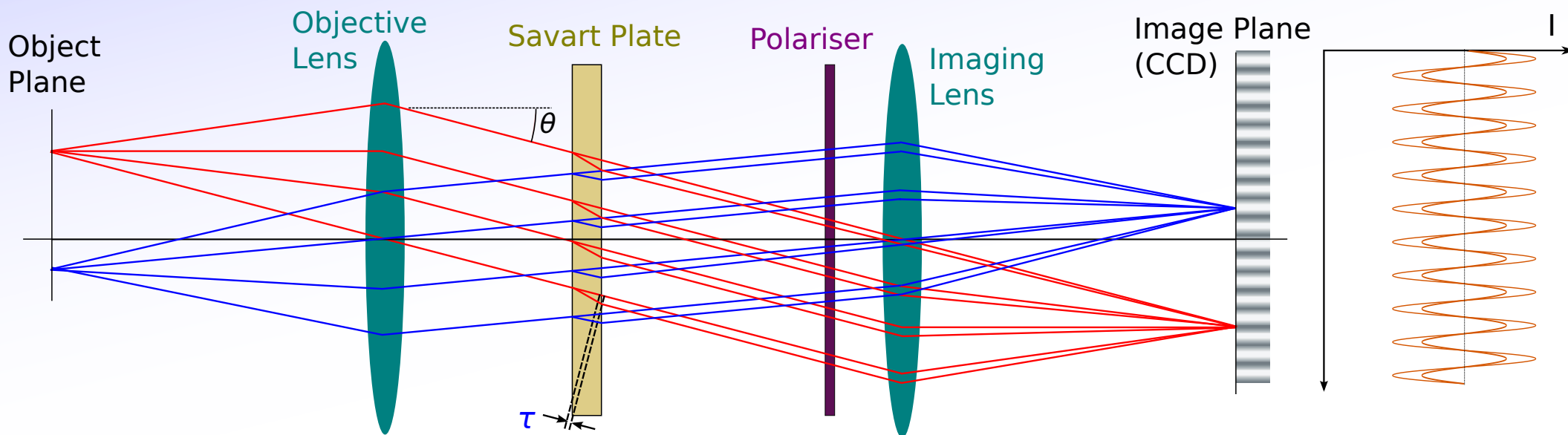
Oscillation amplitude proportional to polarisation angle.

$$I \propto 1 + \cos 2\theta \cos(x)$$



# Savart Plates

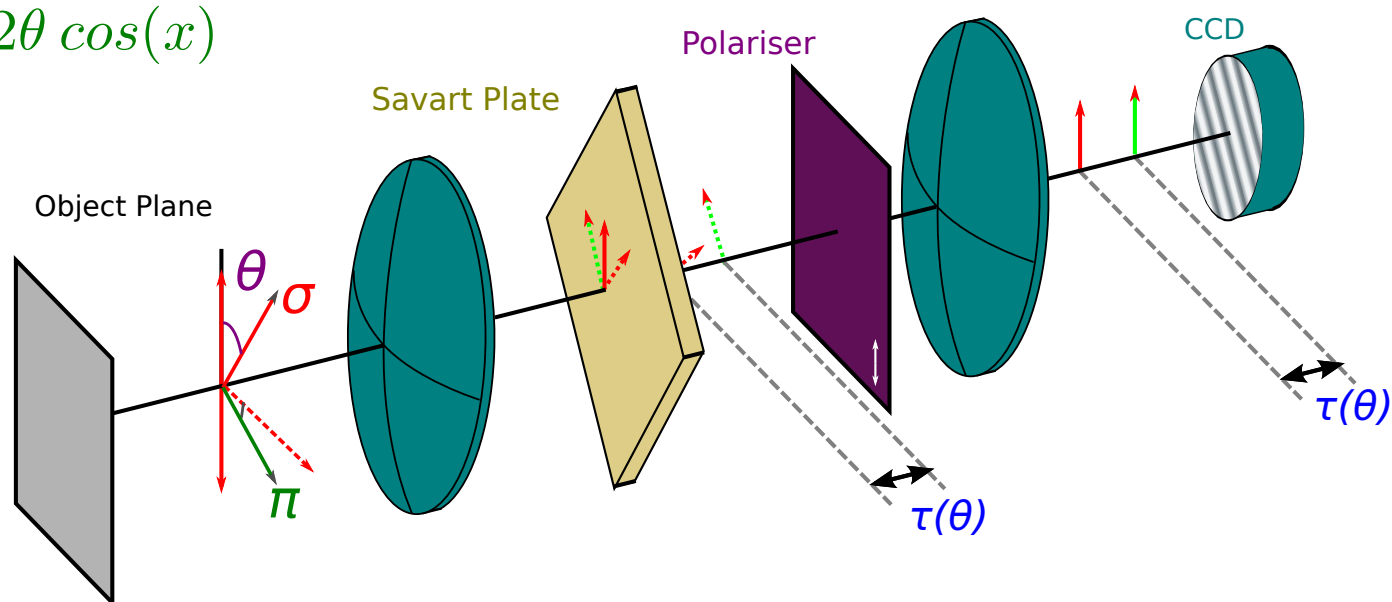
Savart Plate: Angle dependent phase shift --> Interference pattern across image.



Oscillation amplitude proportional to polarisation angle.

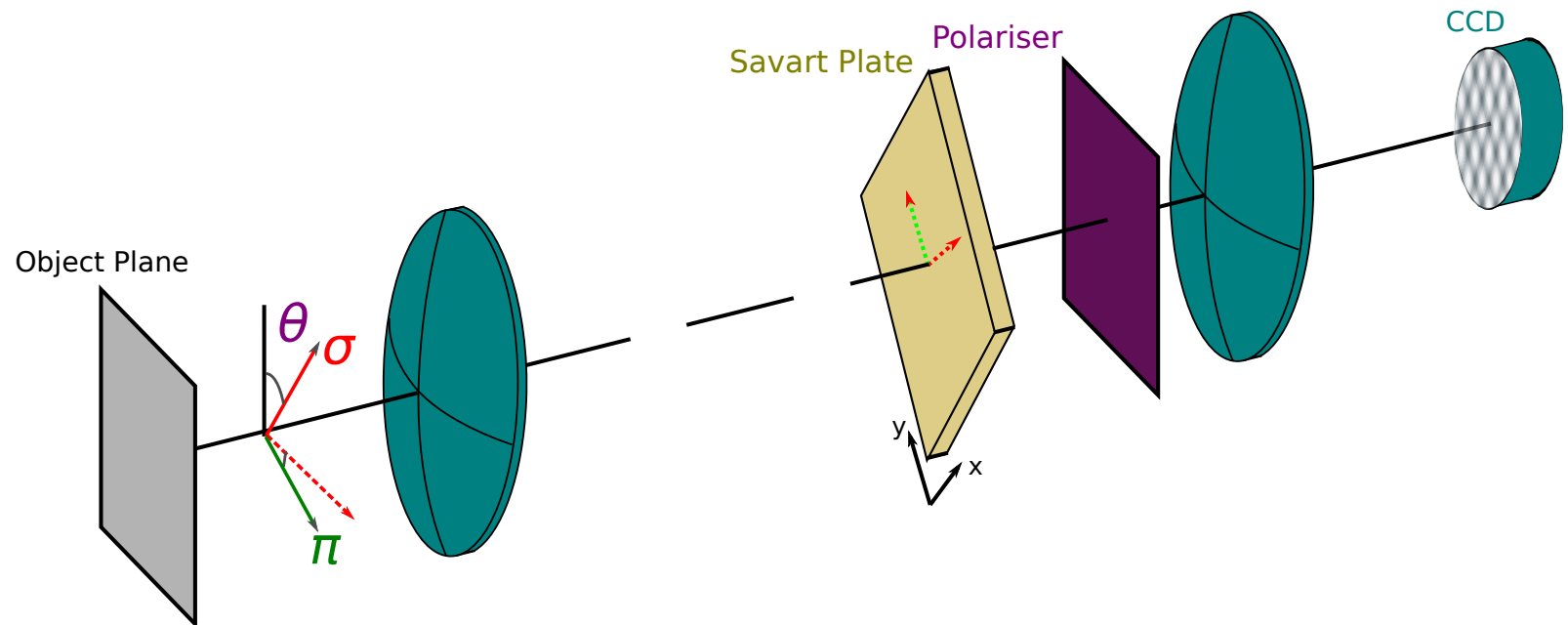
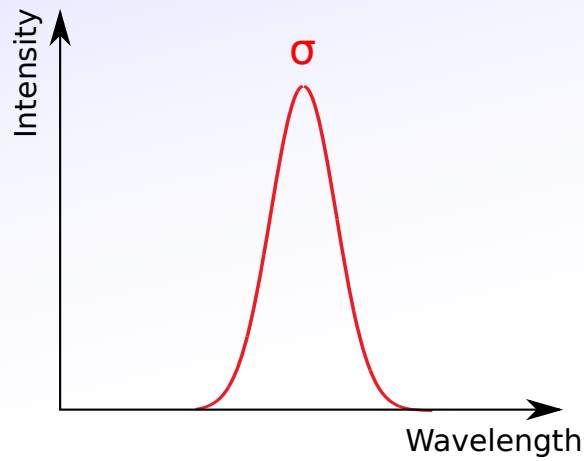
$$I \propto 1 + \cos 2\theta \cos(x) - \cos 2\theta \cos(x)$$

but  $\sigma$  and  $\pi$  are orthogonal.  
If they were monochromatic,  
they would cancel out...



# Spectral Coherence

$\pi$  and  $\sigma$  orthogonal and always the same intensity, but different spectral profiles.

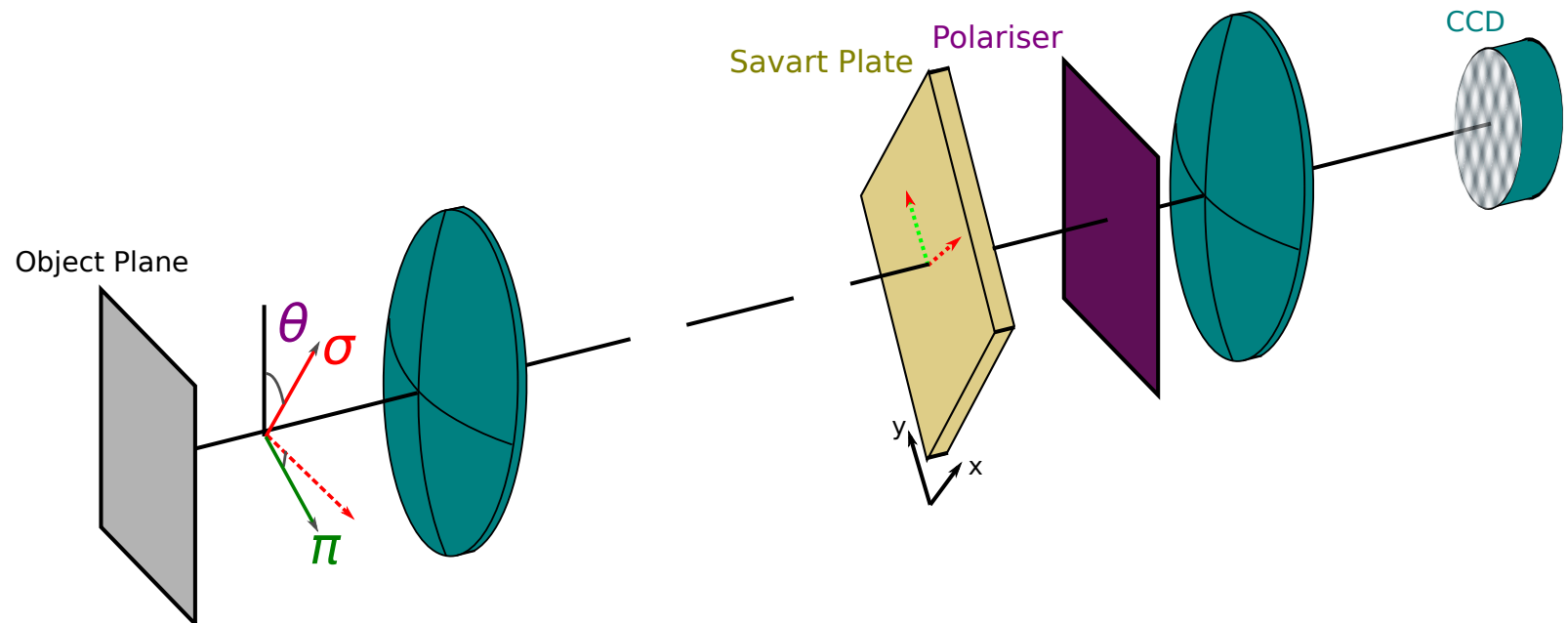
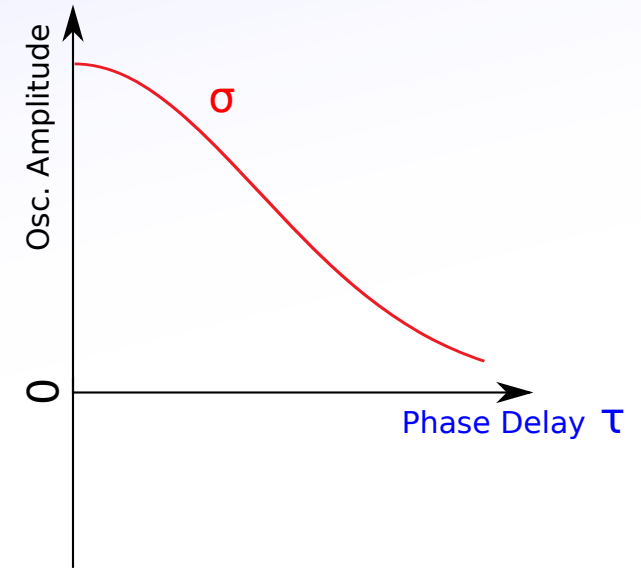
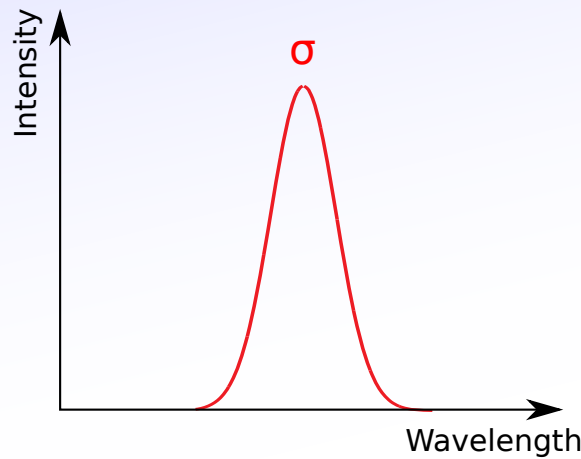




# Spectral Coherence

$\pi$  and  $\sigma$  orthogonal and always the same intensity, but different spectral profiles.

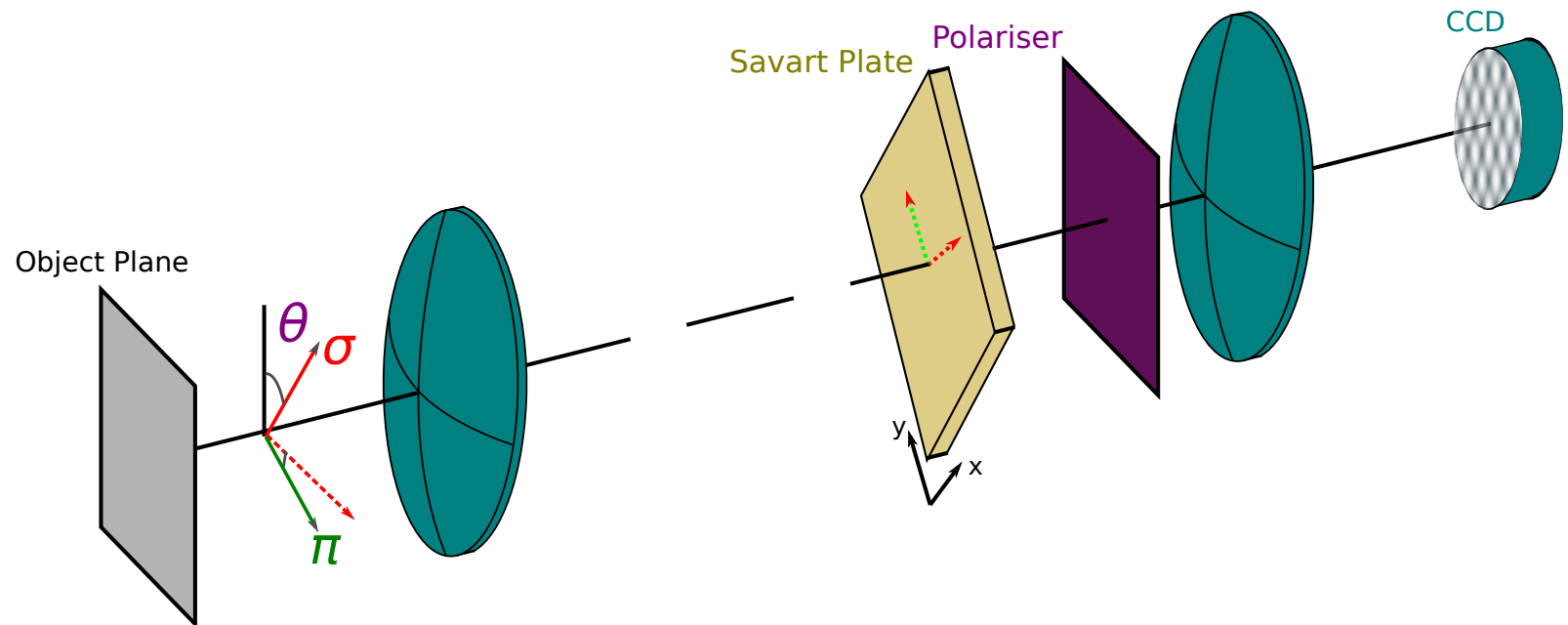
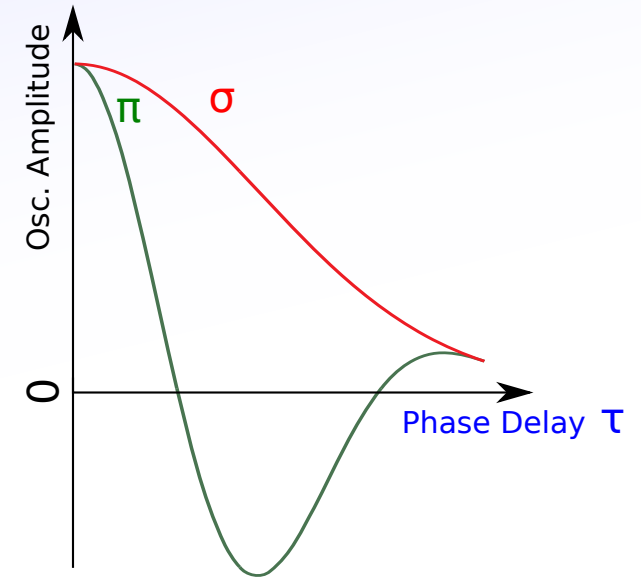
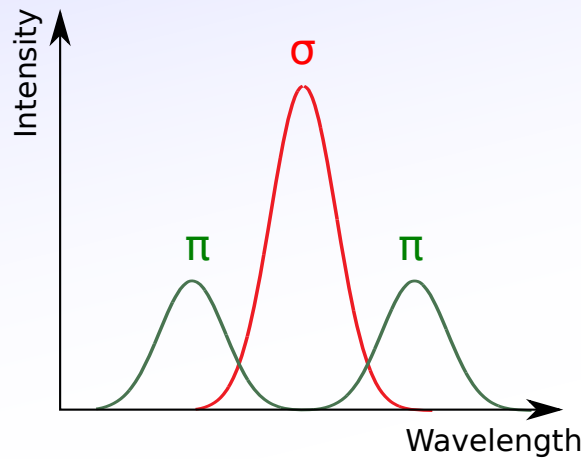
For large  $\tau$ , different wavelengths have different phases --> decoherence.



# Spectral Coherence

$\pi$  and  $\sigma$  orthogonal and always the same intensity, but different spectral profiles.

For large  $\tau$ , different wavelengths have different phases --> decoherence.

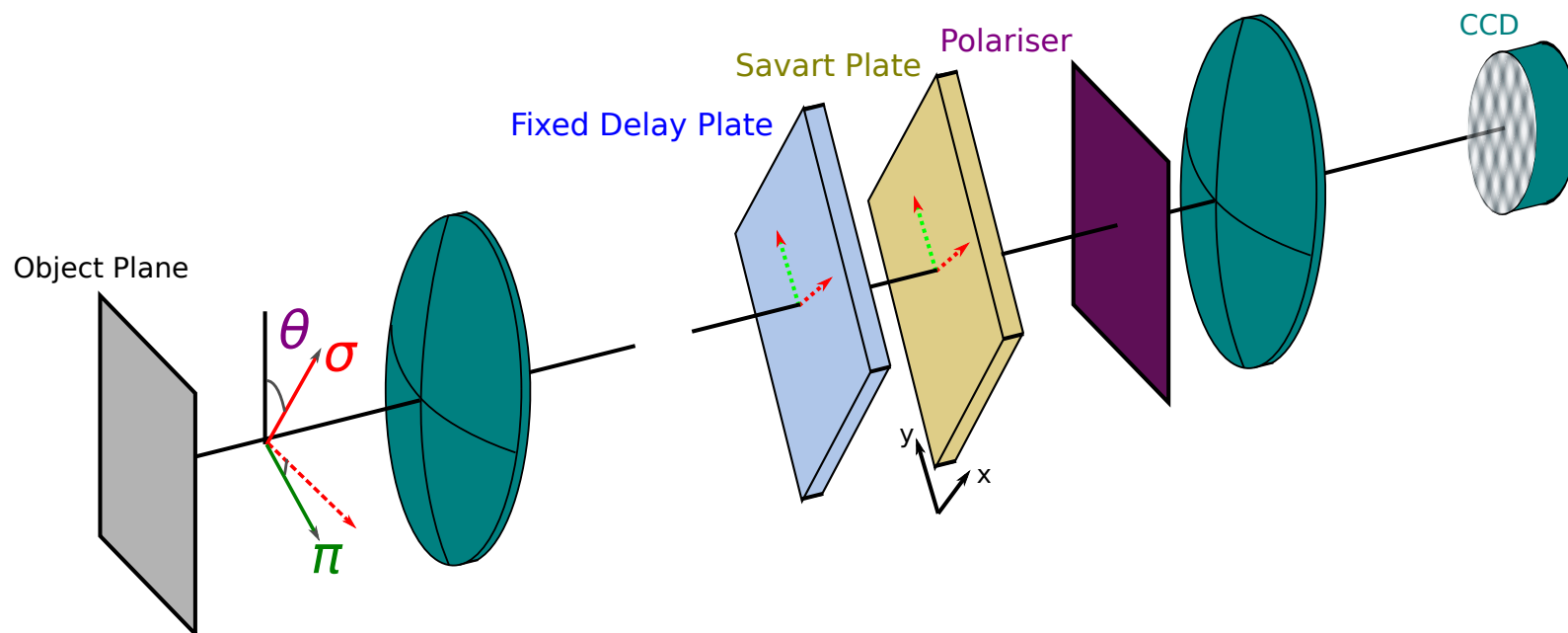
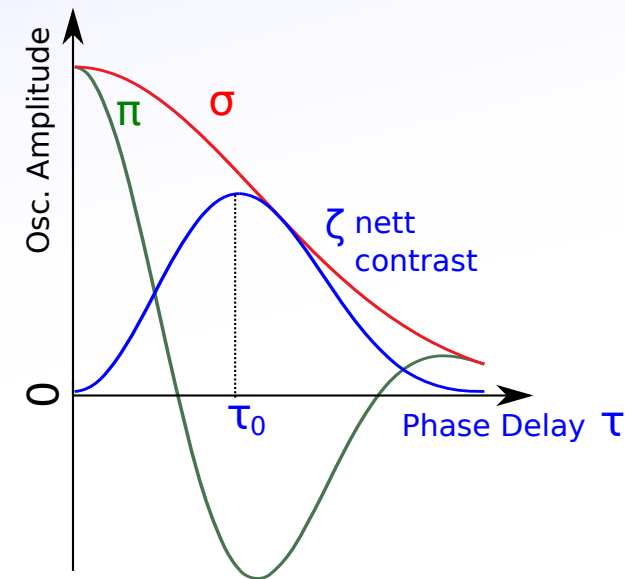
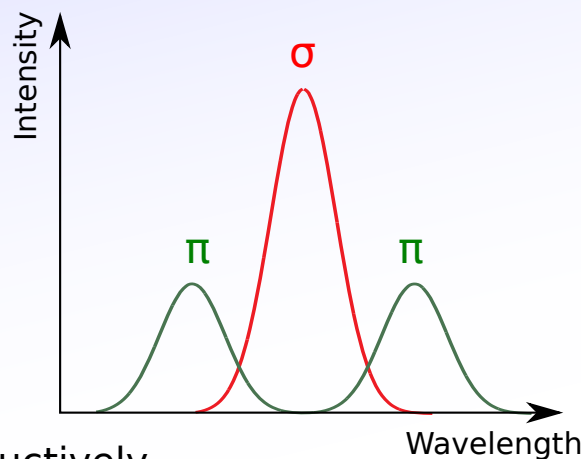


# Spectral Coherence

$\pi$  and  $\sigma$  orthogonal and always the same intensity, but different spectral profiles.

For large  $\tau$ , different wavelengths have different phases --> decoherence.

Add a delay plate to introduce the best  $\tau_0$  - where  $\pi$  and  $\sigma$  combine constructively.



# Spectral Coherence

$\pi$  and  $\sigma$  orthogonal and always the same intensity, but different spectral profiles.

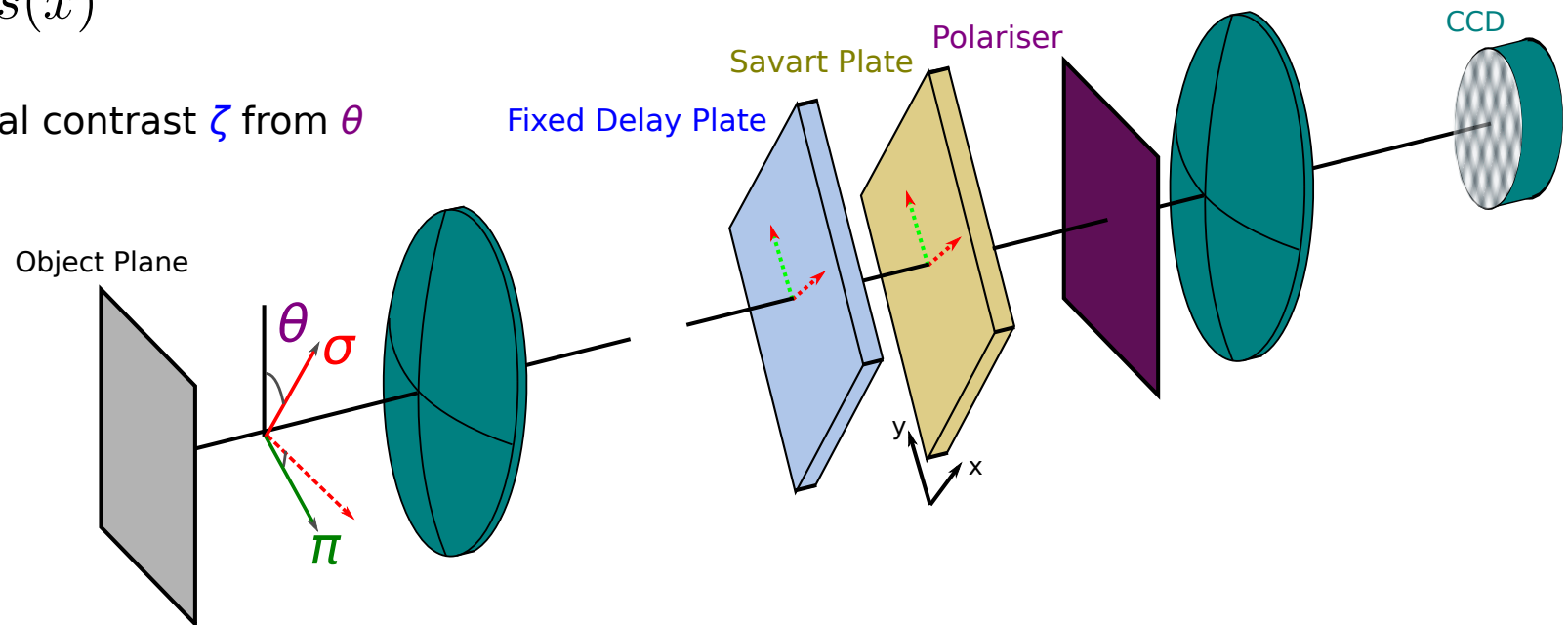
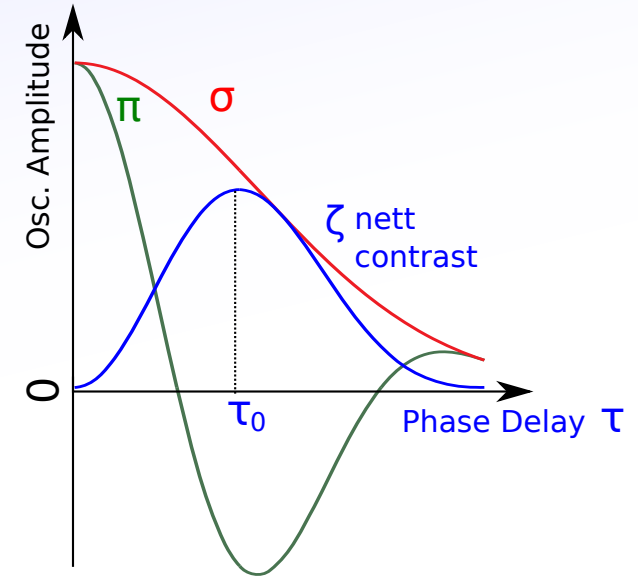
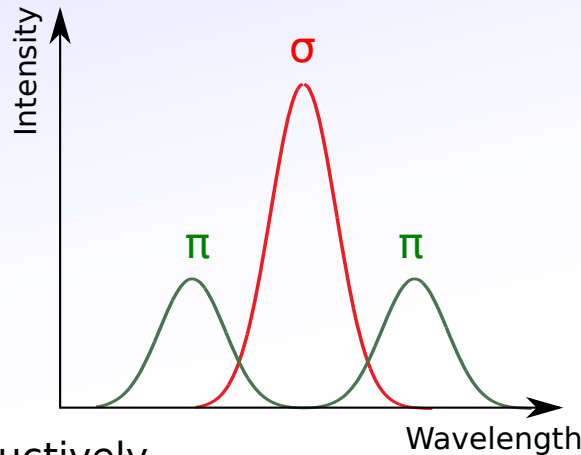
For large  $\tau$ , different wavelengths have different phases --> decoherence.

Add a delay plate to introduce the best  $\tau_0$  - where  $\pi$  and  $\sigma$  combine constructively.

but amplitude now also dependent on contrast:

$$I \propto 1 + \zeta \cos 2\theta \cos(x)$$

Need to separate spectral contrast  $\zeta$  from  $\theta$



# Spectral Coherence

$\pi$  and  $\sigma$  orthogonal and always the same intensity, but different spectral profiles.

For large  $\tau$ , different wavelengths have different phases --> decoherence.

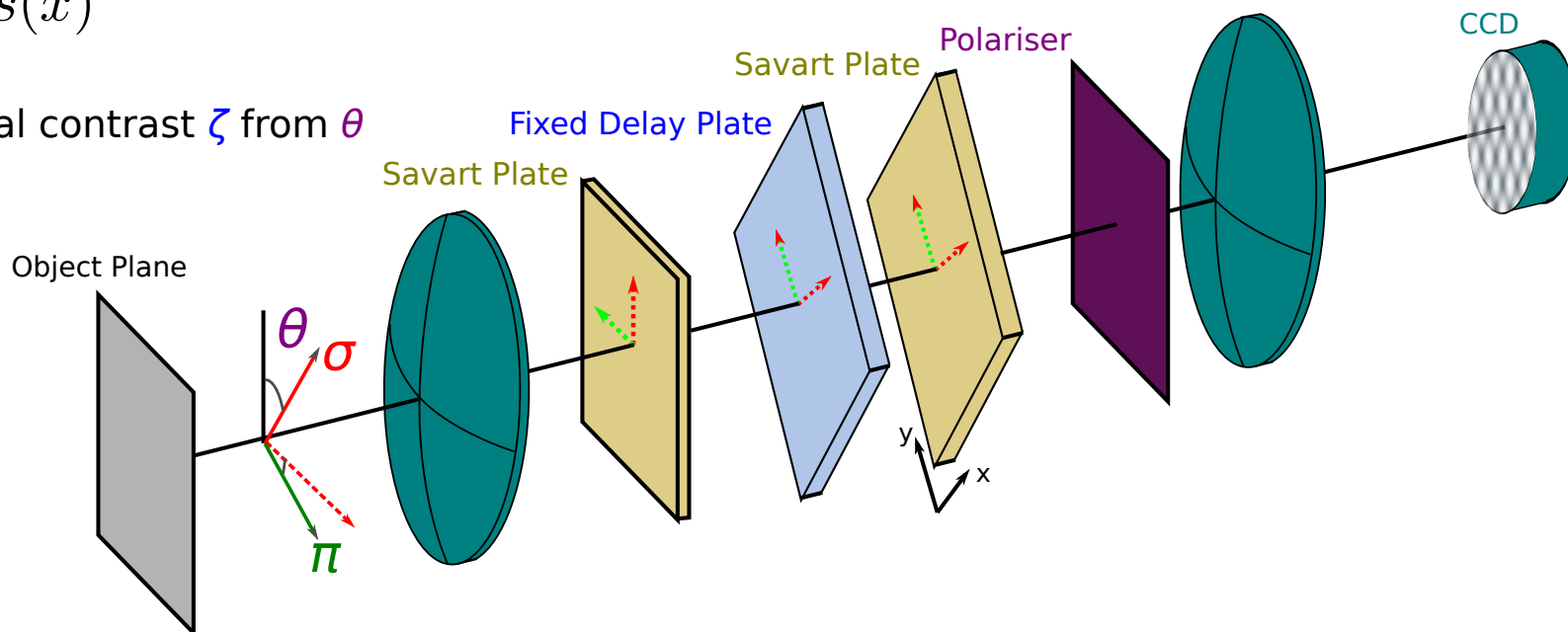
Add a delay plate to introduce the best  $\tau_0$  - where  $\pi$  and  $\sigma$  combine constructively.

but amplitude now also dependent on contrast:

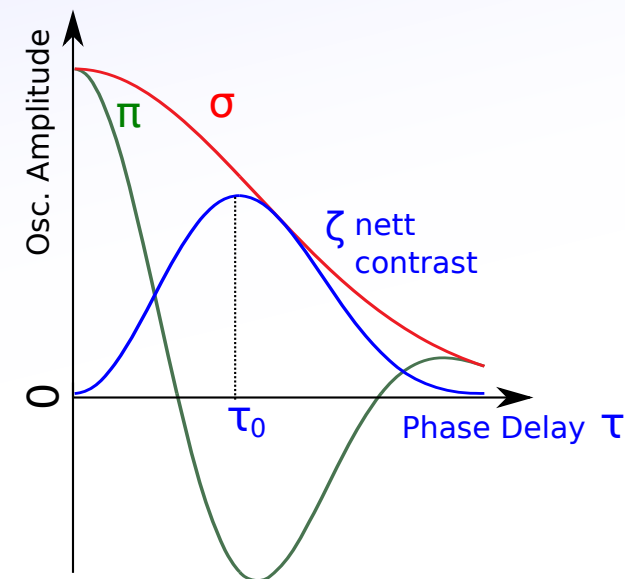
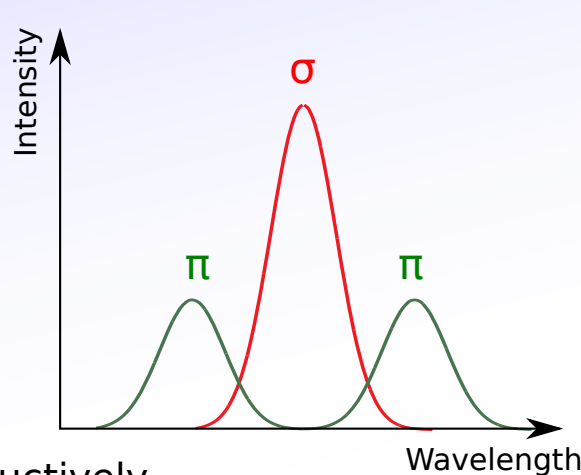
$$I \propto 1 + \zeta \cos 2\theta \cos(x)$$

Need to separate spectral contrast  $\zeta$  from  $\theta$

add another Savart plate at  $45^\circ$ .  
Combined effect adds 2 extra terms:

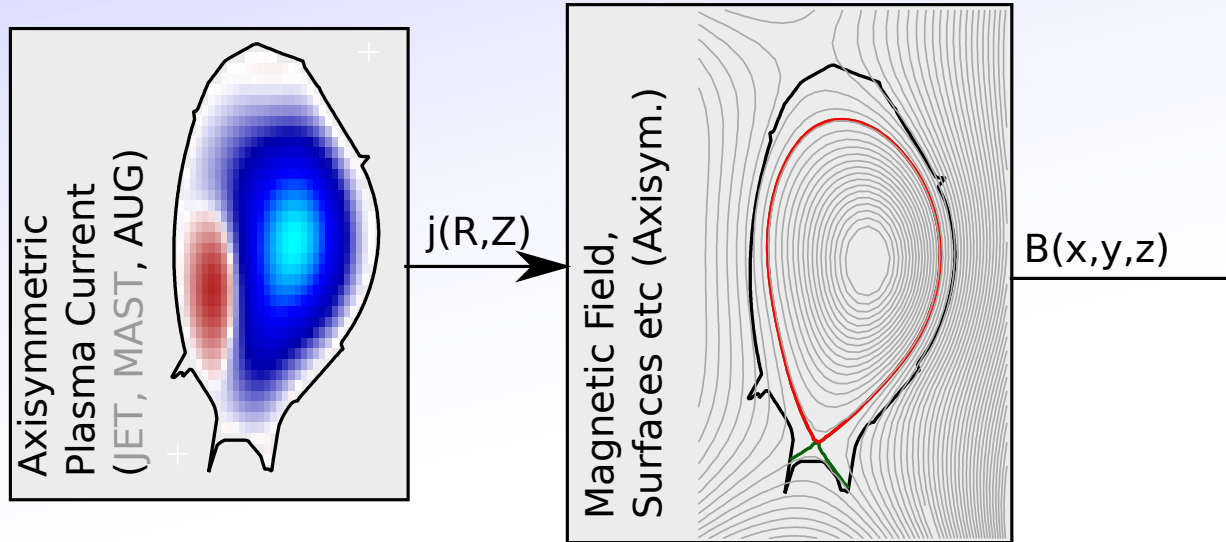


$$I \propto 1 + \zeta \cos 2\theta \cos(x) + \zeta \sin 2\theta \cos(x - y) - \zeta \sin 2\theta \cos(x + y)$$



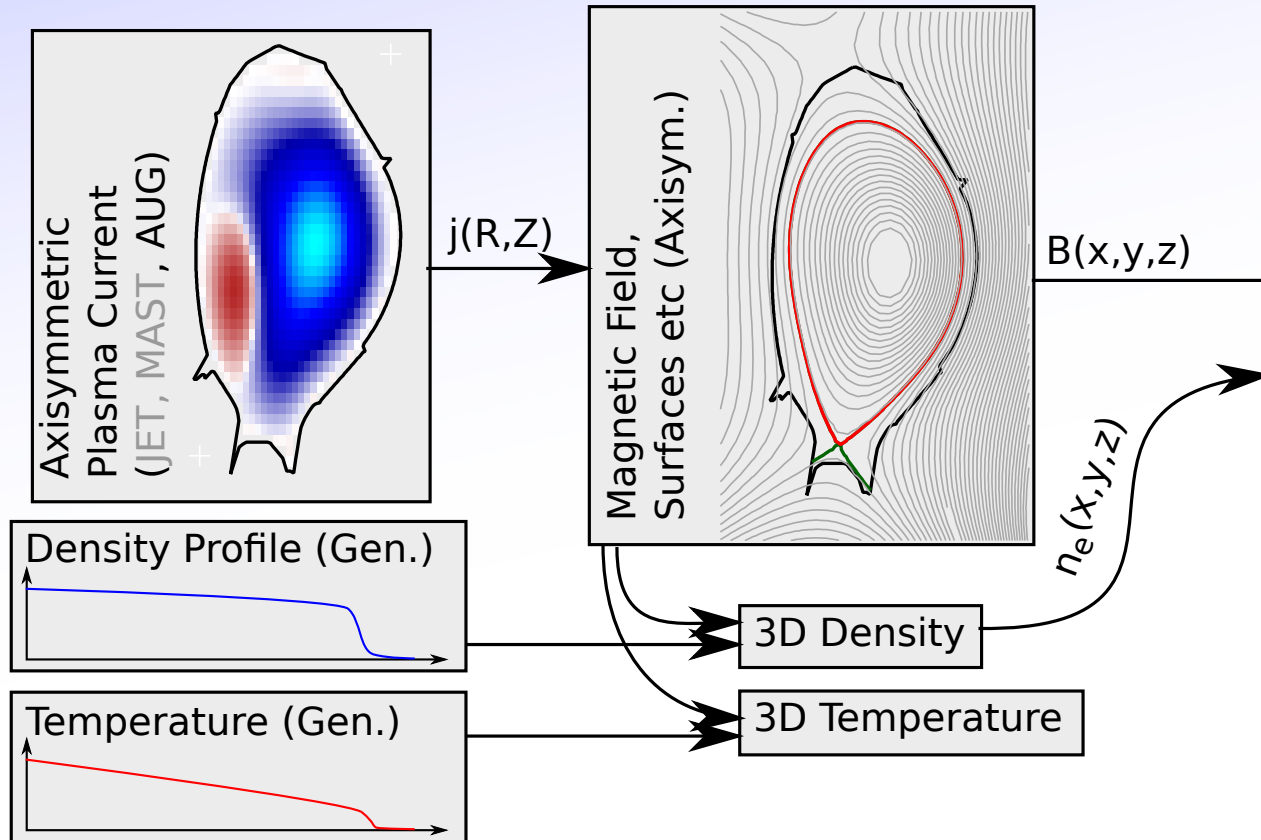
# Forward Model

Developed several components for the Bayesian / forward modelling framework (Minerva).



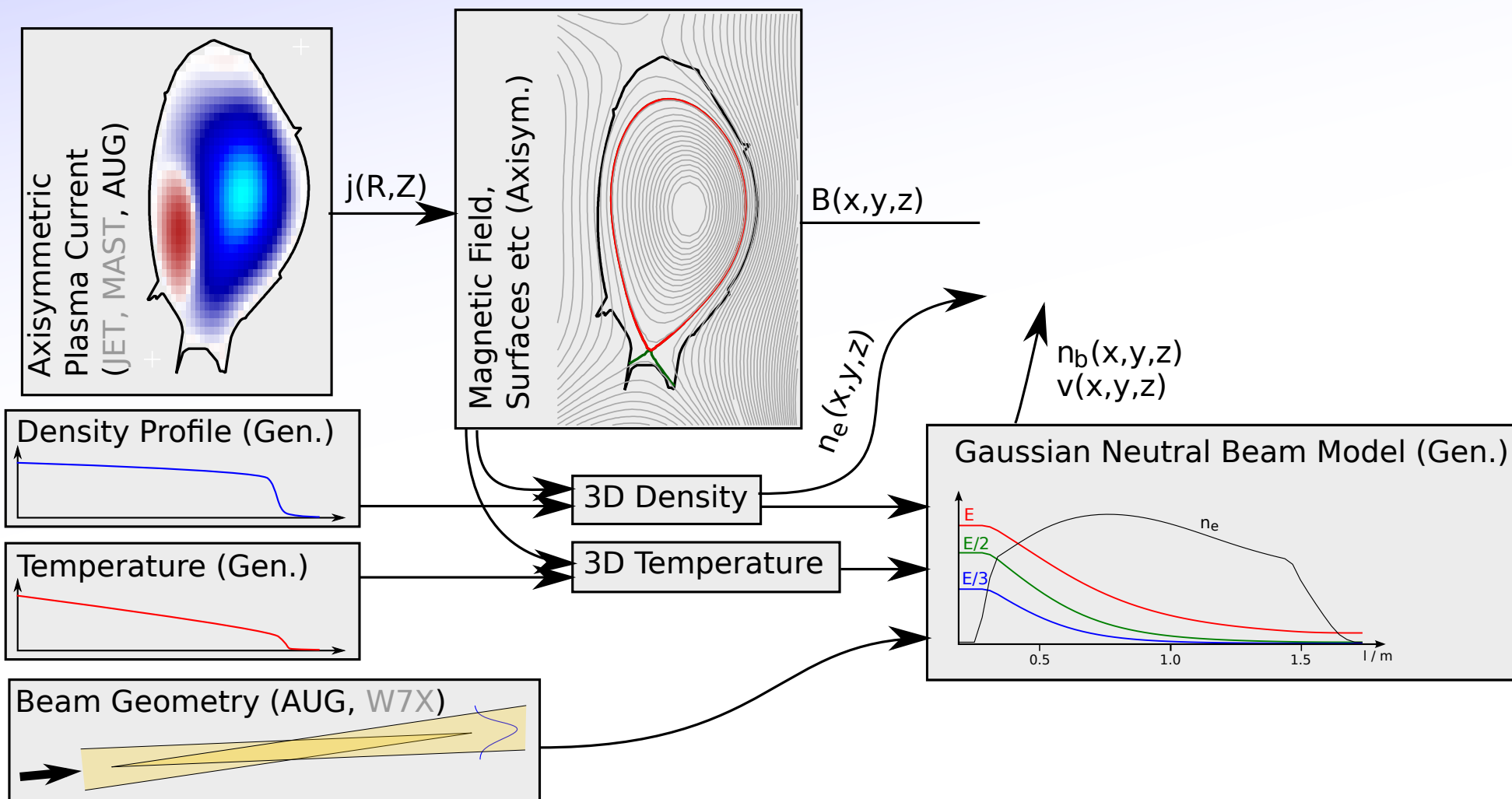
# Forward Model

Developed several components for the Bayesian / forward modelling framework (Minerva).



# Forward Model

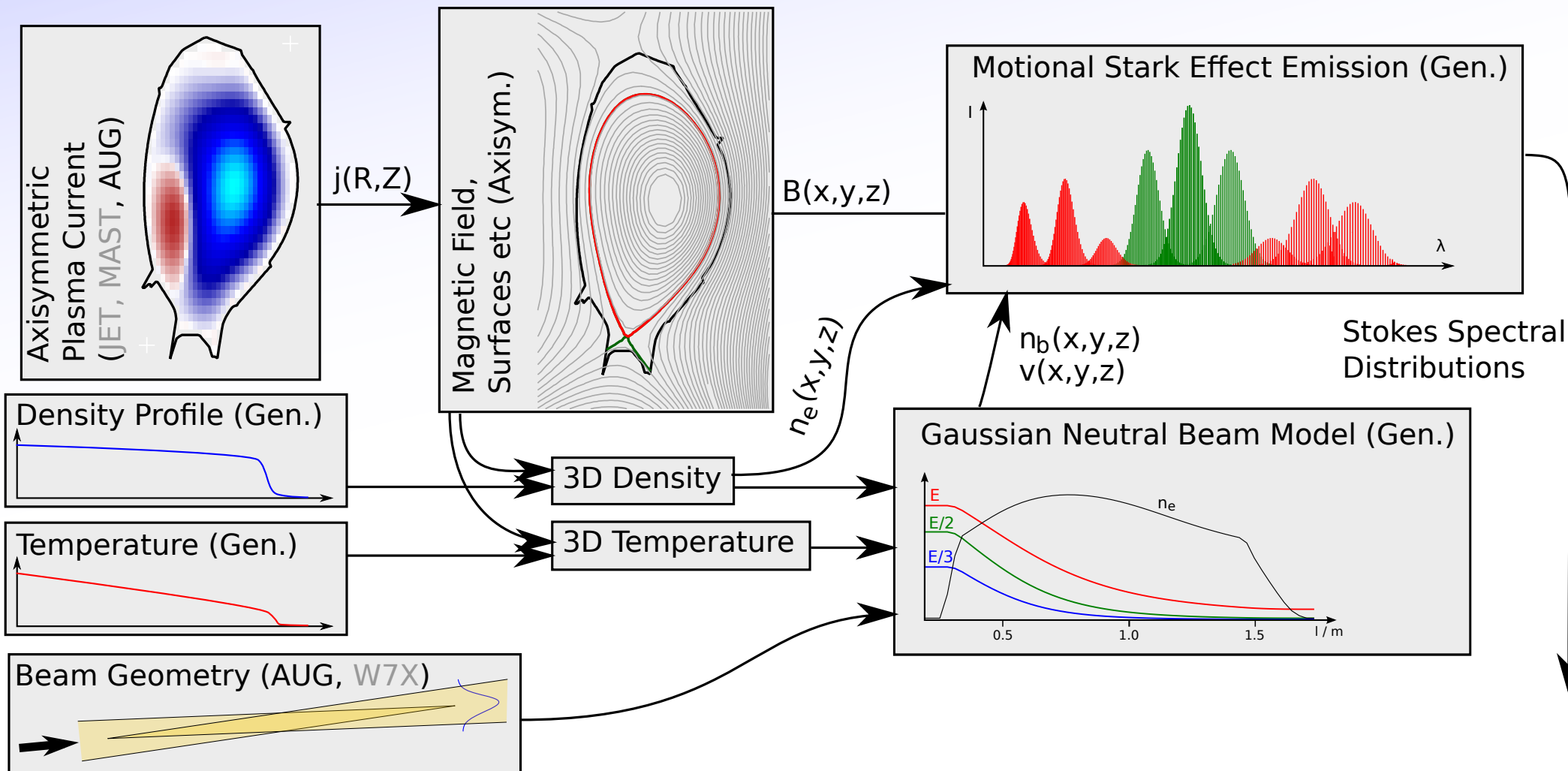
Developed several components for the Bayesian / forward modelling framework (Minerva).





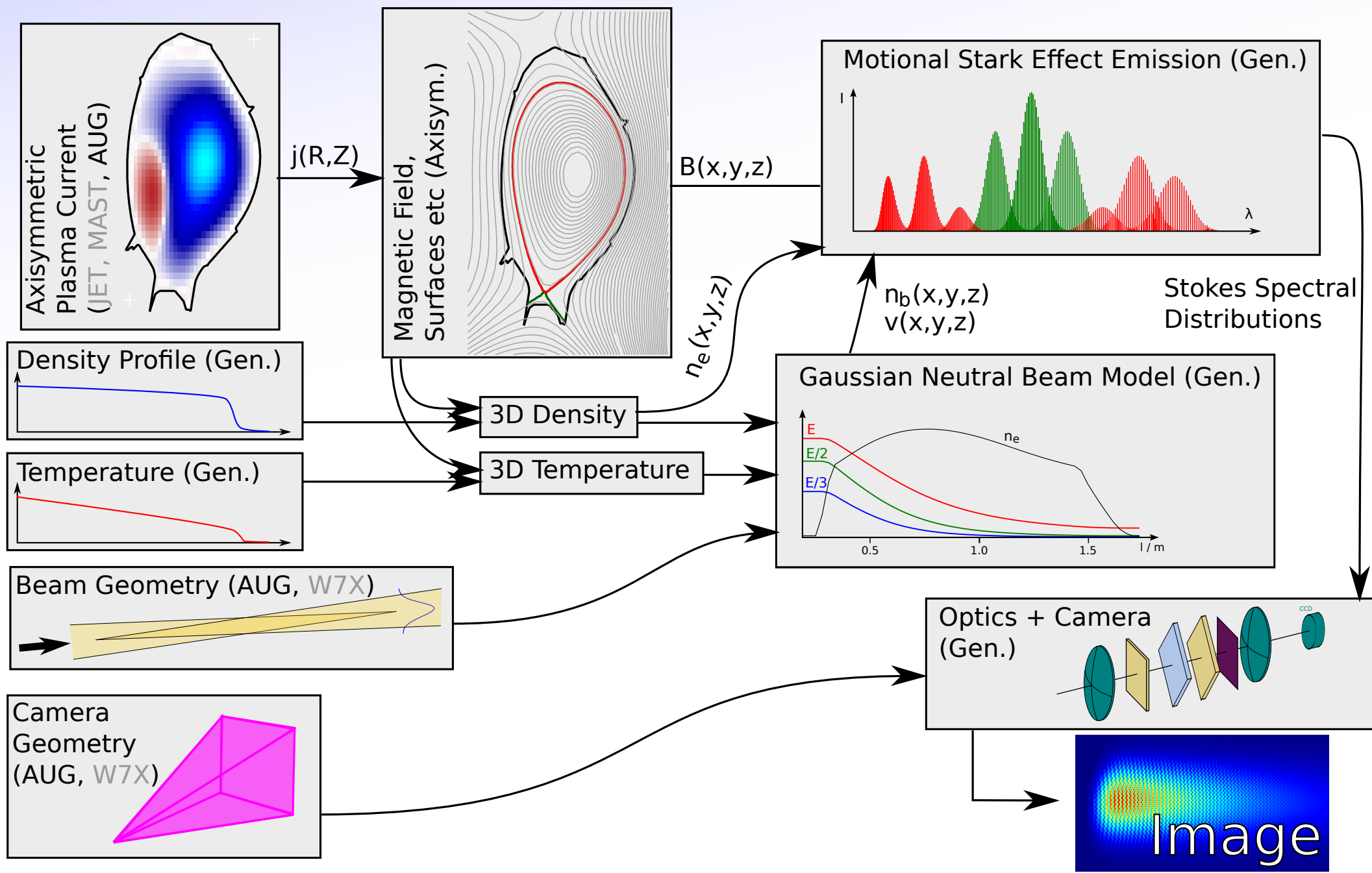
# Forward Model

Developed several components for the Bayesian / forward modelling framework (Minerva).



# Forward Model

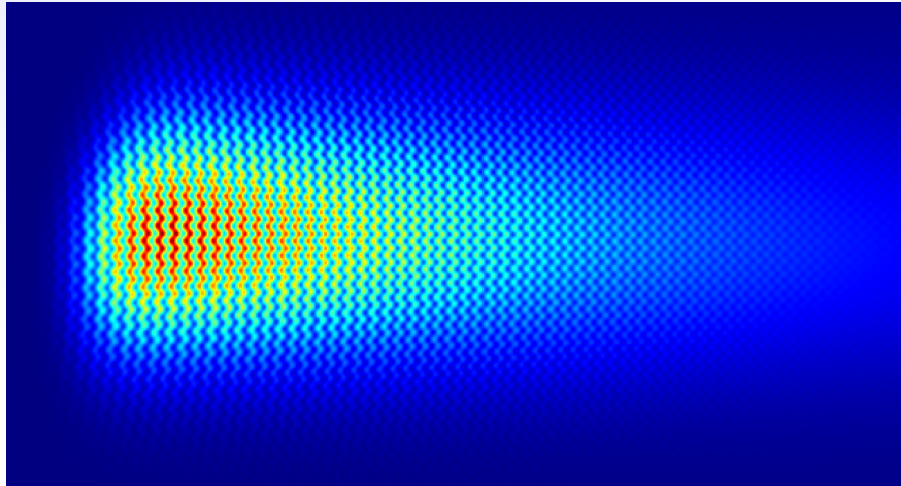
Developed several components for the Bayesian / forward modelling framework (Minerva).





# Savart Plates

(For the record: This is the 'Amplitude  
Modulated Double Spatial Hetrodyne' system).



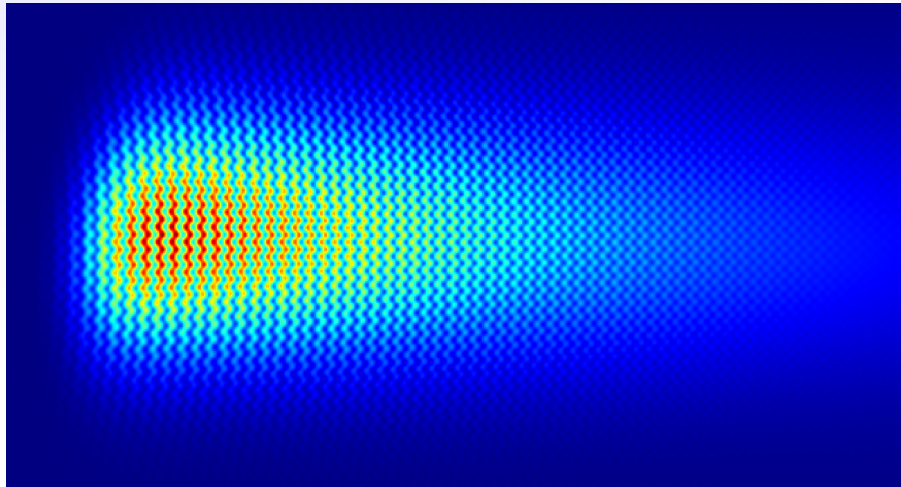
# Savart Plates

(For the record: This is the 'Amplitude Modulated Double Spatial Heterodyne' system).

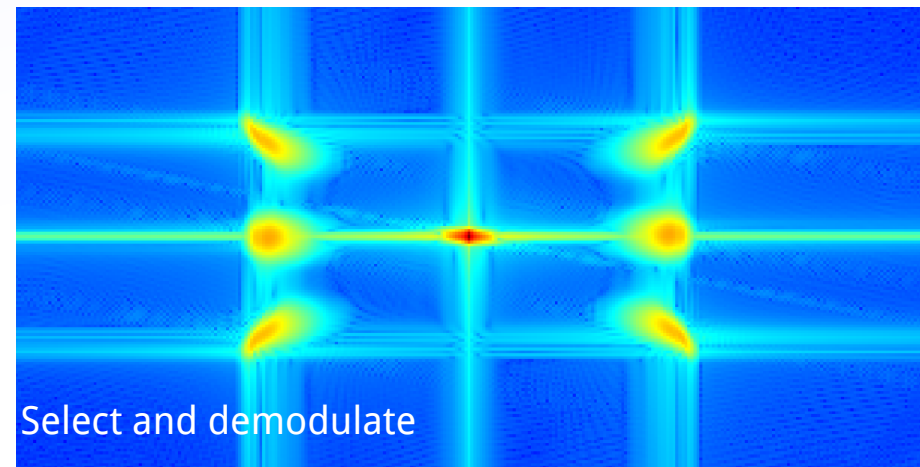
$$\frac{I}{I_0} = 1 + \zeta \cos 2\theta \cos(x) + \zeta \sin 2\theta \cos(x - y) - \zeta \sin 2\theta \cos(x + y)$$

Contrast

Polarisation Angle



FT  
→



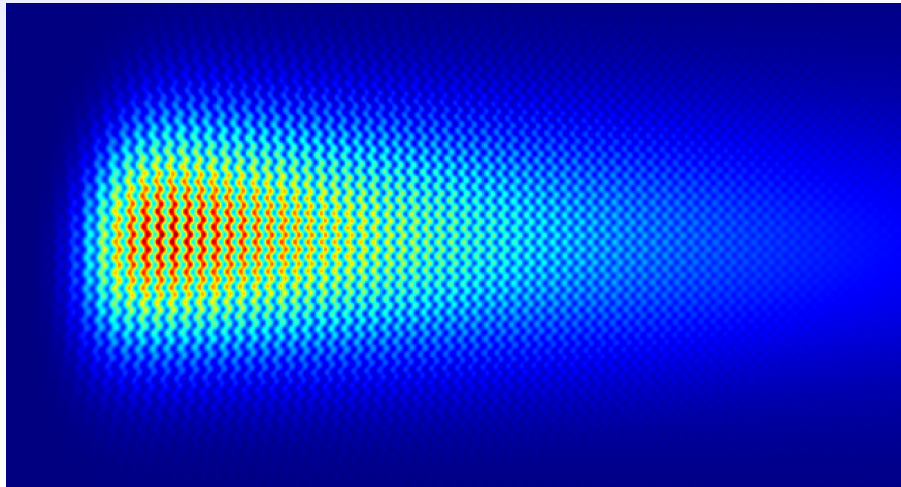
# Savart Plates

(For the record: This is the 'Amplitude Modulated Double Spatial Hetrodyne' system).

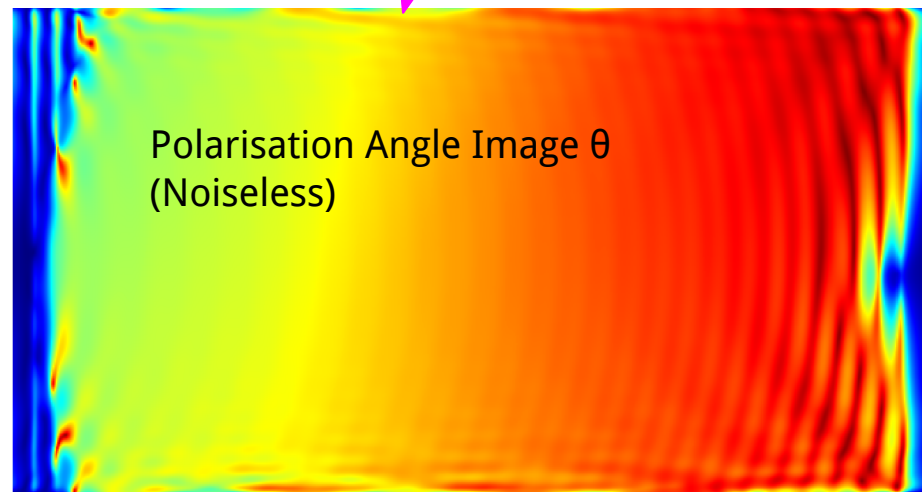
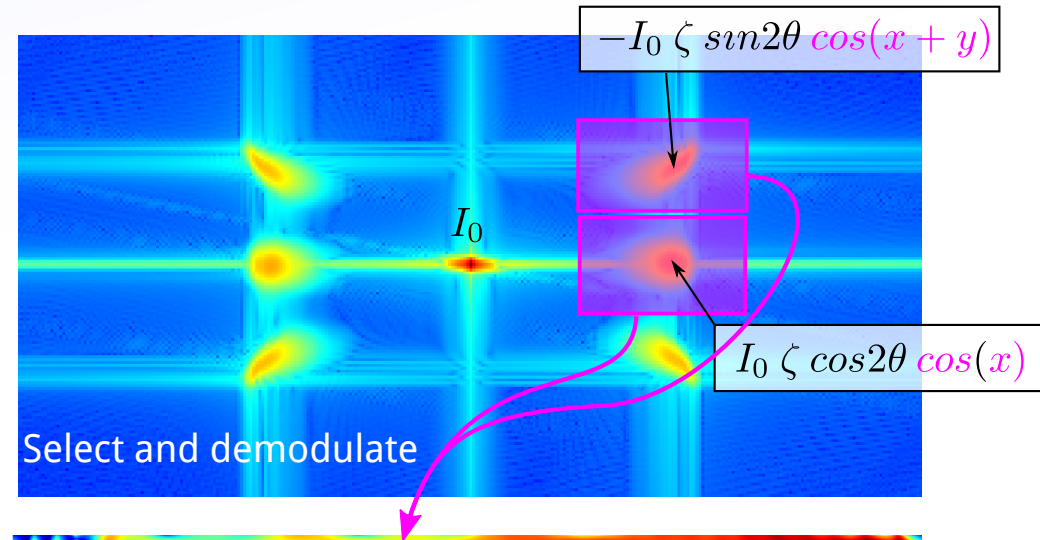
$$\frac{I}{I_0} = 1 + \zeta \cos 2\theta \cos(x) + \zeta \sin 2\theta \cos(x - y) - \zeta \sin 2\theta \cos(x + y)$$

Contrast

Polarisation Angle



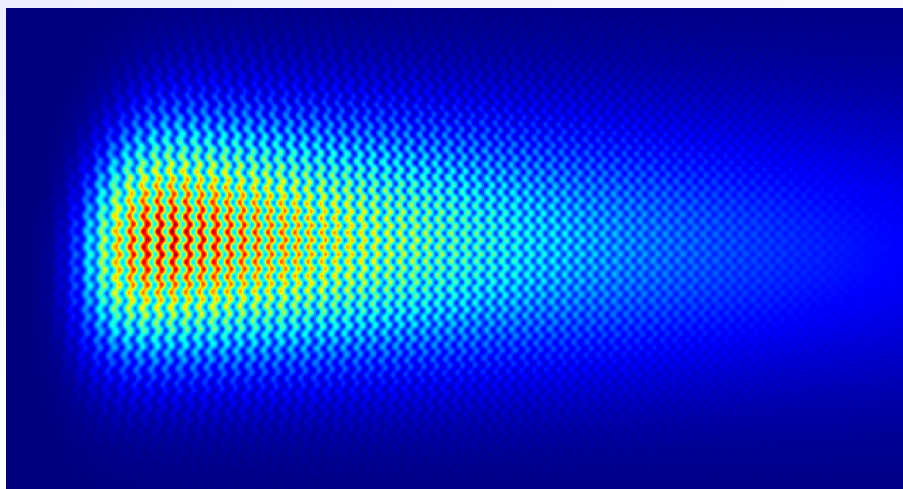
FT  
→



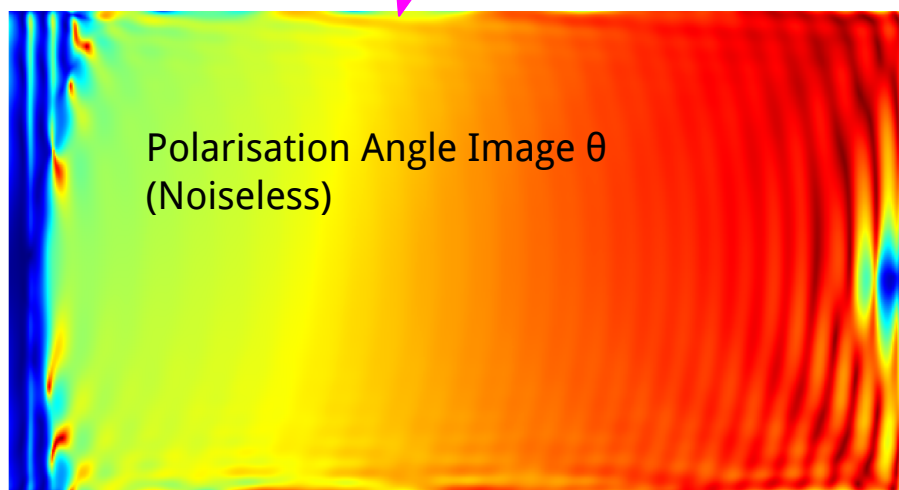
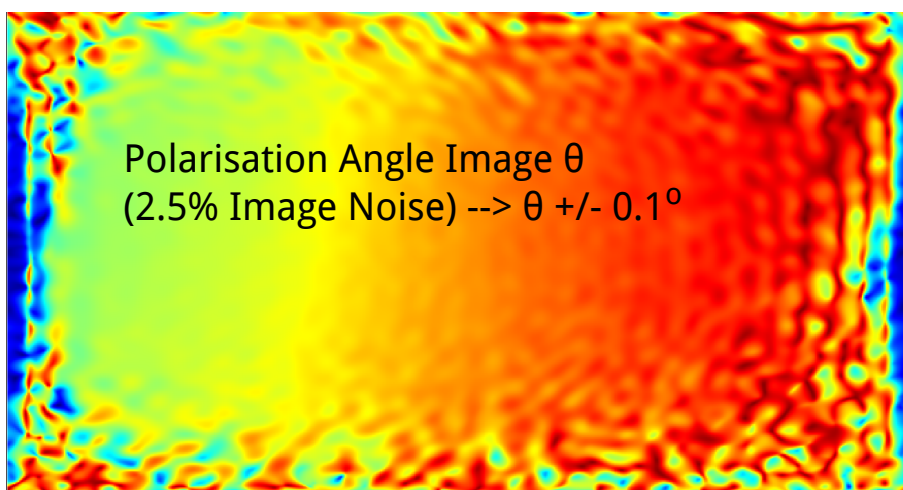
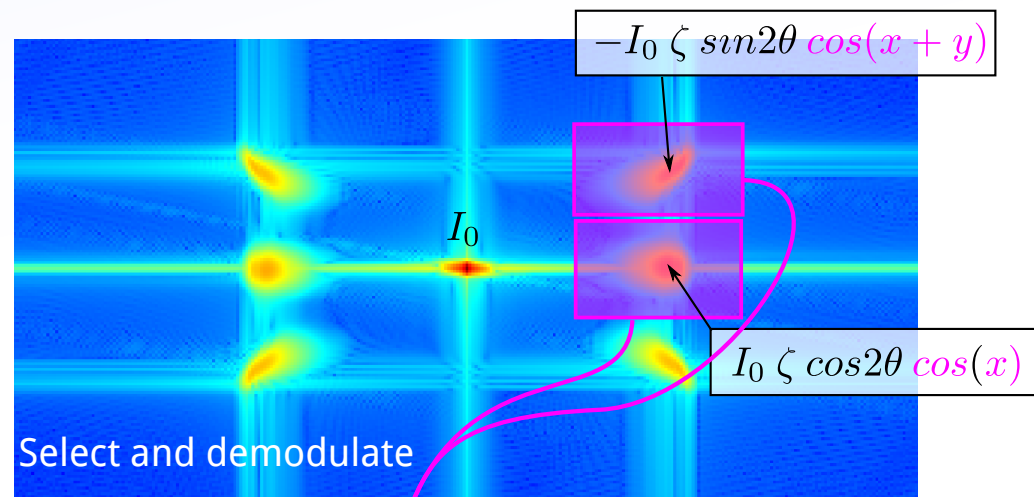
# Savart Plates

(For the record: This is the 'Amplitude Modulated Double Spatial Heterodyne' system).

$$\frac{I}{I_0} = 1 + \underbrace{\zeta}_{\text{Contrast}} \underbrace{\cos 2\theta}_{\text{Polarisation Angle}} \underbrace{\cos(x)}_{\phi?} + \zeta \sin 2\theta \cos(x - y) - \zeta \sin 2\theta \cos(x + y)$$



FT  
→



Demodulated  $\theta$  matches LOS average (with some extra phases).



# Recovery of plasma current - Axisymmetric

Final objective is plasma current -  $j(R, Z)$ .

Normally  $\theta$  used as a constraint for equilibrium.

With 2D measurements, can we calculate  $j$  without equilibrium?

Assuming toroidal symmetry:

$$-\mu_0 j_\phi = \frac{\partial B_z}{\partial R} + \frac{1}{R} \frac{\partial^2}{\partial Z^2} \int_0^R R' B_z(R', Z) dR'$$

Assume known  $B_\phi$  (vacuum field), calculate  $B_z$  from  $\theta$ .

$$\begin{aligned} \psi(R, Z) &= \int_0^R R' B_z(R', Z) dR' \\ -\mu_0 j_\phi &= \frac{\partial}{\partial R} \psi + \frac{1}{R} \frac{\partial^2 \psi}{\partial Z^2} \\ -\mu_0 j_\phi &= \frac{\partial \psi}{\partial R} + \frac{1}{R} \frac{\partial^2 \psi}{\partial Z^2} \\ -\mu_0 j_\phi &= \frac{\partial \psi}{\partial R} + \frac{1}{R} \frac{\partial^2 \psi}{\partial Z^2} \end{aligned}$$

# Recovery of plasma current - Axisymmetric

Final objective is plasma current -  $j(R, Z)$ .

Normally  $\theta$  used as a constraint for equilibrium.

With 2D measurements, can we calculate  $j$  without equilibrium?

Assuming toroidal symmetry:

$$-\mu_0 j_\phi = \frac{\partial B_z}{\partial R} + \frac{1}{R} \frac{\partial^2}{\partial Z^2} \int_0^R R' B_z(R', Z) dR'$$

Assume known  $B_\phi$  (vacuum field), calculate  $B_z$  from  $\theta$ .

We only see where the MSE emission is, so can only integrate from some  $R = R_0$ :

$$-\mu_0 j_\phi = \left( \frac{\partial B_z}{\partial R} \right) + \frac{1}{R} \frac{\partial^2 \psi(R_0, Z)}{\partial Z^2} + \frac{1}{R} \frac{\partial^2}{\partial Z^2} \int_{R_0}^R R' B_z(R', Z) dR'$$

This we have  
with 1D MSE.





# Recovery of plasma current - Axisymmetric

Final objective is plasma current -  $j(R, Z)$ .

Normally  $\theta$  used as a constraint for equilibrium.

With 2D measurements, can we calculate  $j$  without equilibrium?

Assuming toroidal symmetry:

$$-\mu_0 j_\phi = \frac{\partial B_z}{\partial R} + \frac{1}{R} \frac{\partial^2}{\partial Z^2} \int_0^R R' B_z(R', Z) dR'$$

Assume known  $B_\phi$  (vacuum field), calculate  $B_z$  from  $\theta$ .

We only see where the MSE emission is, so can only integrate from some  $R = R_0$ :

$$-\mu_0 j_\phi = \left( \frac{\partial B_z}{\partial R} \right) + \left( \frac{1}{R} \frac{\partial^2 \psi(R_0, Z)}{\partial Z^2} \right) + \frac{1}{R} \frac{\partial^2}{\partial Z^2} \int_{R_0}^R R' B_z(R', Z) dR'$$

This we have with 1D MSE.

Function of Z that we still cannot know.

$$\begin{aligned} \psi(R, Z) &= \int_0^R R' B_z(R', Z) dR' \\ -\mu_0 j_\phi &= \frac{\partial}{\partial R} \int_0^R R' B_z(R', Z) dR' + \frac{1}{R} \frac{\partial^2}{\partial Z^2} \int_0^R R' B_z(R', Z) dR' \\ -\mu_0 j_\phi &= \frac{\partial B_z}{\partial R} + \frac{1}{R} \frac{\partial^2}{\partial Z^2} \int_0^R R' B_z(R', Z) dR' \\ -\mu_0 j_\phi &= \frac{\partial B_z}{\partial R} + \frac{1}{R} \frac{\partial^2 \psi(R_0, Z)}{\partial Z^2} + \frac{1}{R} \frac{\partial^2}{\partial Z^2} \int_{R_0}^R R' B_z(R', Z) dR' \end{aligned}$$

# Recovery of plasma current - Axisymmetric

Final objective is plasma current -  $j(R, Z)$ .

Normally  $\theta$  used as a constraint for equilibrium.

With 2D measurements, can we calculate  $j$  without equilibrium?

Assuming toroidal symmetry:

$$-\mu_0 j_\phi = \frac{\partial B_z}{\partial R} + \frac{1}{R} \frac{\partial^2}{\partial Z^2} \int_0^R R' B_z(R', Z) dR'$$

Assume known  $B_\phi$  (vacuum field), calculate  $B_z$  from  $\theta$ .

We only see where the MSE emission is, so can only integrate from some  $R = R_0$ :

$$-\mu_0 j_\phi = \underbrace{\frac{\partial B_z}{\partial R}}_{\text{This we have with 1D MSE.}} + \underbrace{\frac{1}{R} \frac{\partial^2 \psi(R_0, Z)}{\partial Z^2}}_{\text{Function of Z that we still cannot know.}} + \underbrace{\frac{1}{R} \frac{\partial^2}{\partial Z^2} \int_{R_0}^R R' B_z(R', Z) dR'}_{\text{The new term gives localisation of current in Z (~via curvature of field).}}$$

~10% of  $j_\phi$  and measurement too noisy.

No: It still cannot be directly calculated.

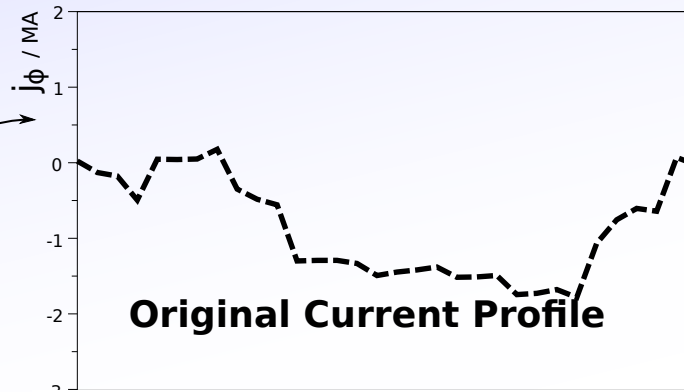
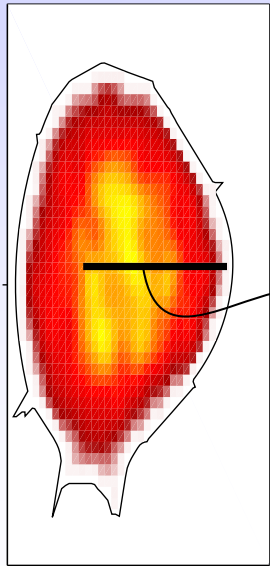
However, we gain  $dB_z/dR$  at different Zs.

Complex tomography problem, but we may not need equilibrium...

$$\begin{aligned} \psi(R, Z) &= \int_0^R R' B_z(R', Z) dR' \\ -\mu_0 j_\phi &= \frac{\partial}{\partial R} \int_0^R R' B_z(R', Z) dR' + \frac{1}{R} \frac{\partial^2}{\partial Z^2} \int_0^R R' B_z(R', Z) dR' \\ -\mu_0 j_\phi &= \frac{\partial B_z}{\partial R} + \frac{1}{R} \frac{\partial^2}{\partial Z^2} \int_0^R R' B_z(R', Z) dR' \\ -\mu_0 j_\phi &= \frac{\partial B_z}{\partial R} + \frac{1}{R} \frac{\partial^2}{\partial Z^2} \psi(R, Z) + \frac{1}{R} \frac{\partial^2}{\partial Z^2} \int_{R_0}^R R' B_z(R', Z) dR' \end{aligned}$$

## By current tomography...

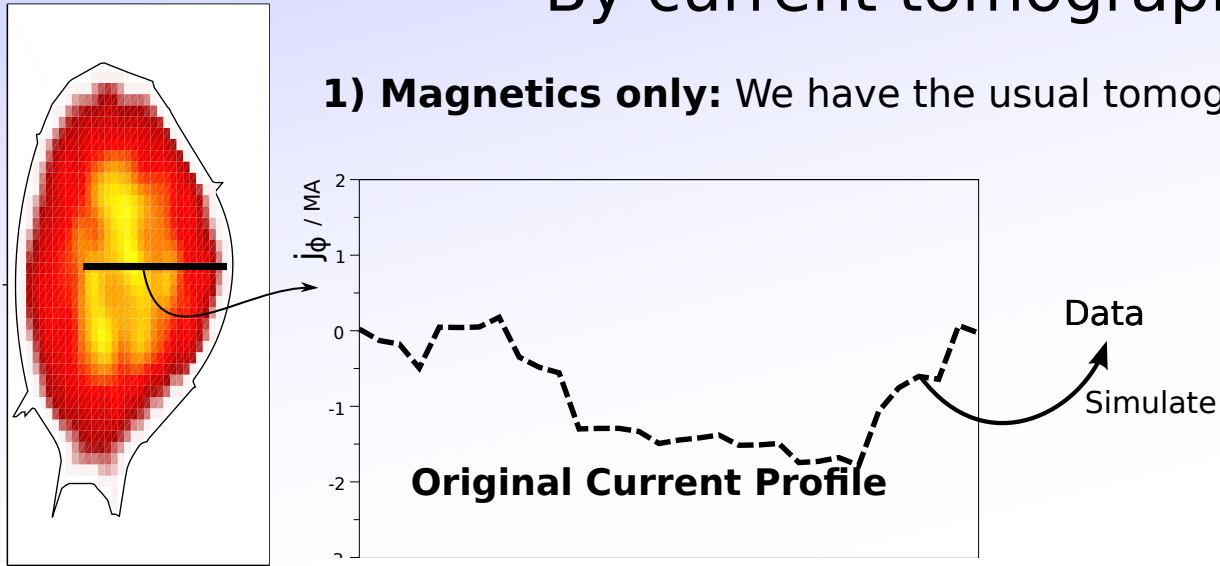
**1) Magnetics only:** We have the usual tomography situation:



Each case has 900 measurements at  $\sigma = 10mT$ . So difference is only in the **type** of information.

## By current tomography...

**1) Magnetics only:** We have the usual tomography situation:

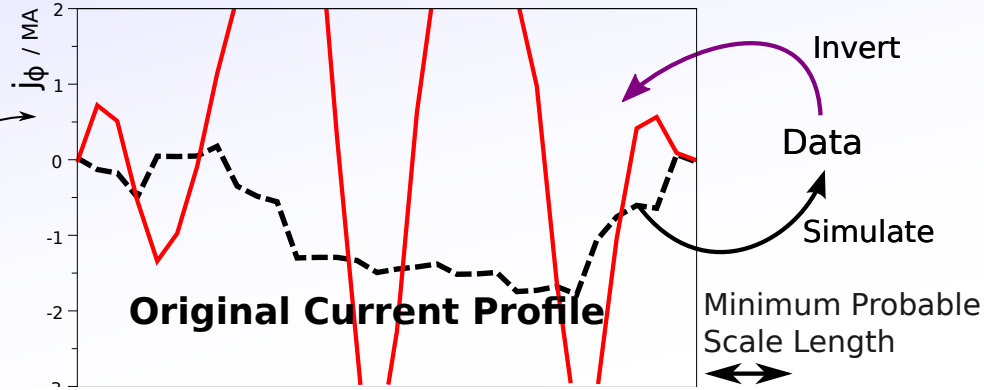
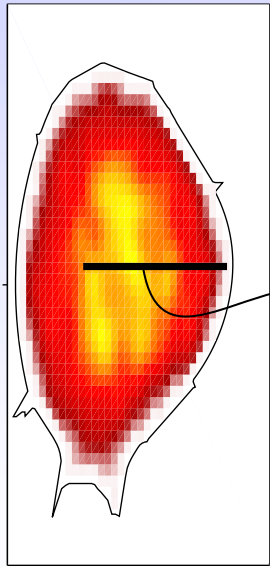


Each case has 900 measurements at  $\sigma = 10\text{mT}$ . So difference is only in the **type** of information.

# By current tomography...

**1) Magnetics only:** We have the usual tomography situation:

**P(J | D): Possible current profiles given data**



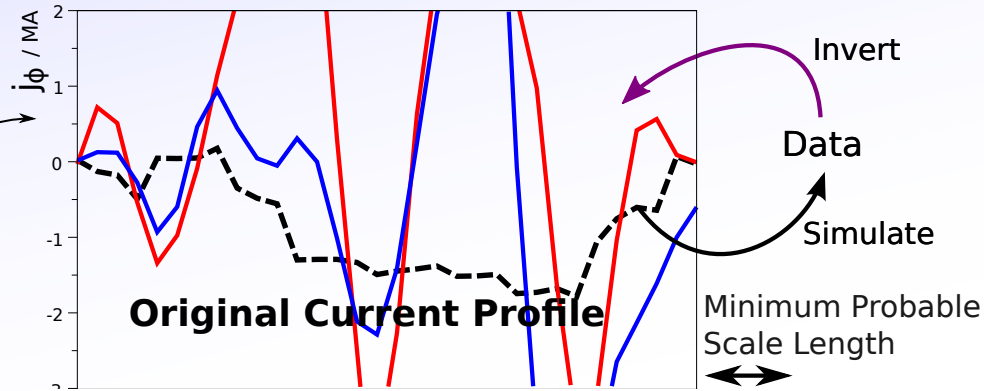
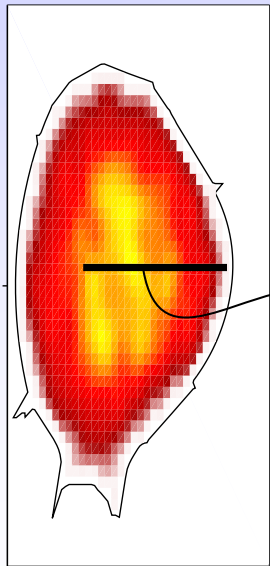
Only weak short scale length  
prior/regularisation.

Each case has 900 measurements at  $\sigma = 10mT$ . So difference is only in the **type** of information.

# By current tomography...

**1) Magnetics only:** We have the usual tomography situation:

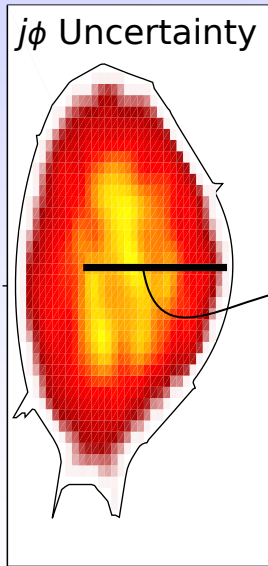
**P(J | D): Possible current profiles given data**



Only weak short scale length  
prior/regularisation.

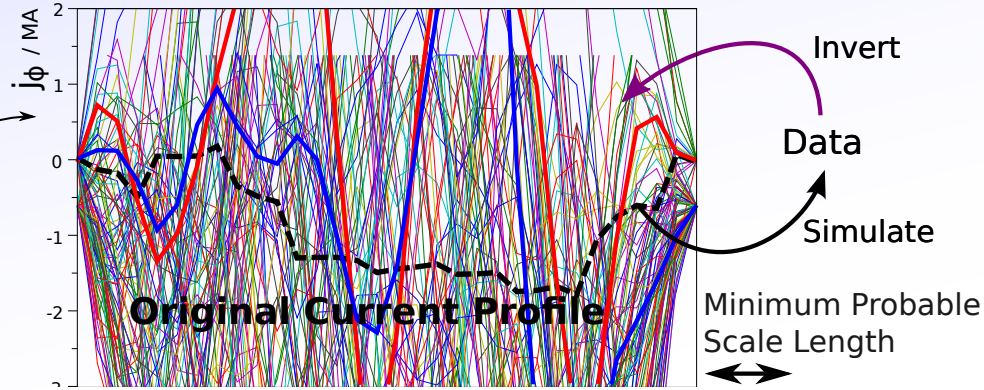
Each case has 900 measurements at  $\sigma = 10mT$ . So difference is only in the **type** of information.

# By current tomography...



**1) Magnetics only:** We have the usual tomography situation:

**P(J | D): Possible current profiles given data**



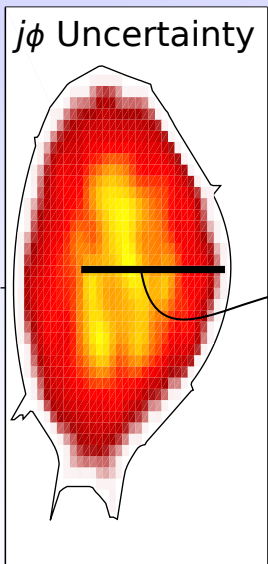
Only weak short scale length prior/regularisation.



(Almost) infinite uncertainty  
(but B and flux still good)

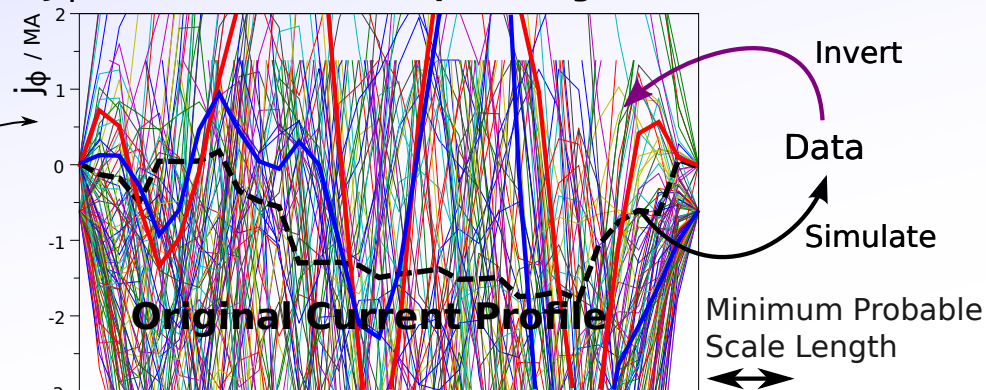
Each case has 900 measurements at  $\sigma = 10mT$ . So difference is only in the **type** of information.

# By current tomography...



**1) Magnetics only:** We have the usual tomography situation:

**P(J | D): Possible current profiles given data**



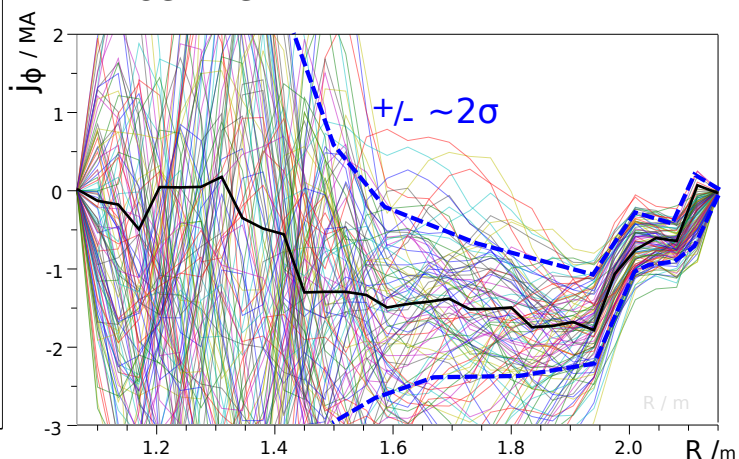
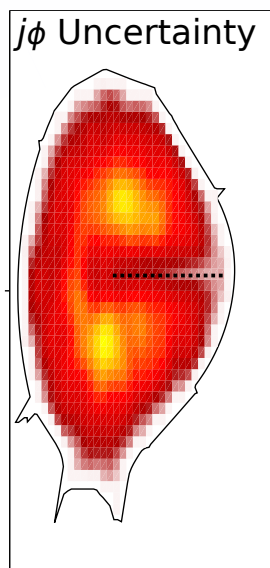
Only weak short scale length prior/regularisation.



(Almost) infinite uncertainty  
(but B and flux still good)

**2) +Normal MSE system:**

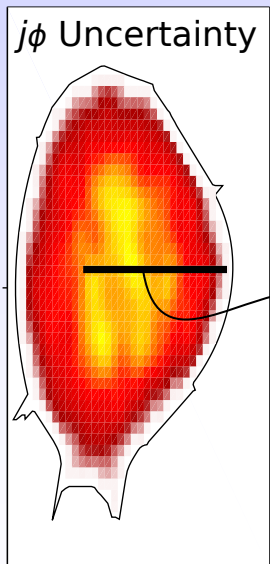
30 x  $B_z$  at 30 positions along NBI centre.



Each case has 900 measurements at  $\sigma = 10mT$ . So difference is only in the **type** of information.

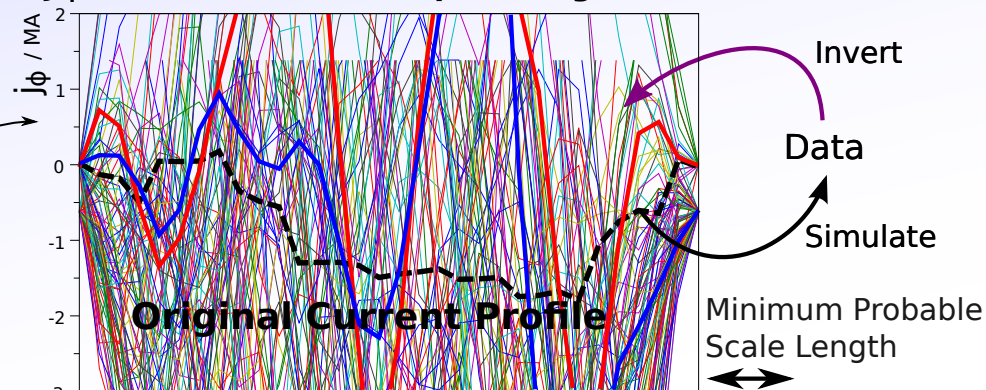


# By current tomography...



**1) Magnetics only:** We have the usual tomography situation:

**P(J | D): Possible current profiles given data**



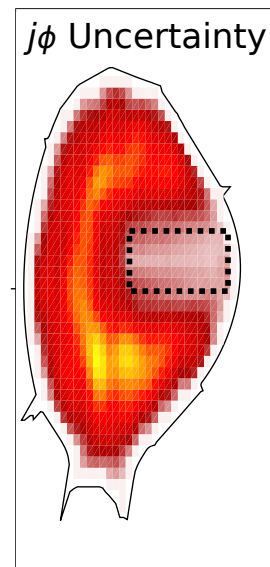
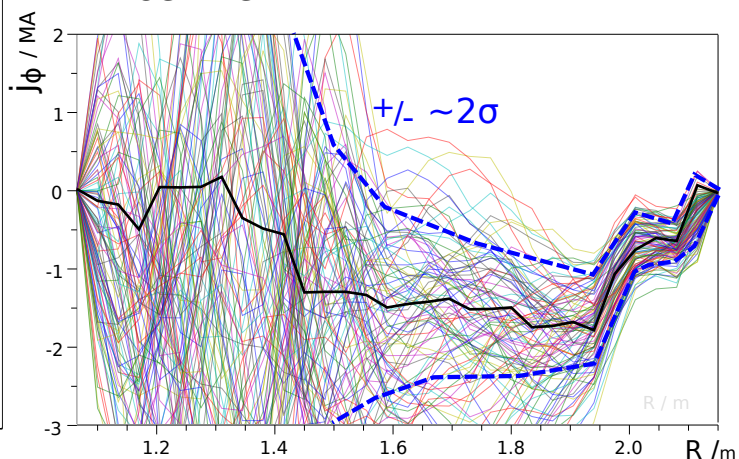
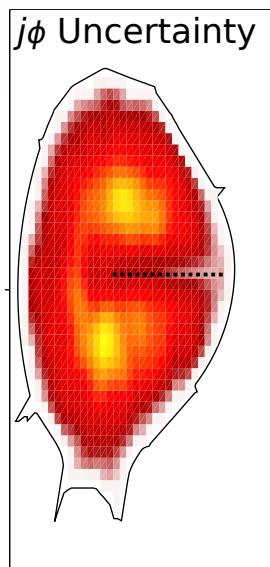
Only weak short scale length prior/regularisation.



(Almost) infinite uncertainty  
(but B and flux still good)

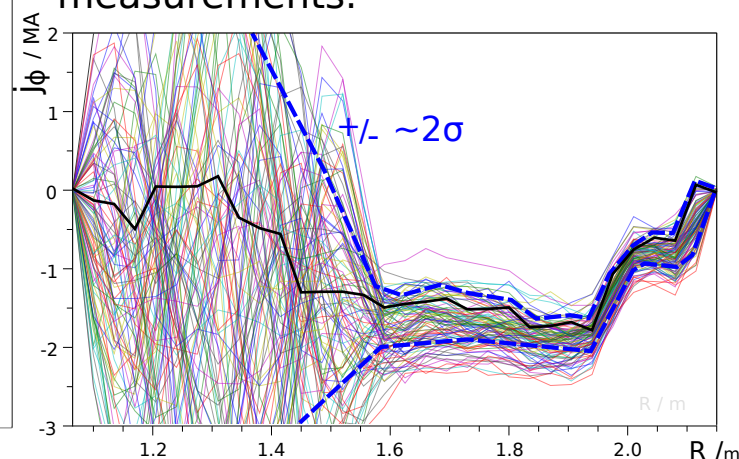
**2) +Normal MSE system:**

30 x  $B_z$  at 30 positions along NBI centre.



**3) +1IMSE System:**

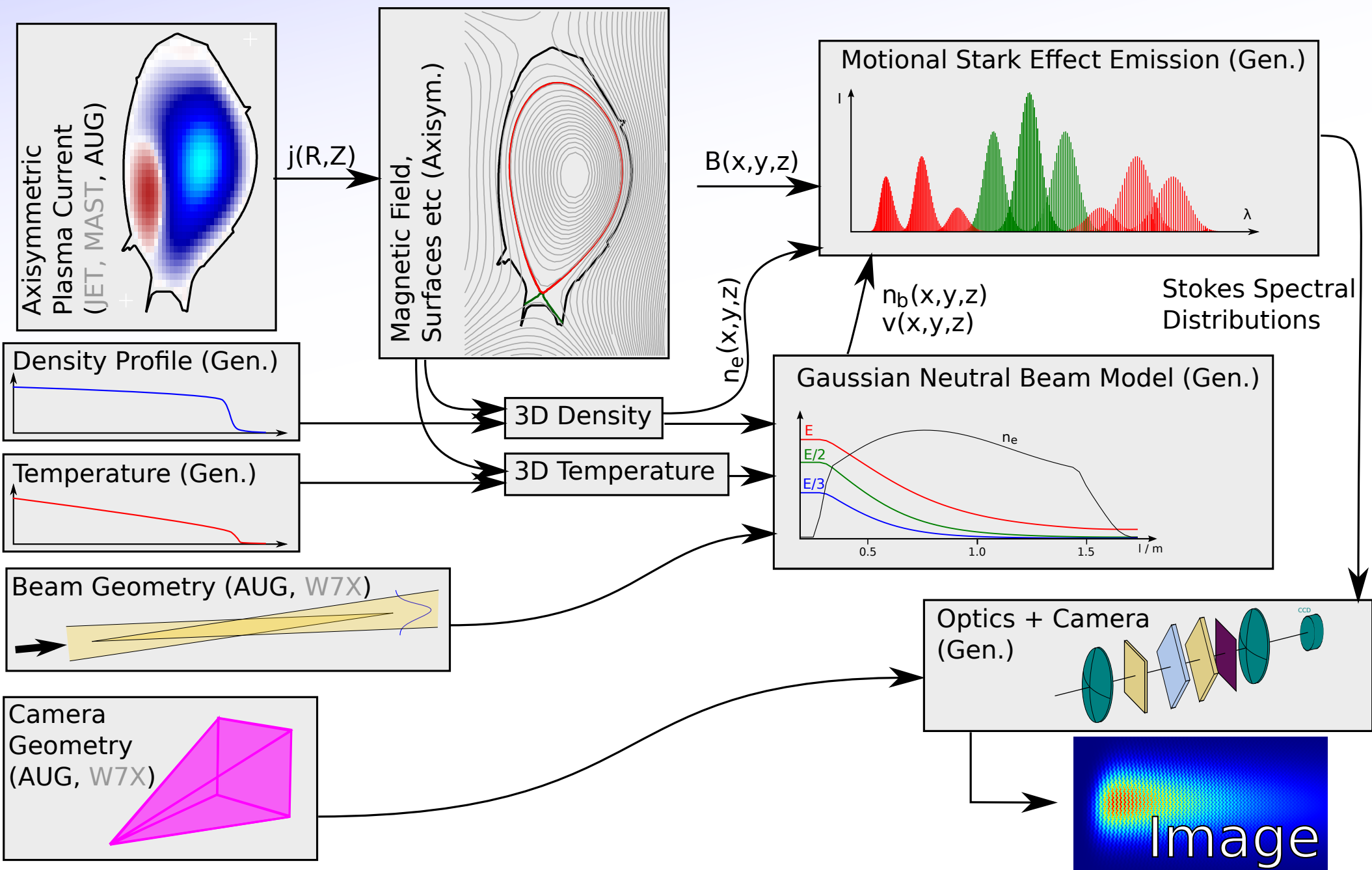
30x30 grid of  $B_z$  measurements.



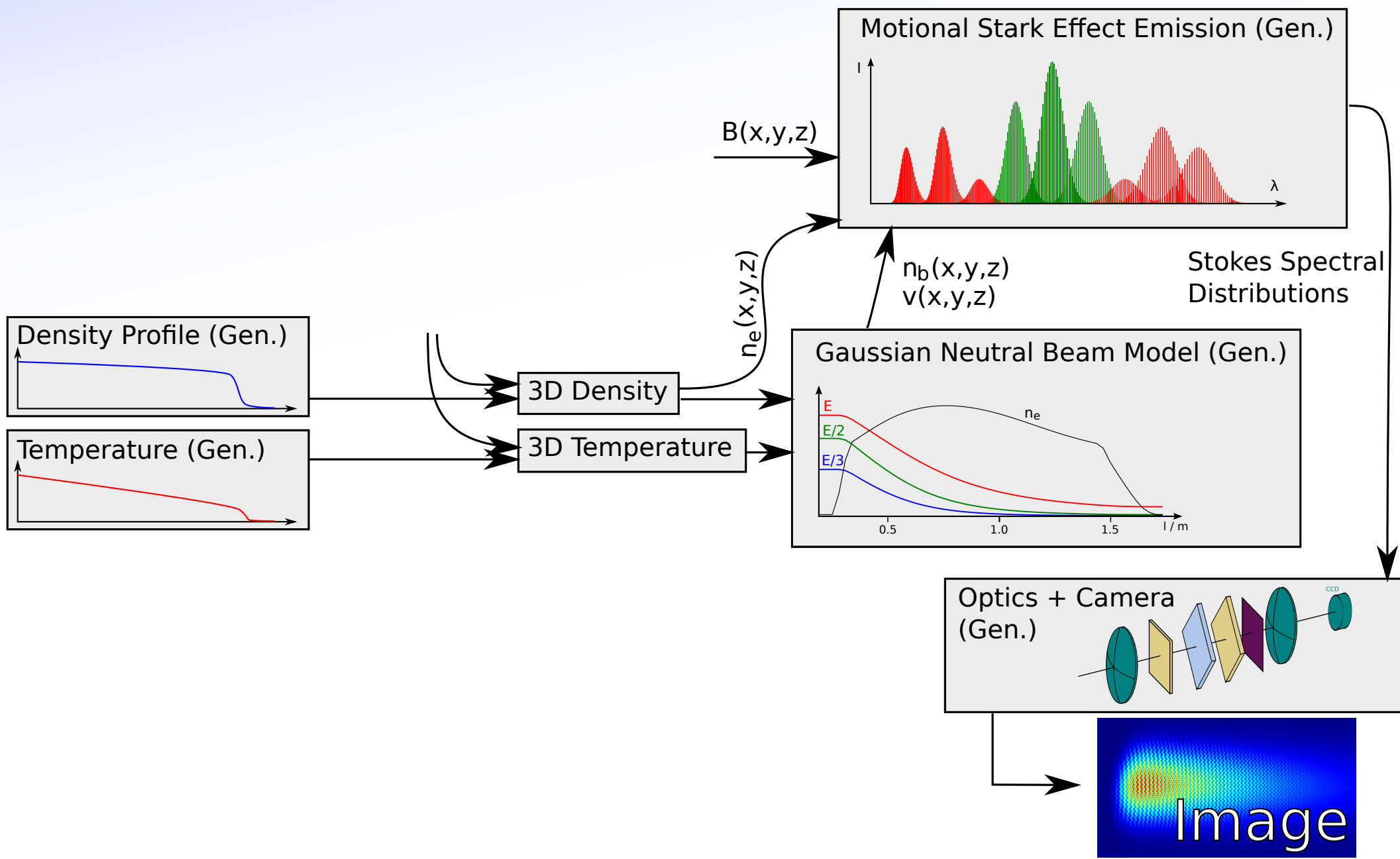
Each case has 900 measurements at  $\sigma = 10mT$ . So difference is only in the **type** of information.

**Conclusion:** 2D information greatly improves current inference ability, even *excluding* increase in data quantity.

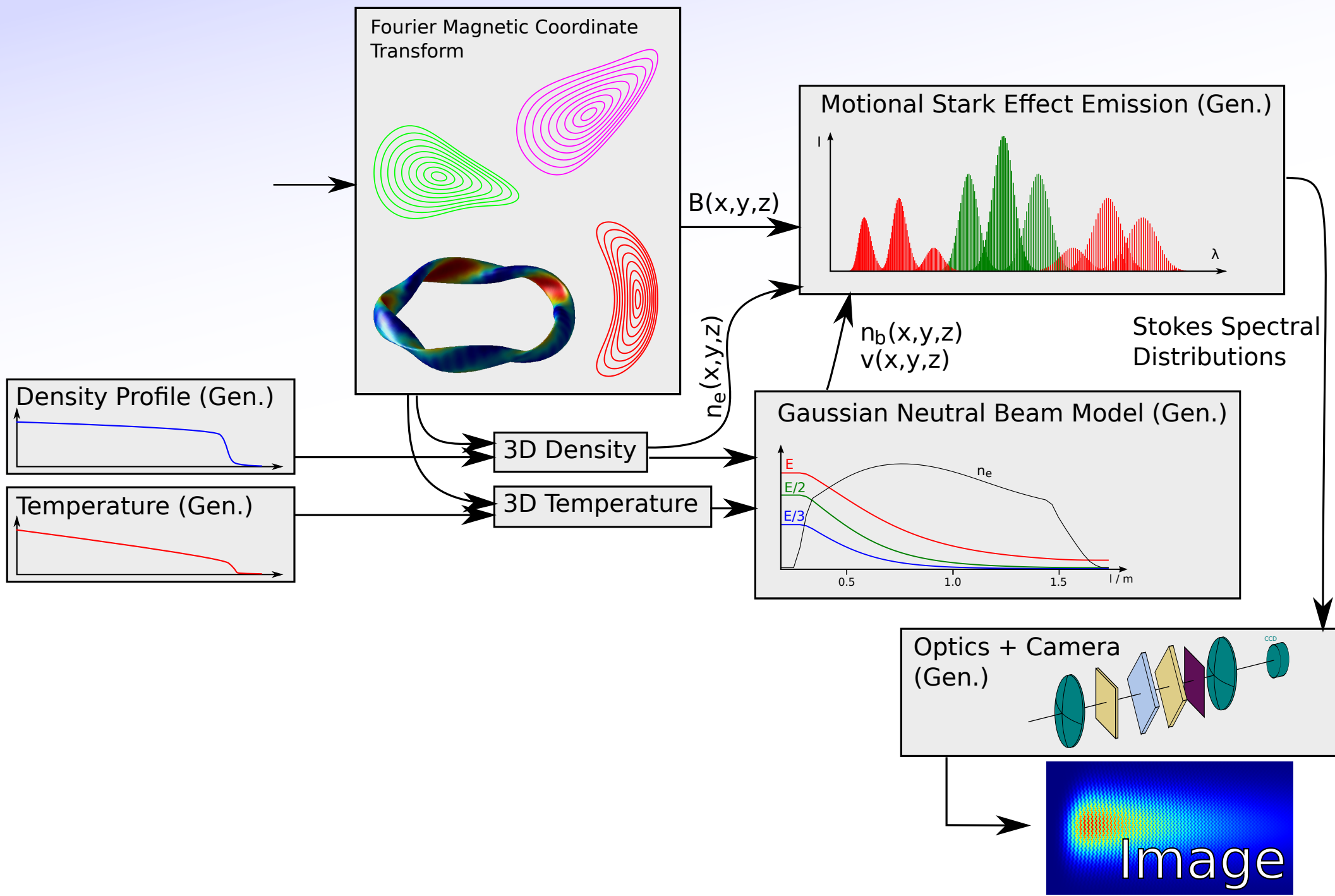
# Forward Model (W7X)



# Forward Model (W7X)

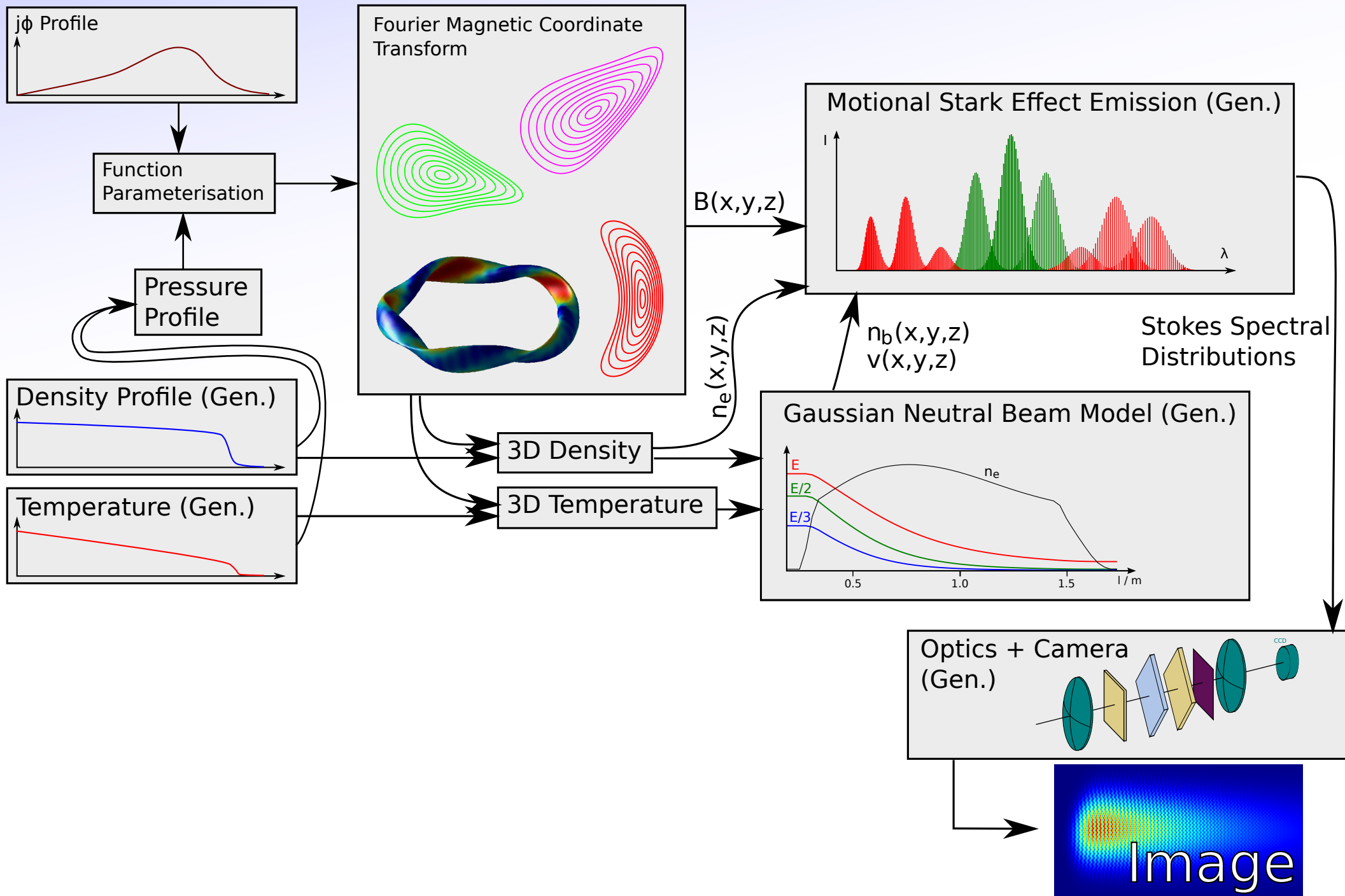


# Forward Model (W7X)

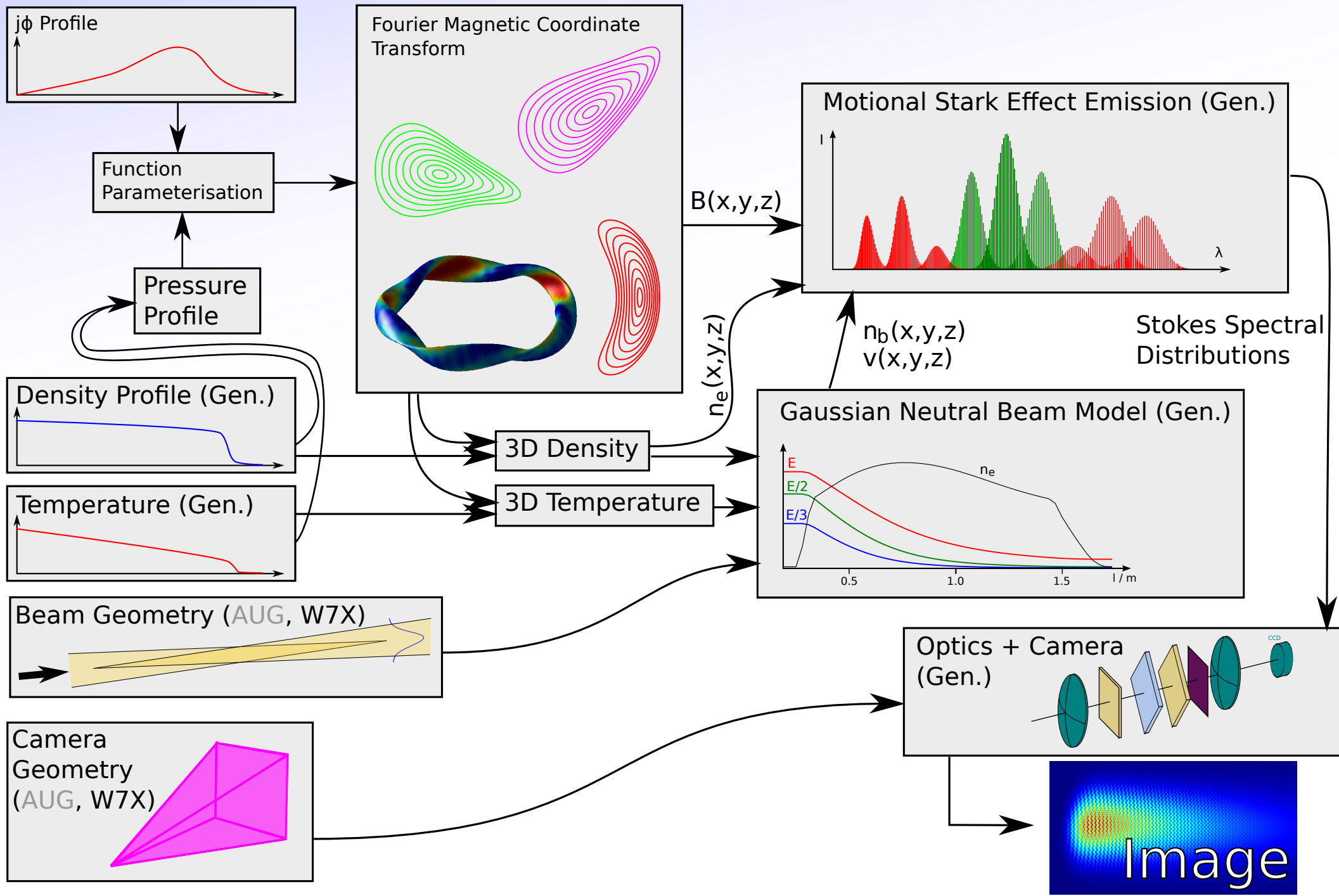




# Forward Model (W7X)



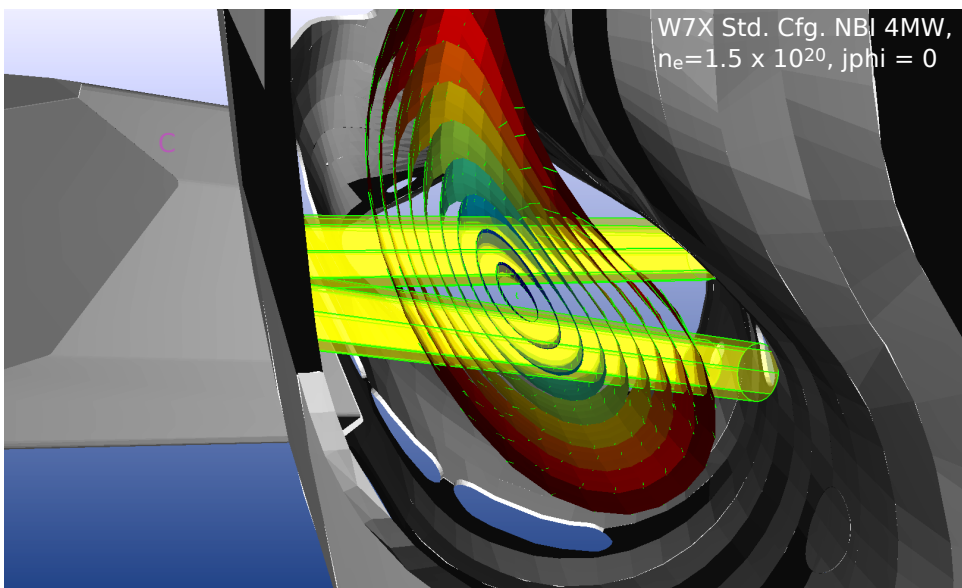
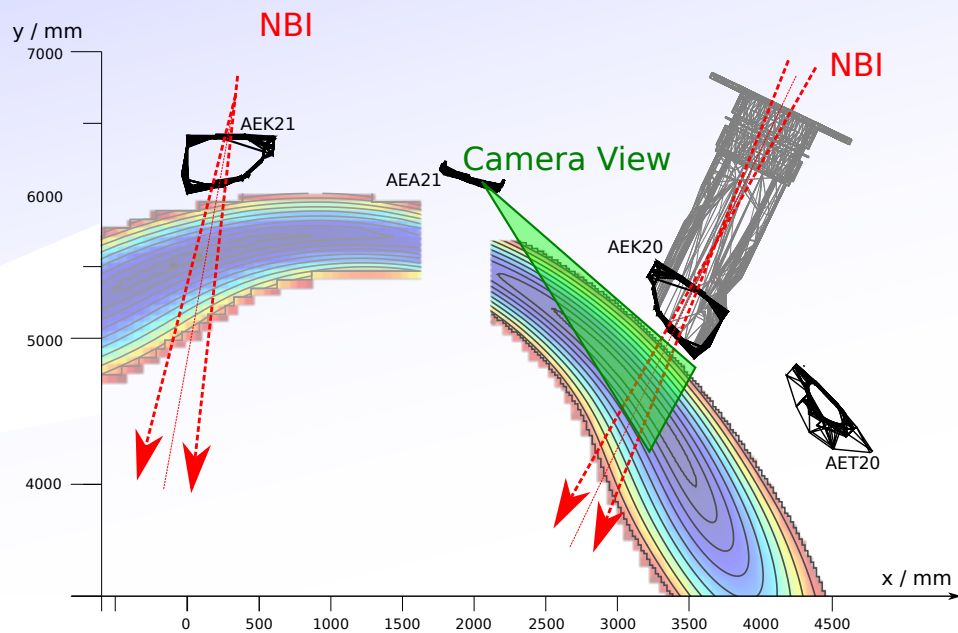
# Forward Model (W7X)



# Geometry (W7X)

Best view of NBI to reduce cross-surface integration.

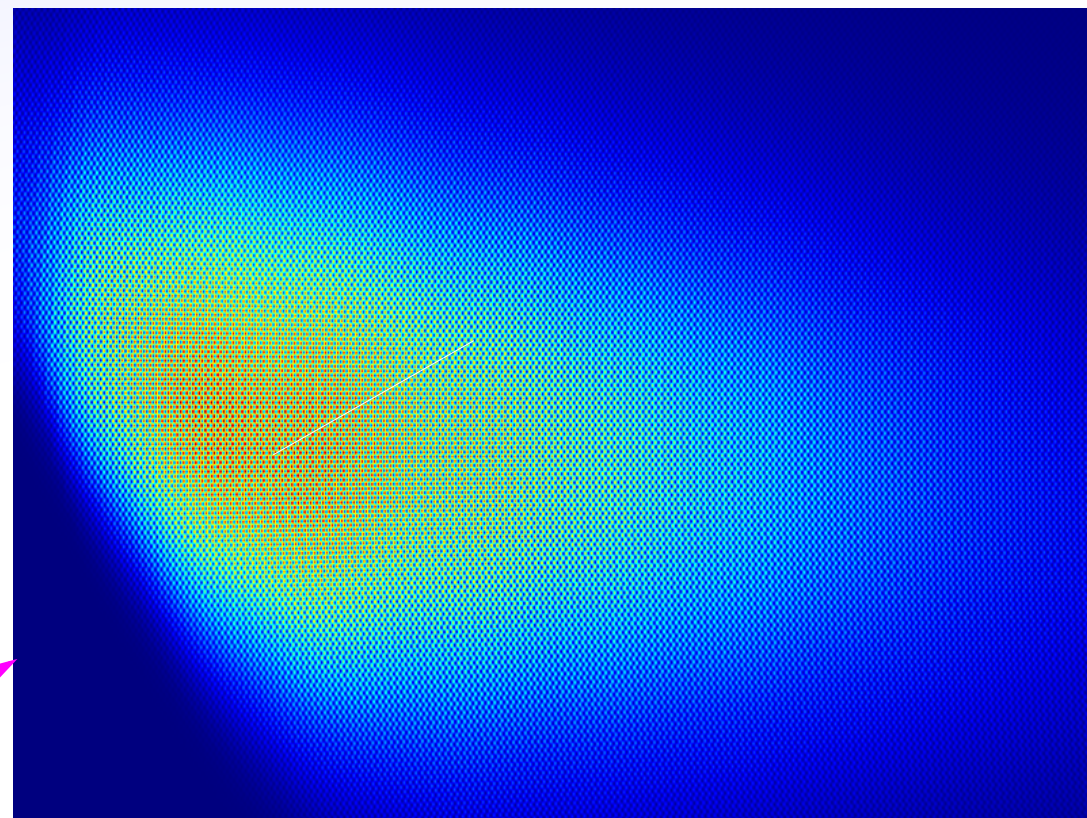
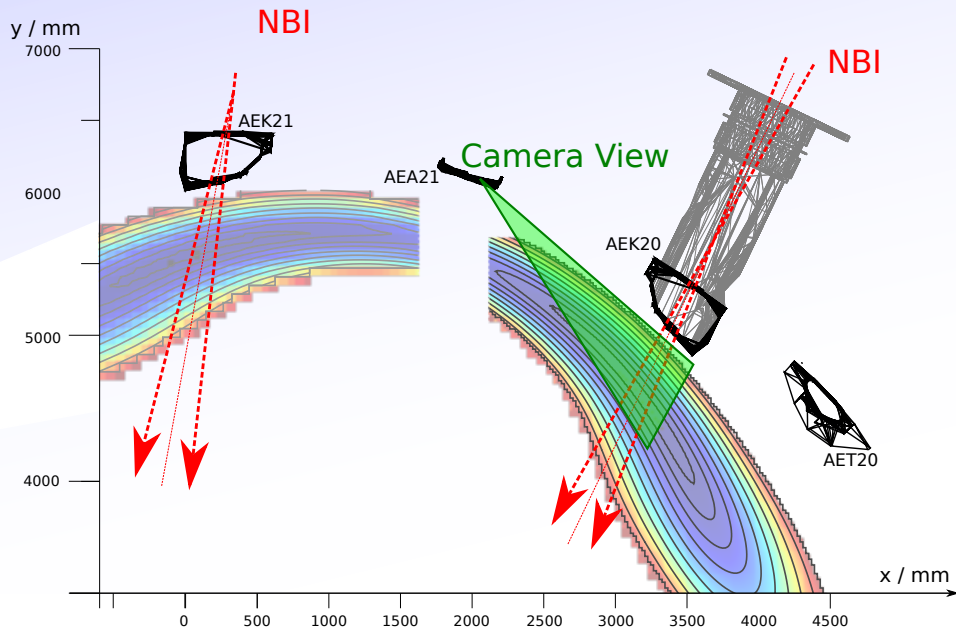
More tangential lower beam gives best Doppler shift --> Better image fringe contrast.



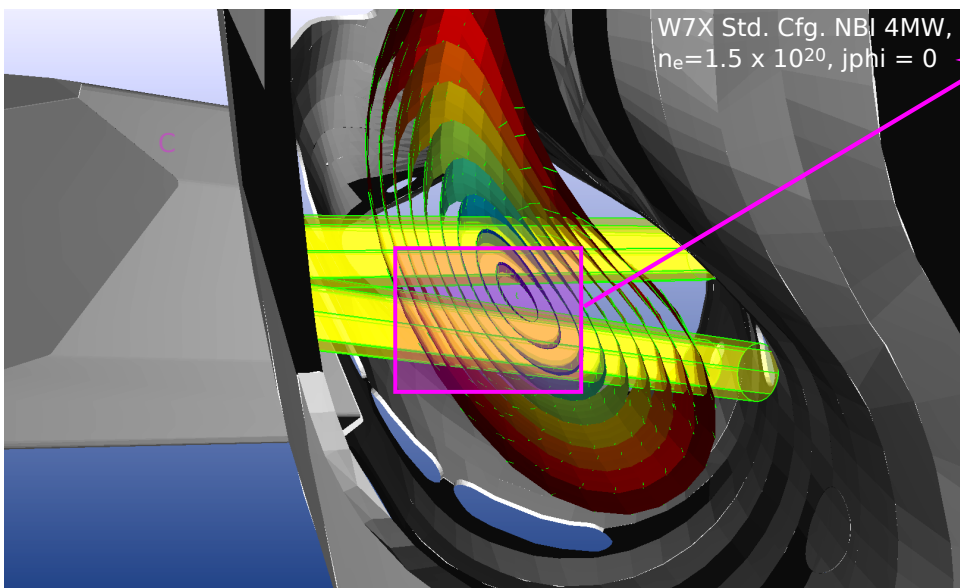
# Geometry (W7X)

Best view of NBI to reduce cross-surface integration.

More tangential lower beam gives best Doppler shift --> Better image fringe contrast.



0 Image intensity.

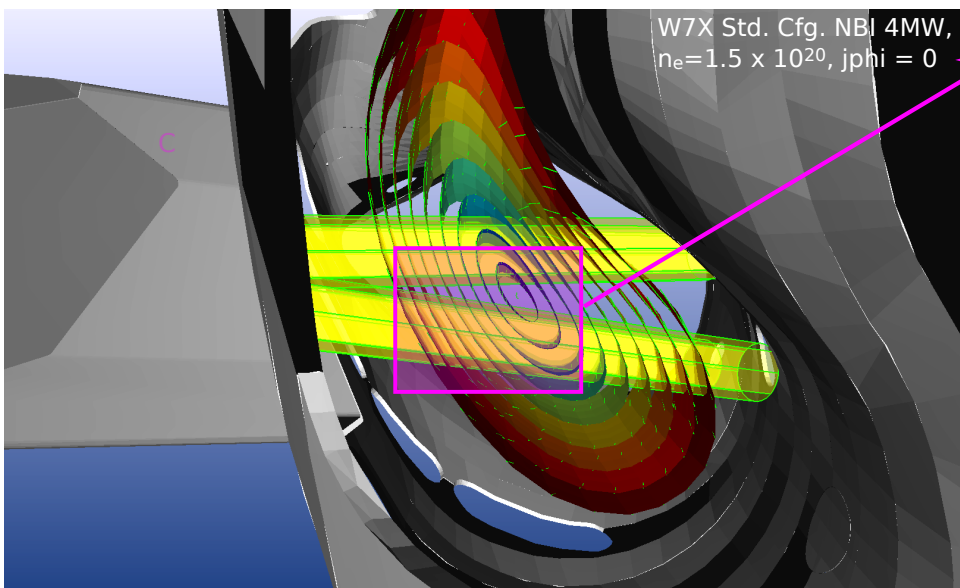
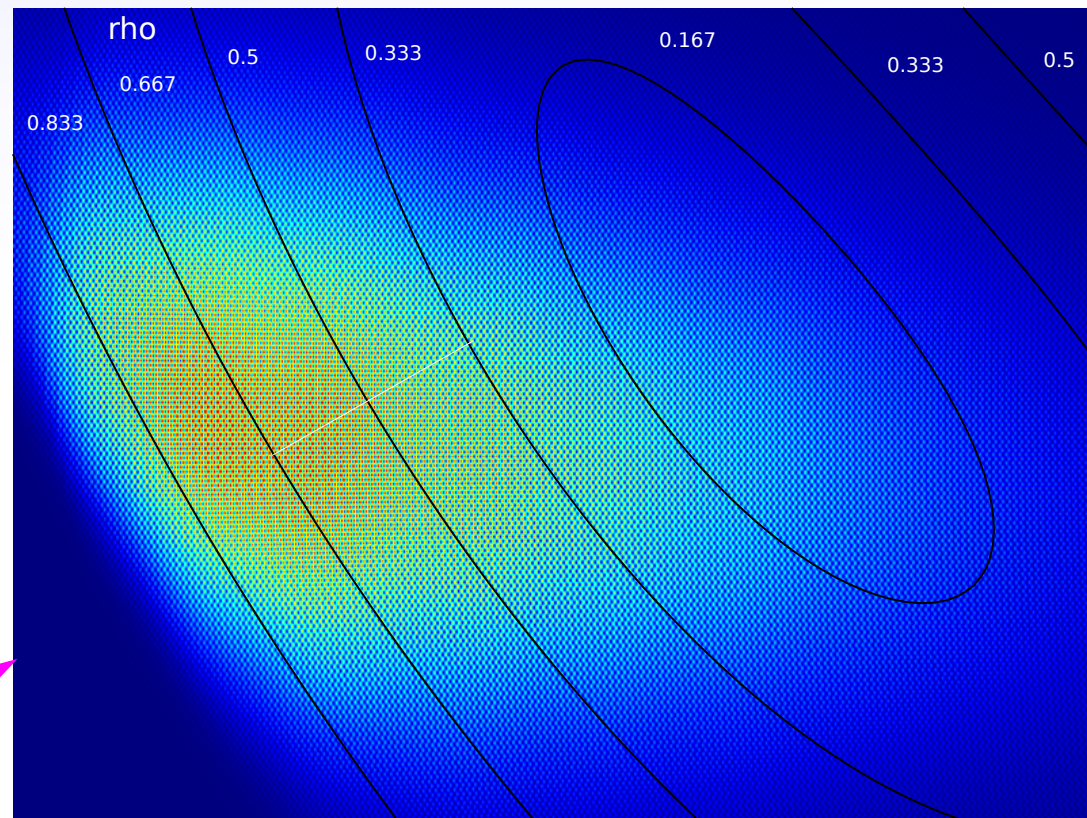
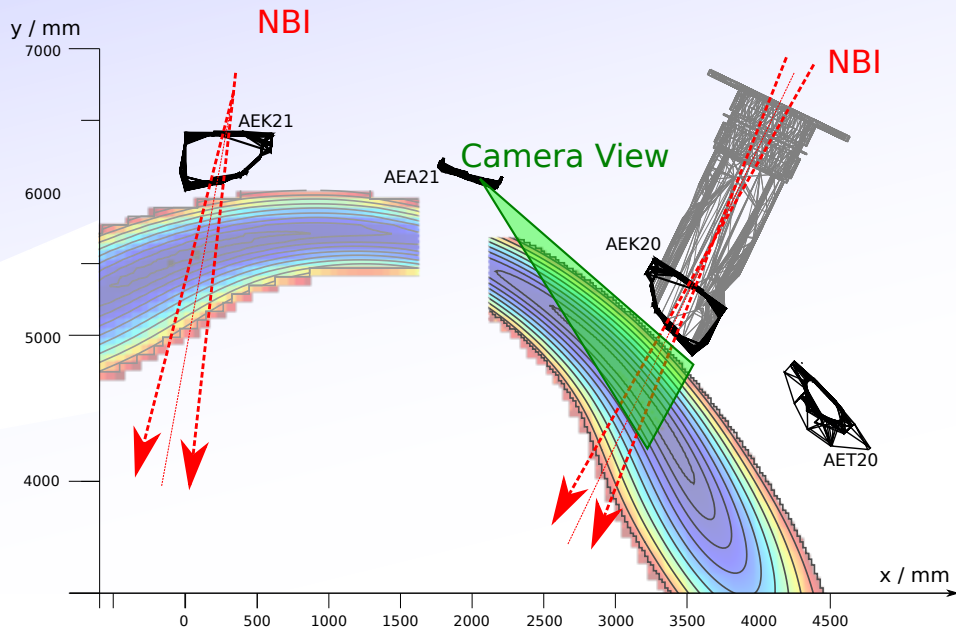




# Geometry (W7X)

Best view of NBI to reduce cross-surface integration.

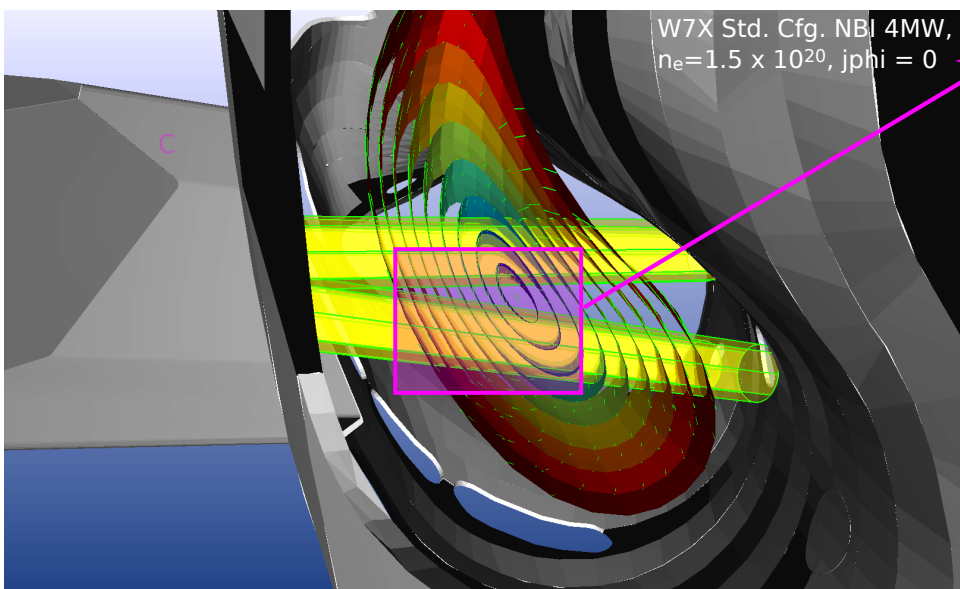
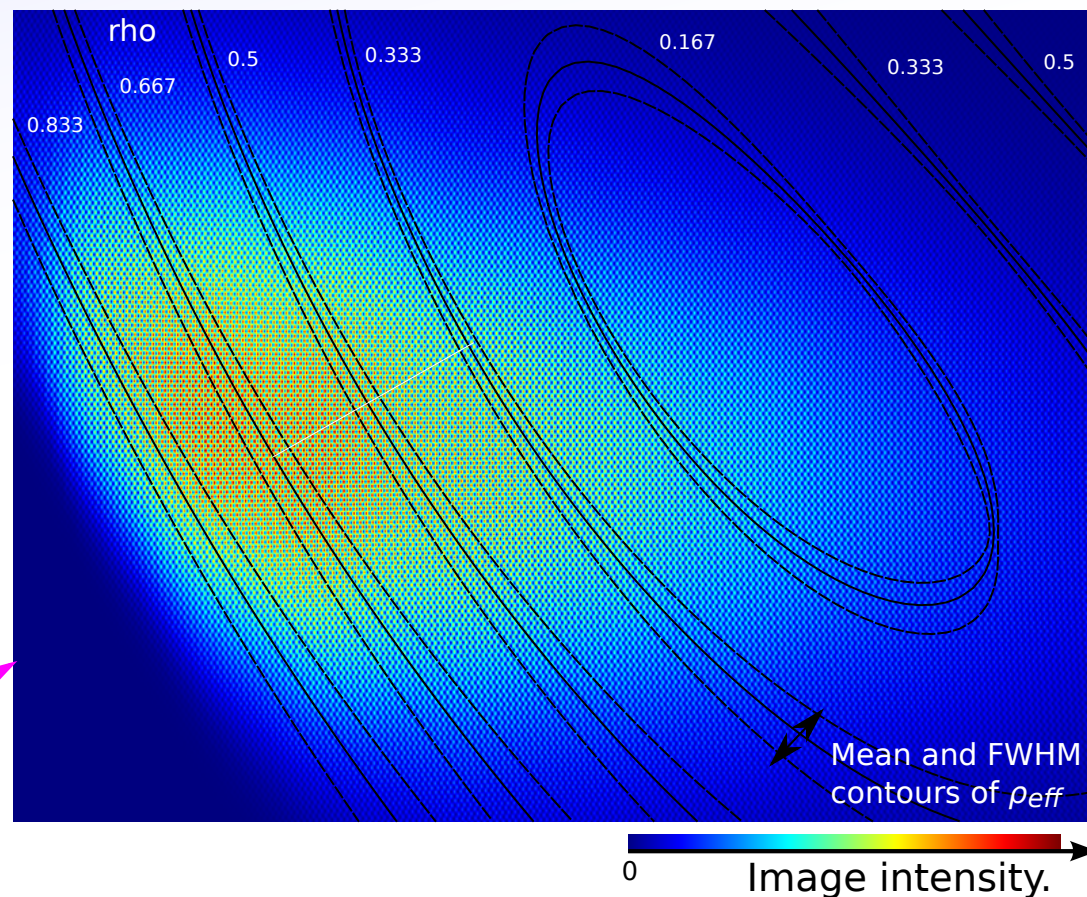
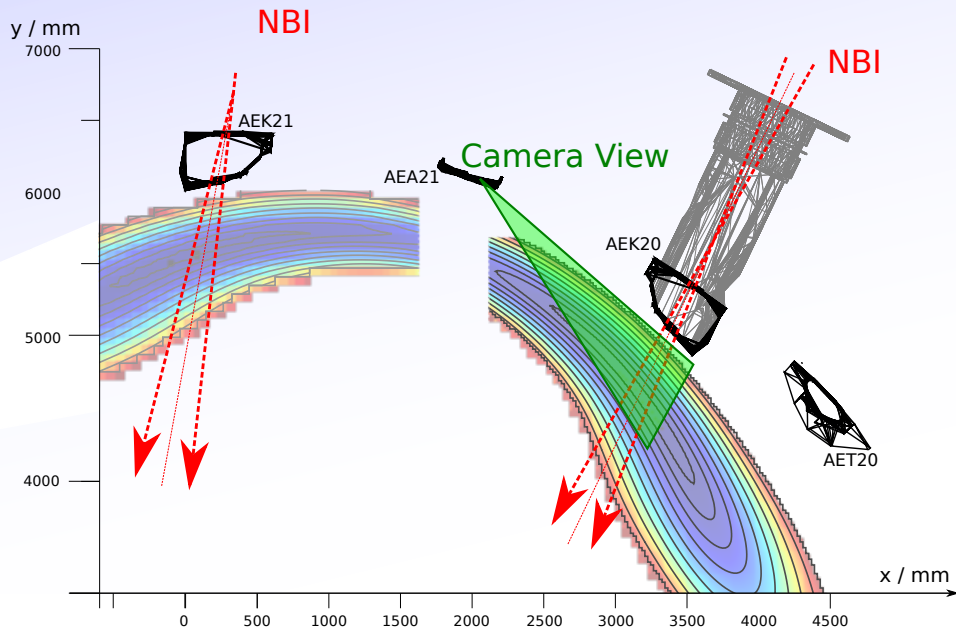
More tangential lower beam gives best Doppler shift --> Better image fringe contrast.



# Geometry (W7X)

Best view of NBI to reduce cross-surface integration.

More tangential lower beam gives best Doppler shift --> Better image fringe contrast.

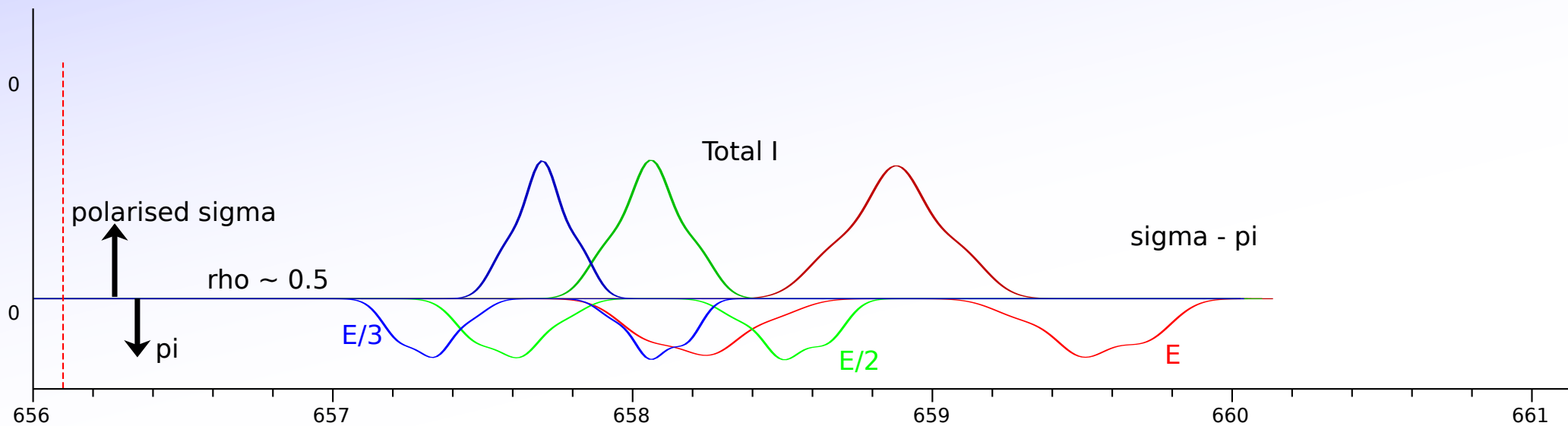


LOS is almost parallel to surfaces  
--> Good flux surface resolution.



# Geometry (W7X)

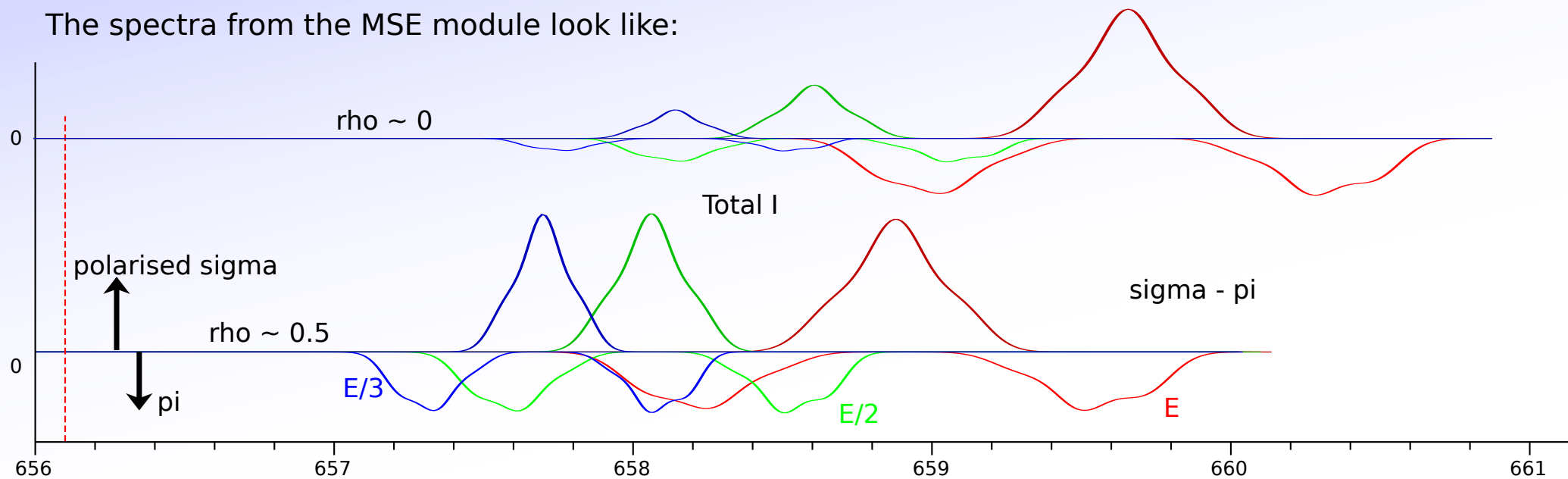
The spectra from the MSE module look like:





# Geometry (W7X)

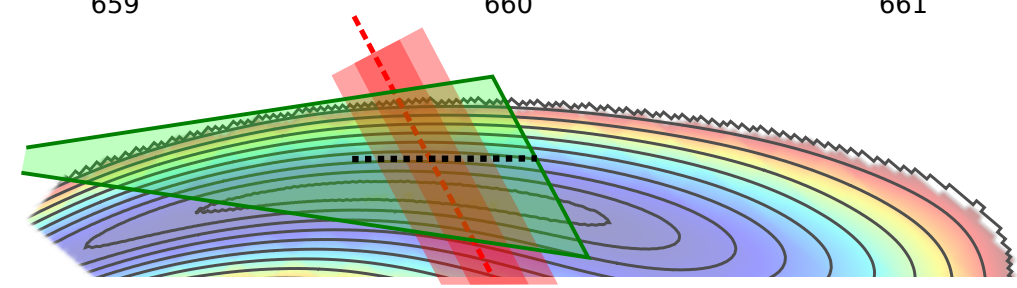
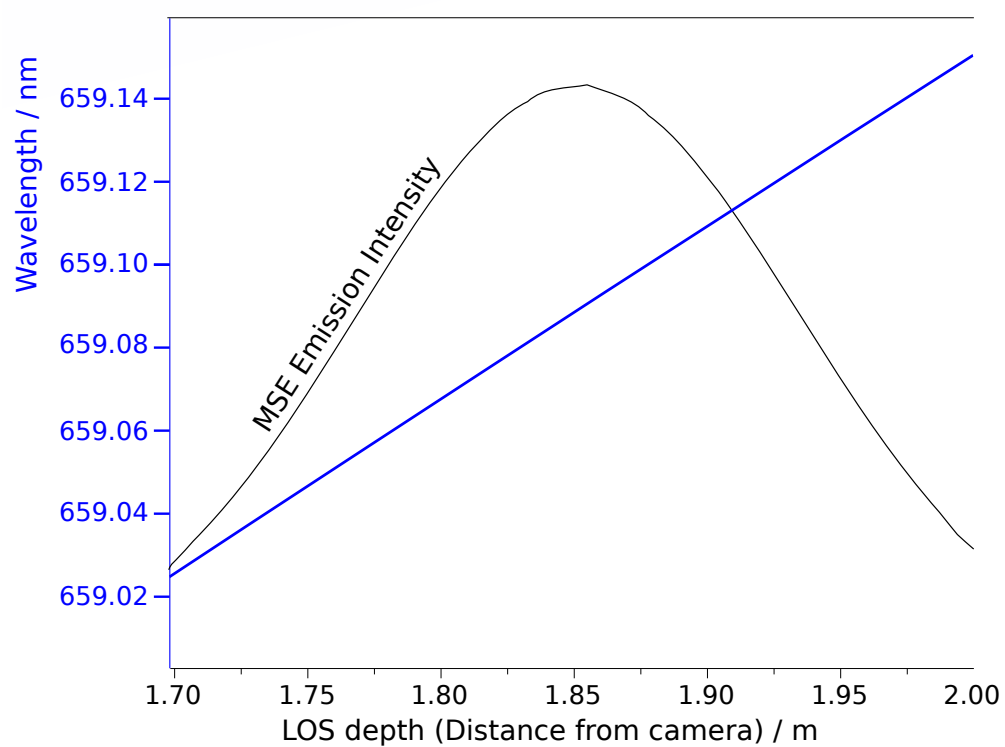
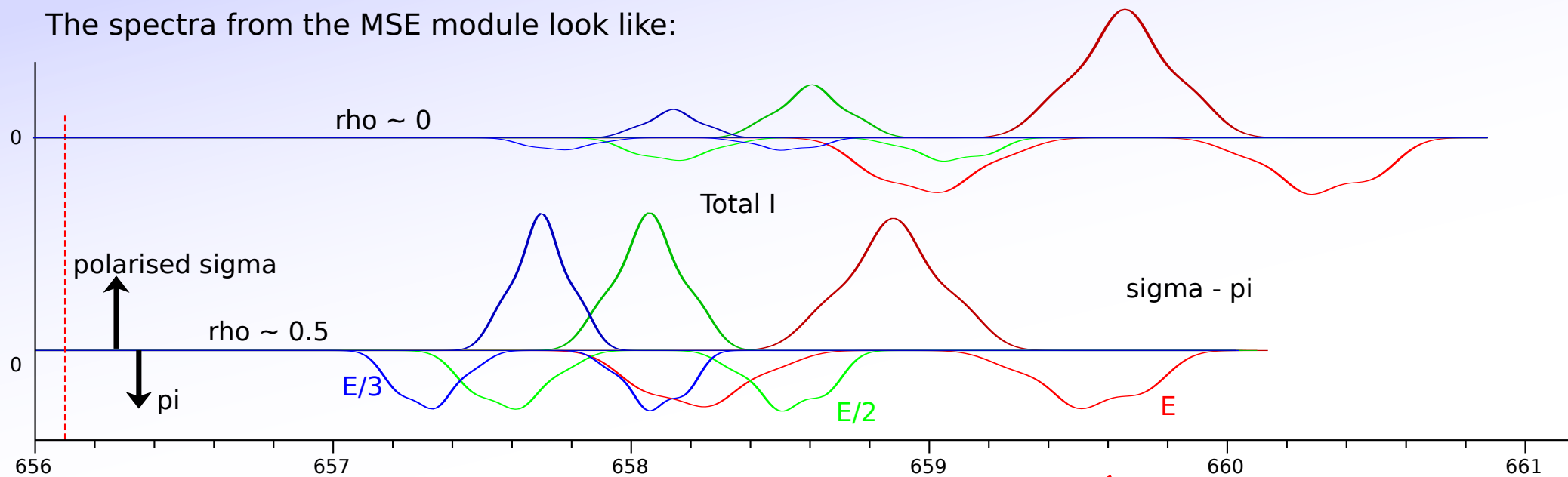
The spectra from the MSE module look like:





# Geometry (W7X)

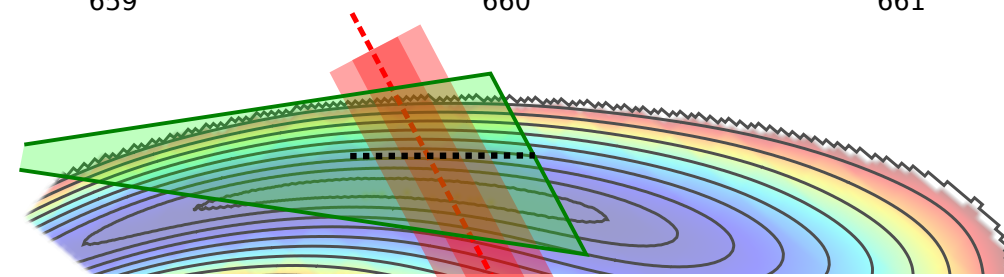
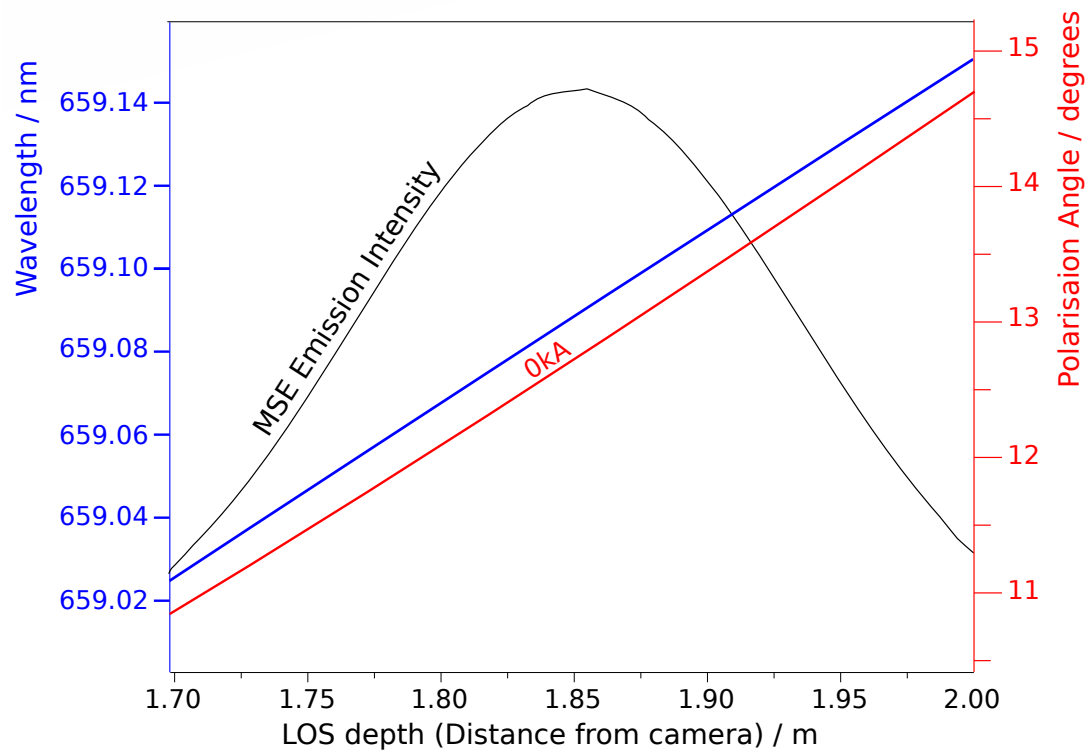
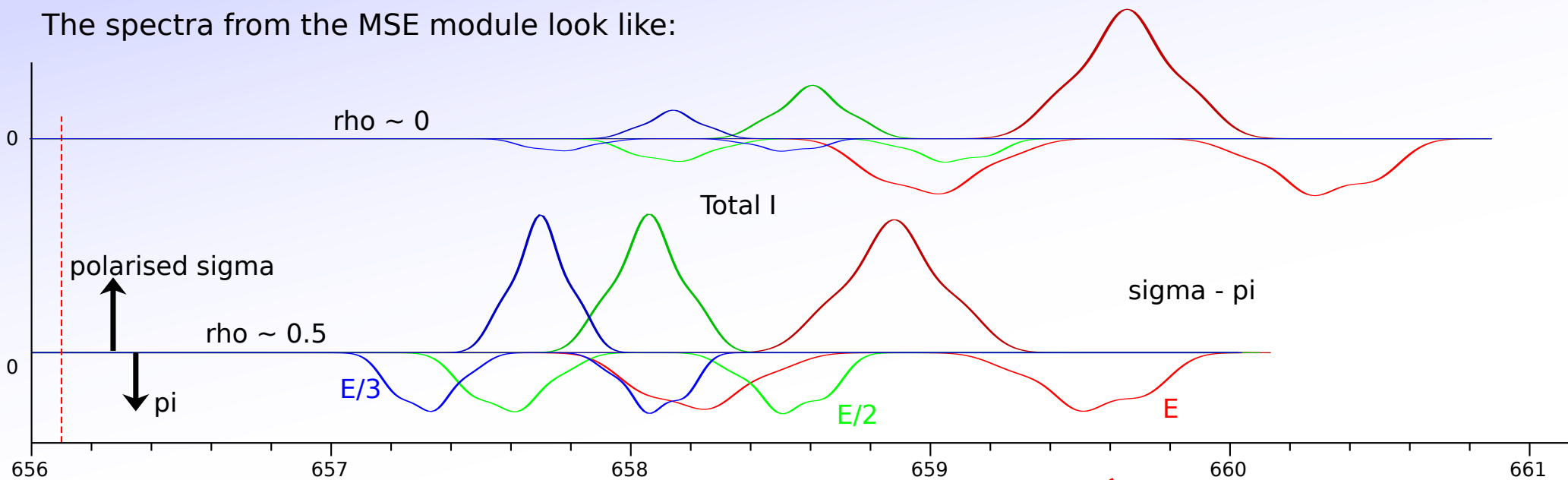
The spectra from the MSE module look like:





# Geometry (W7X)

The spectra from the MSE module look like:

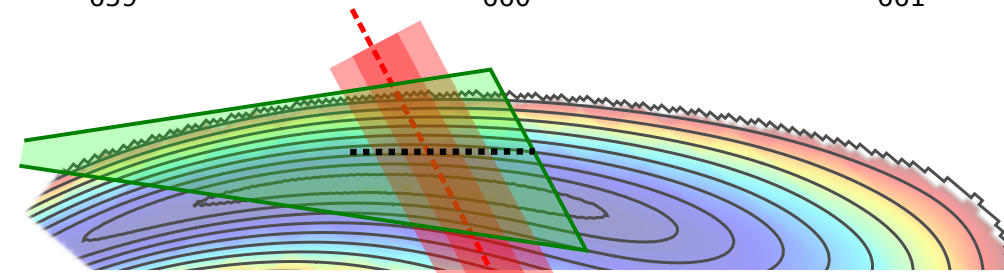
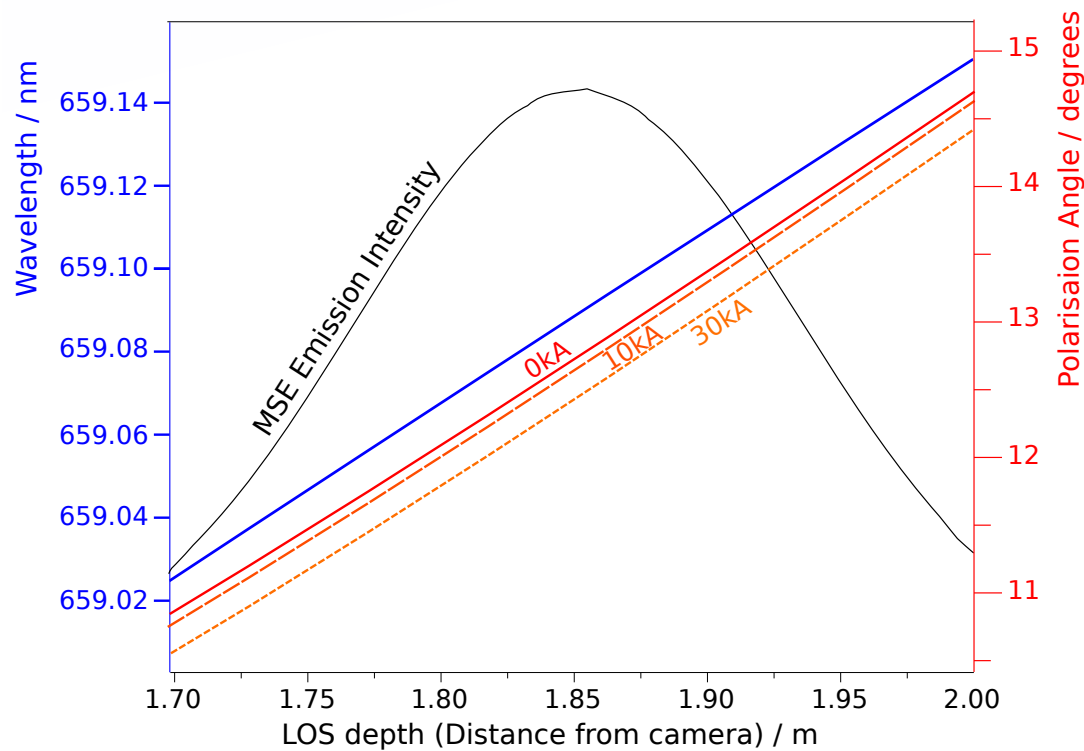
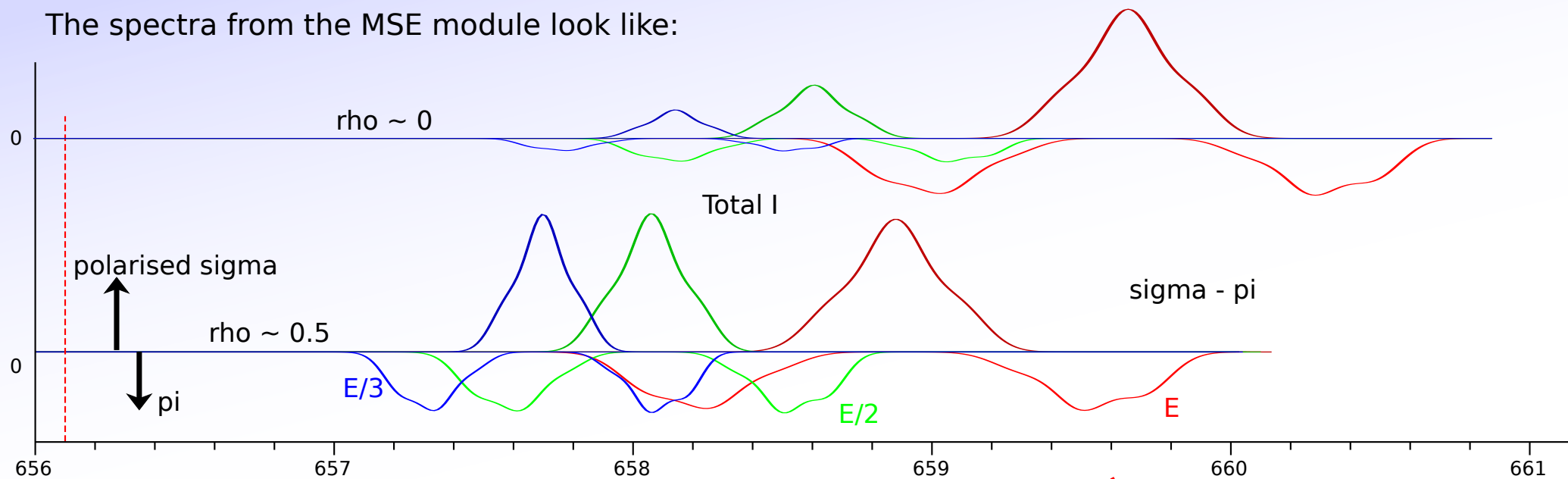


For the Tokamak, pitch change is mostly due to cross-surface LOS integration  $\sim 0.6^\circ$ .

For W7X, pitch changes along  $\phi$  by  $>3^\circ$ .

# Geometry (W7X)

The spectra from the MSE module look like:



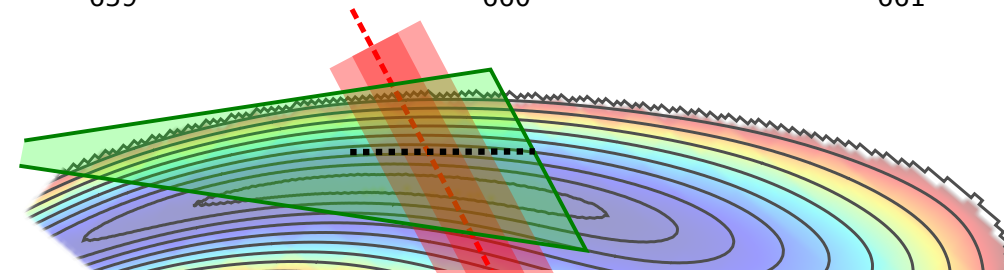
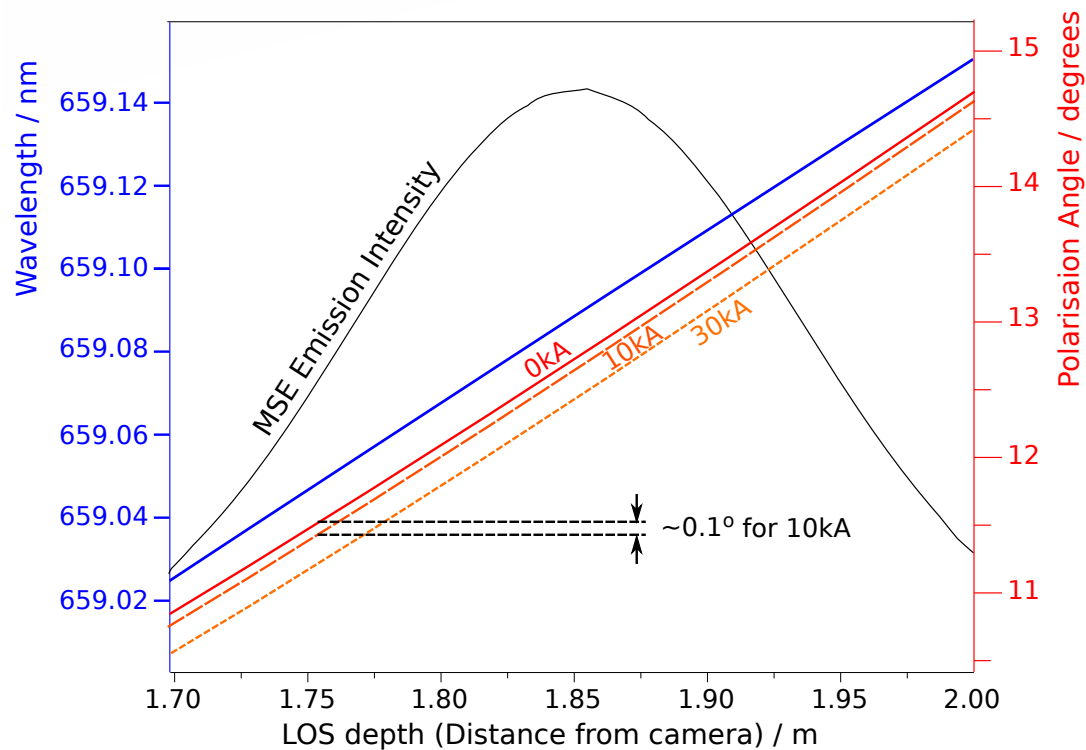
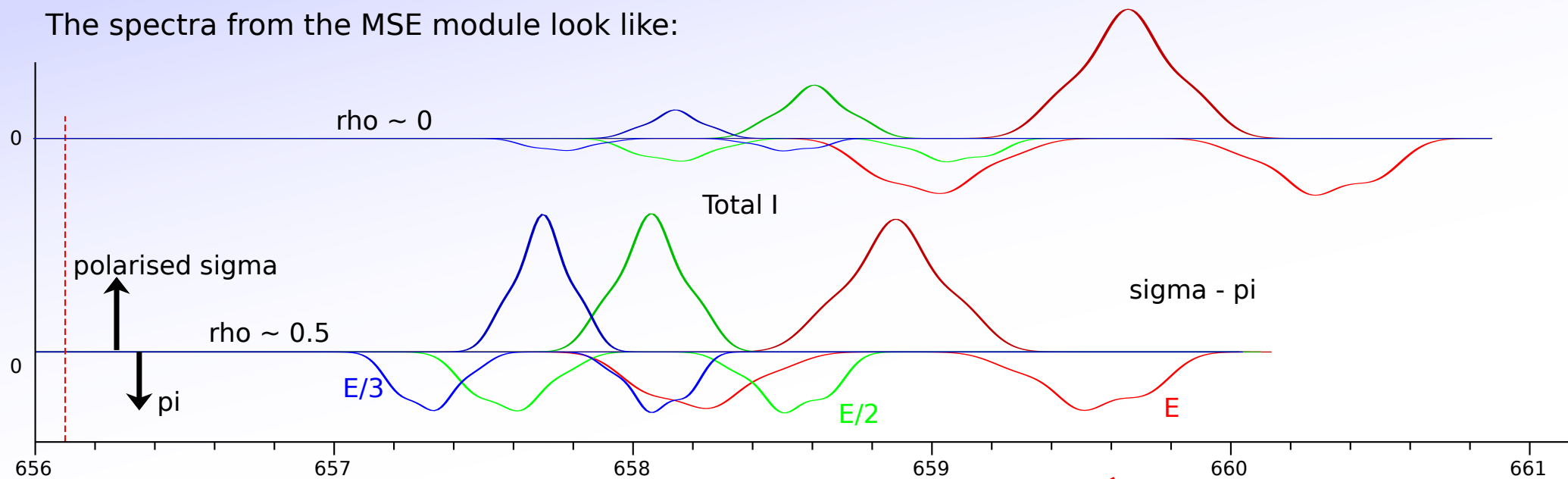
For the Tokamak, pitch change is mostly due to cross-surface LOS integration  $\sim 0.6^\circ$ .

For W7X, pitch changes along  $\phi$  by  $>3^\circ$ .



# Geometry (W7X)

The spectra from the MSE module look like:



For the Tokamak, pitch change is mostly due to cross-surface LOS integration  $\sim 0.6^\circ$ .

For W7X, pitch changes along  $\phi$  by  $>3^\circ$ .

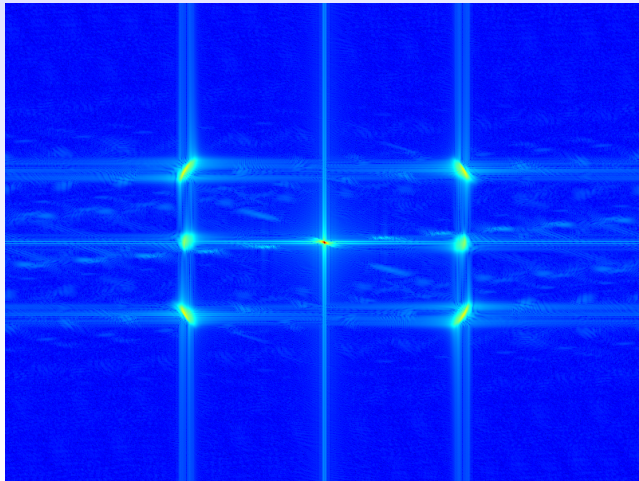
A toroidal current of 10kA will give only  $\sim 0.1^\circ$  change, but is constant.

Need to be able to recover the *average*  $\theta$ .



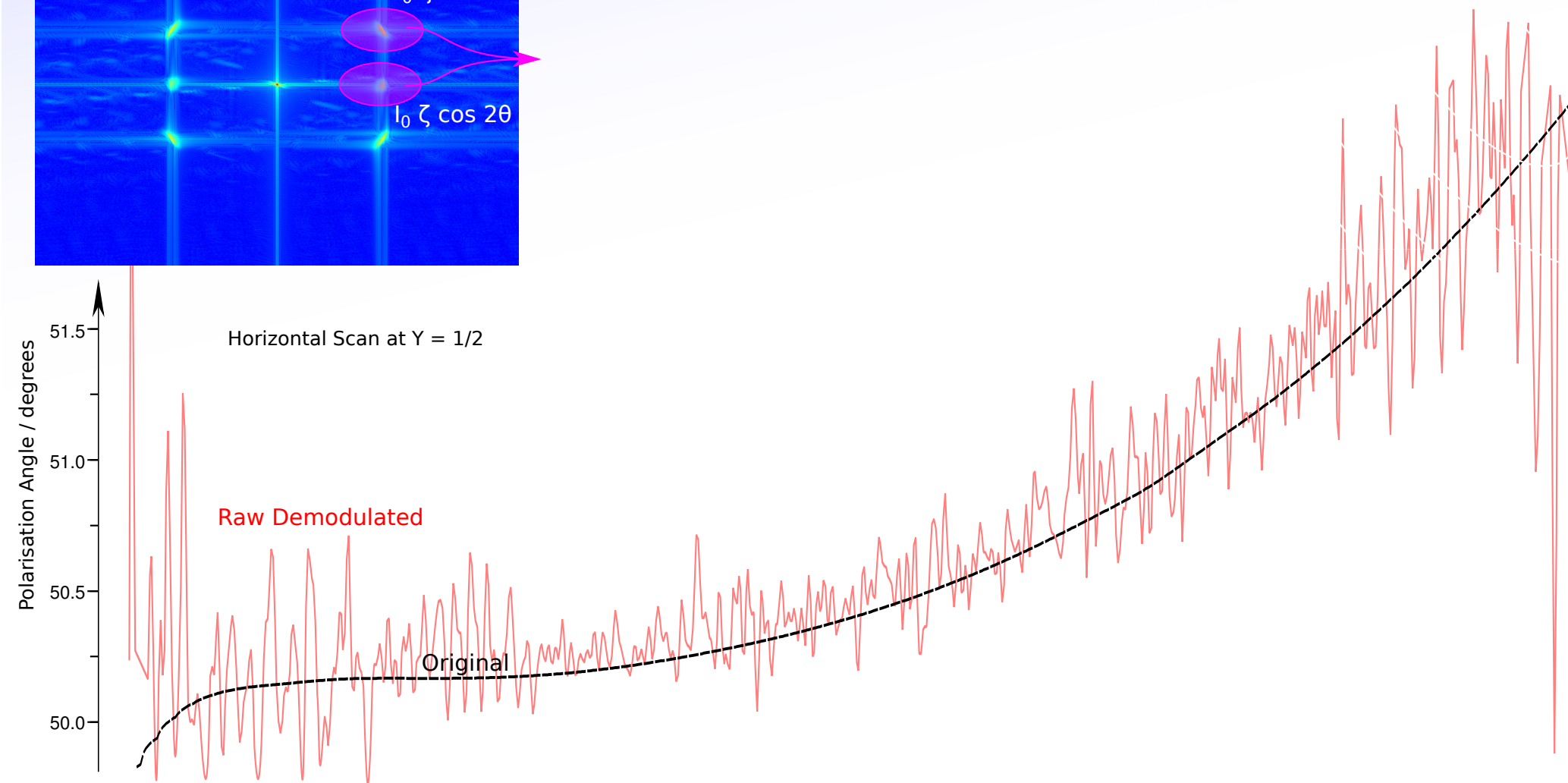
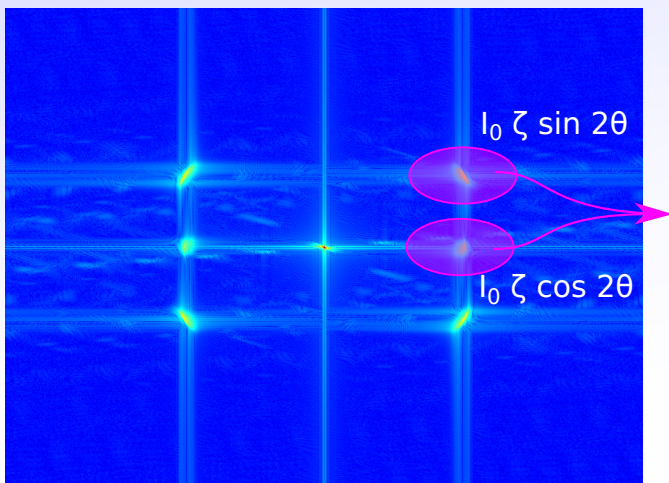
## Demodulation (W7X)

Generated full forward modelled image, add 1% random noise and demodulate:



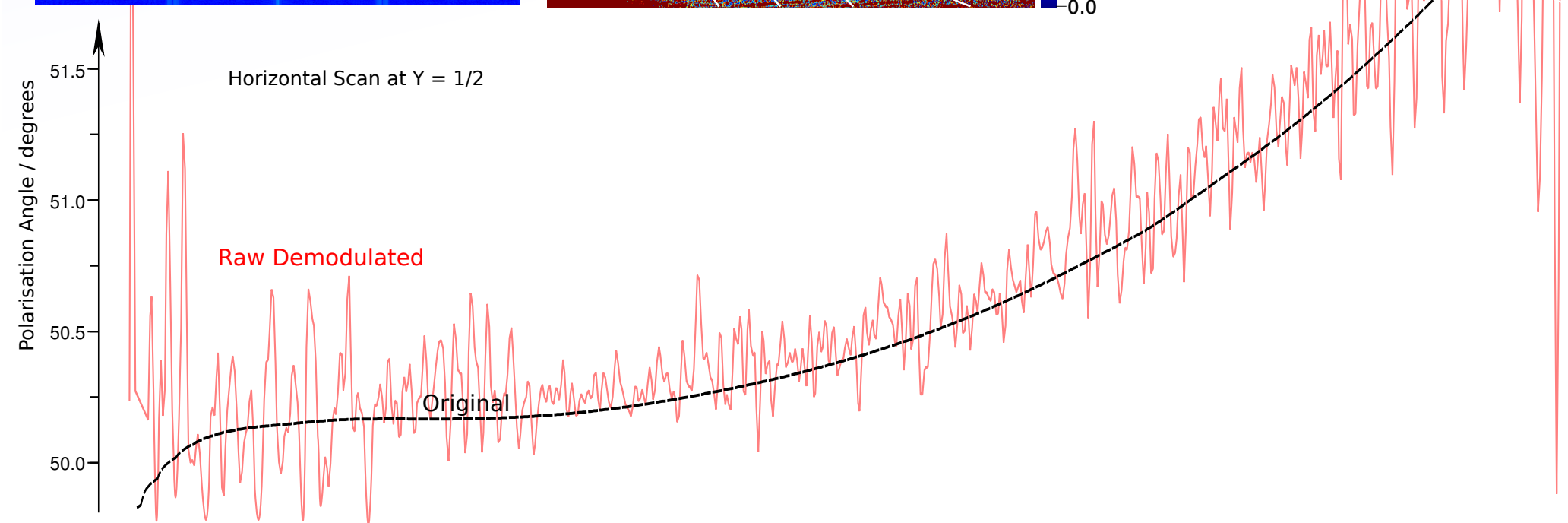
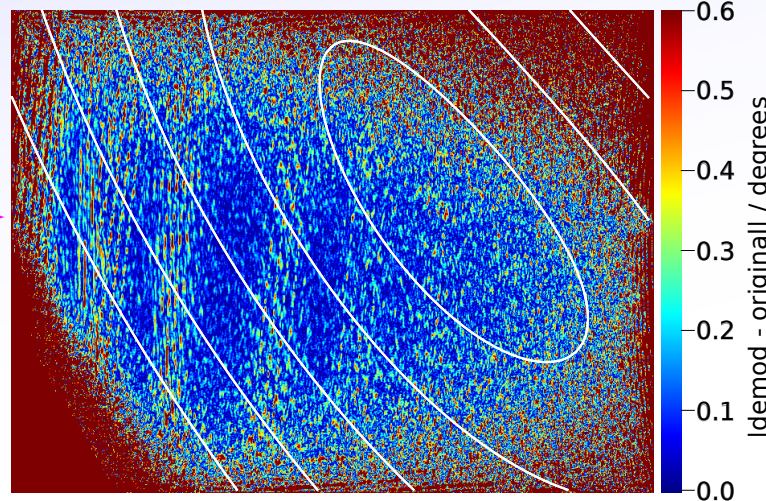
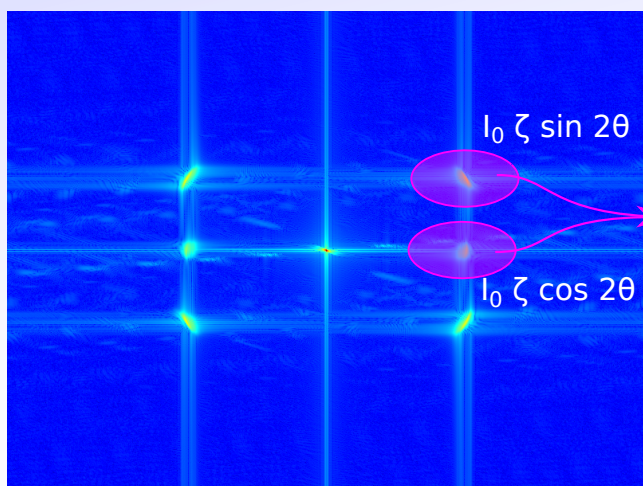
# Demodulation (W7X)

Generated full forward modelled image, add 1% random noise and demodulate:



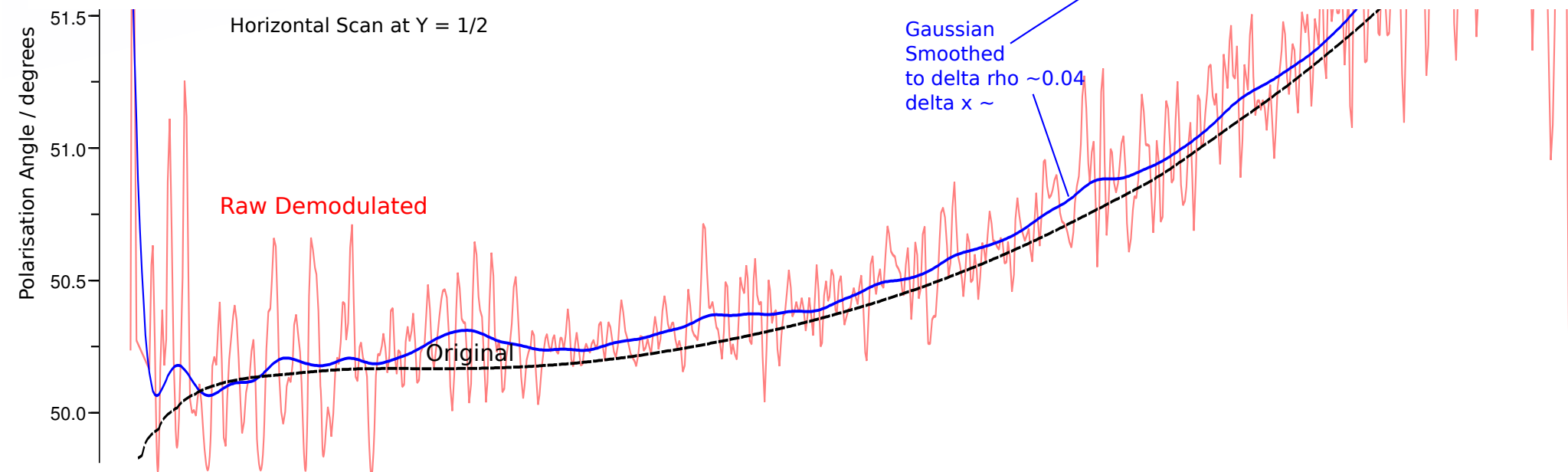
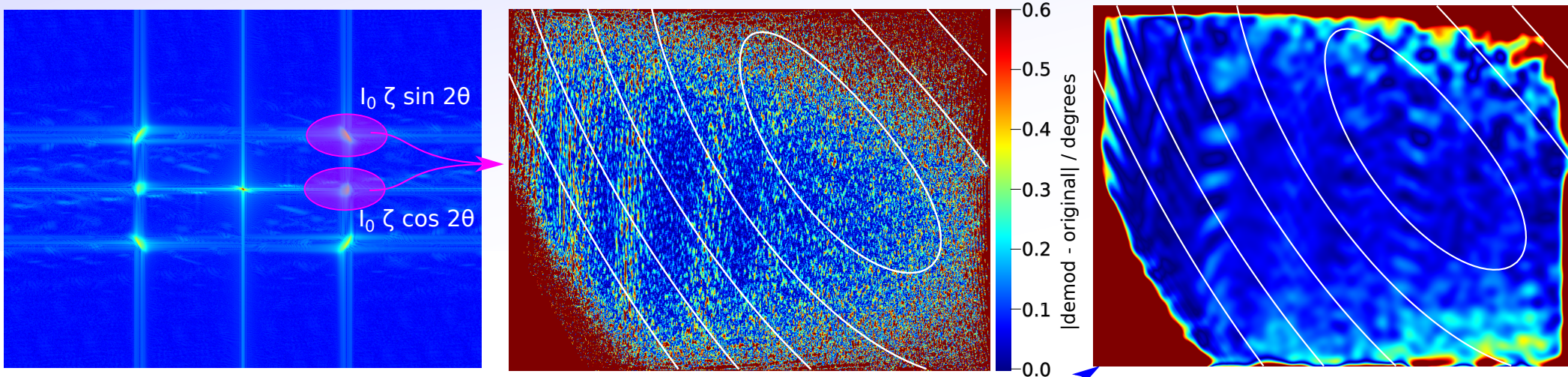
# Demodulation (W7X)

Generated full forward modelled image, add 1% random noise and demodulate:



# Demodulation (W7X)

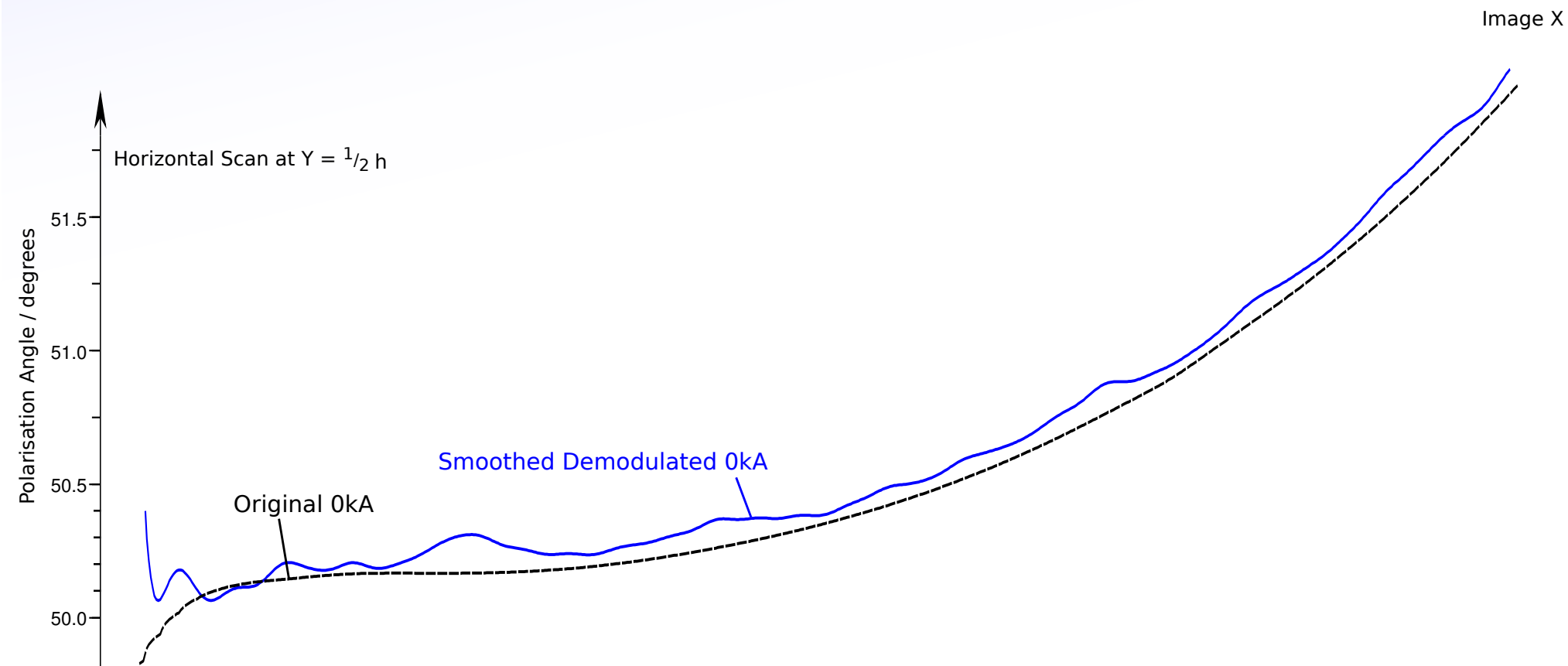
Generated full forward modelled image, add 1% random noise and demodulate:



Demodulation not as good as AUG - possibly due to integration of wide range of  $\theta$  with varying wavelength. Generated image is integration of images but demodulated assuming a single image.



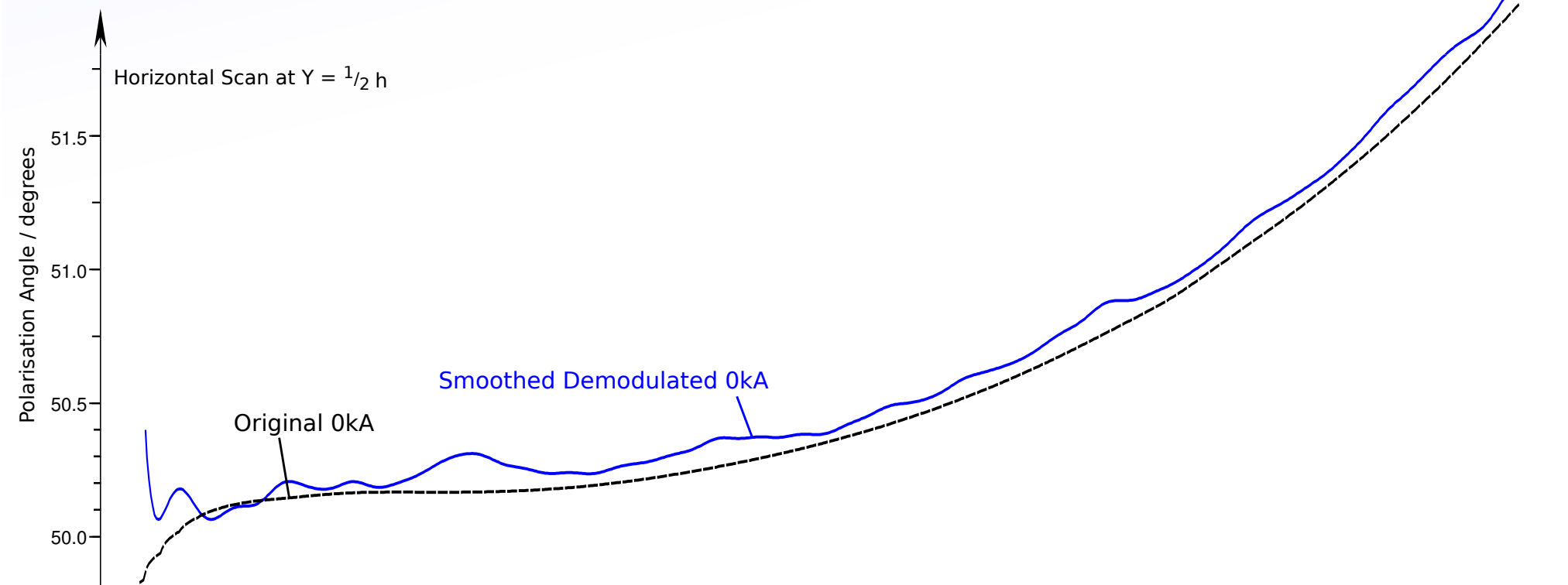
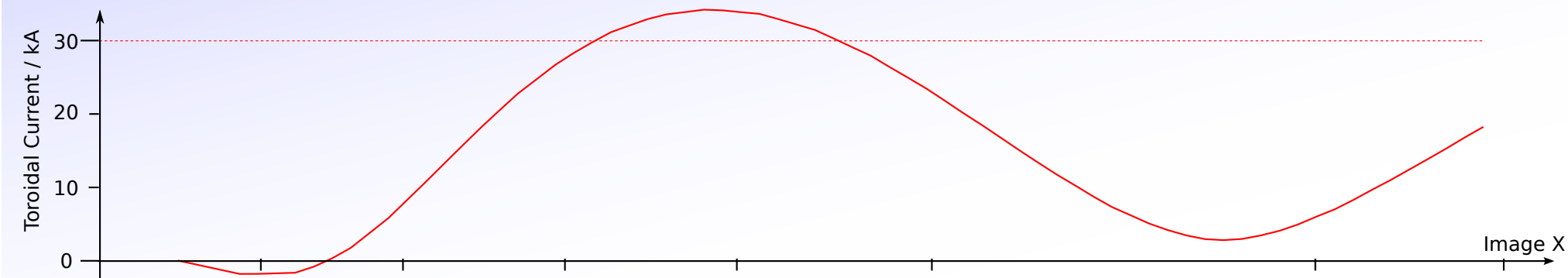
# Demodulation Response to jphi (W7X)





# Demodulation Response to jphi (W7X)

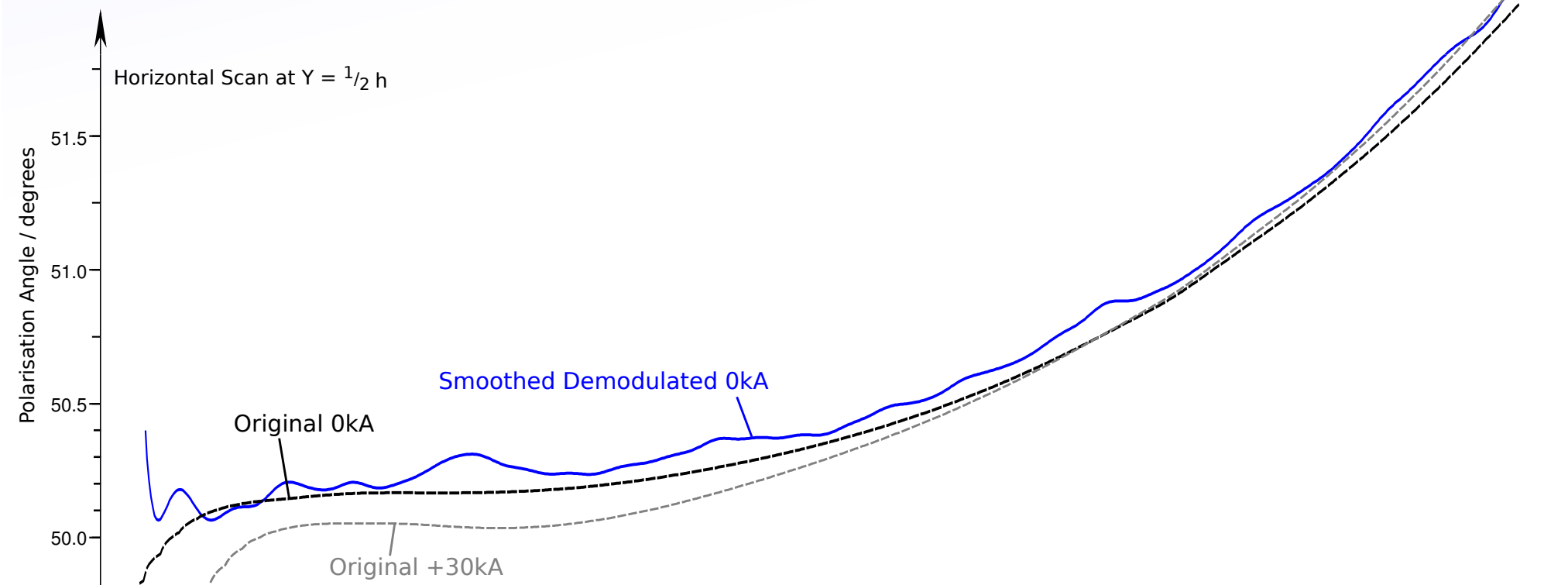
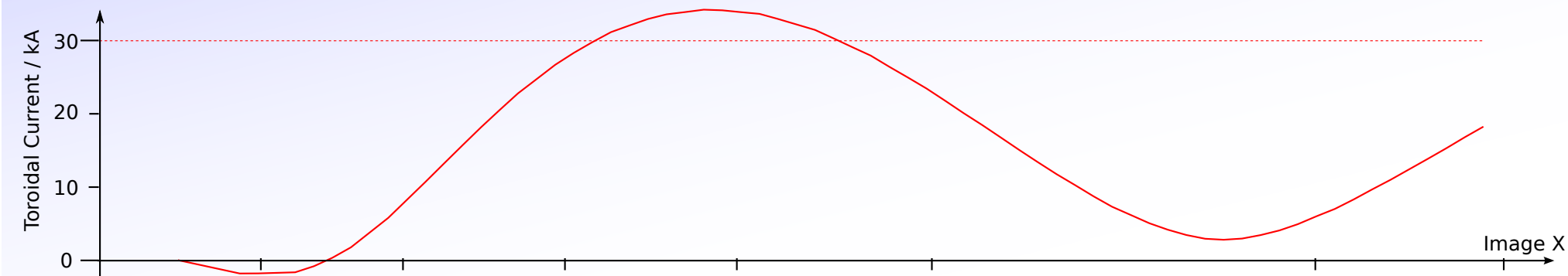
Add 30kA peak modification to toroidal current profile:





# Demodulation Response to jphi (W7X)

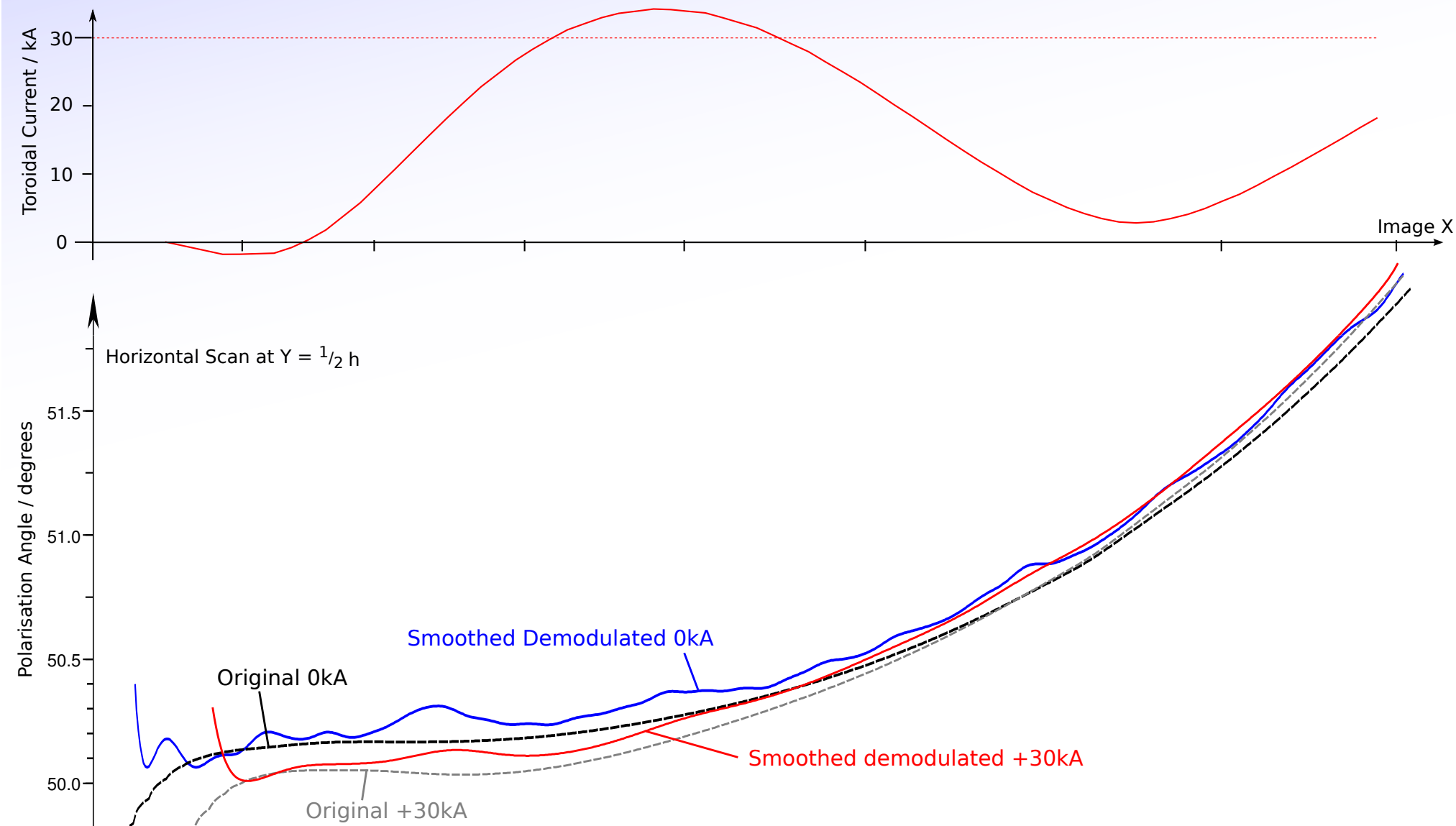
Add 30kA peak modification to toroidal current profile:





# Demodulation Response to jphi (W7X)

Add 30kA peak modification to toroidal current profile:







## Inference of $j_\phi$ (W7X)

Can't do the current tomography in 3D (at present).

For a rough idea of the inference capability - use Function Parameterisation in forward model.  
Assume fixed/known pressure and coil currents and invert 40x30 polarisation angle map to  $j_\phi$ ,  
assuming we can reconstruct to  $\pm 0.14^\circ$ .

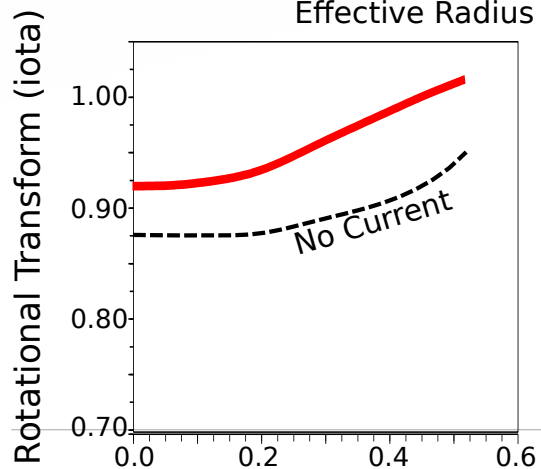
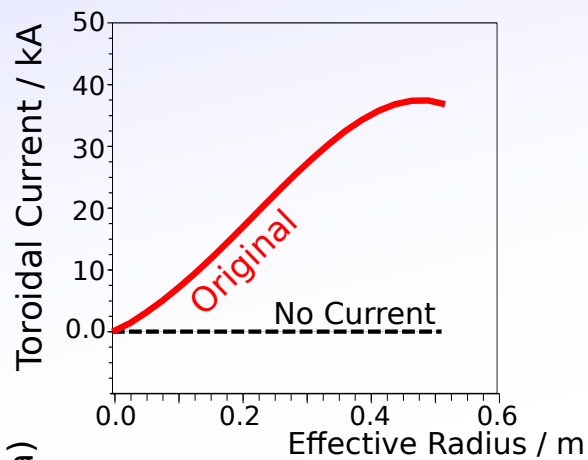
---



# Inference of $j_\phi$ (W7X)

Can't do the current tomography in 3D (at present).

For a rough idea of the inference capability - use Function Parameterisation in forward model.  
Assume fixed/known pressure and coil currents and invert 40x30 polarisation angle map to  $j_\phi$ ,  
assuming we can reconstruct to  $\pm 0.14^\circ$ .



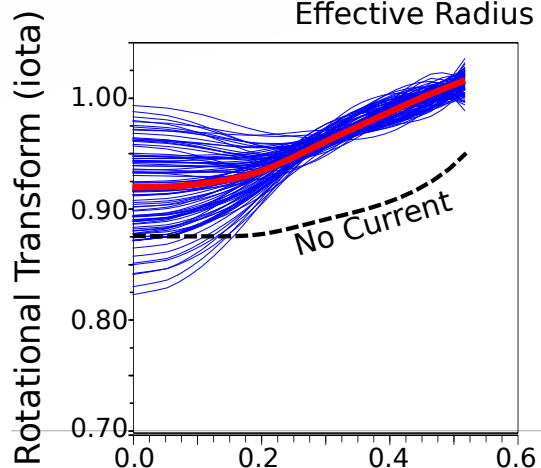
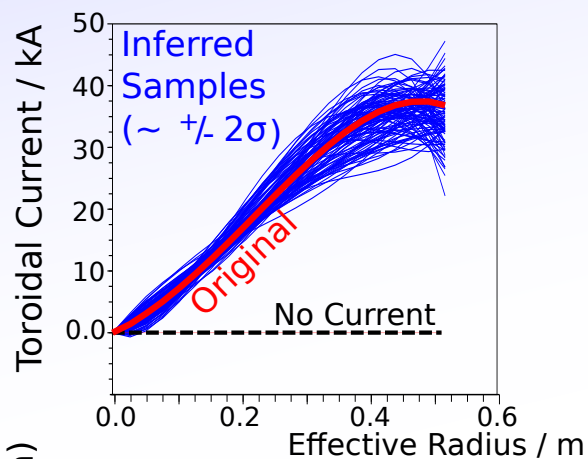


# Inference of $j_\phi$ (W7X)

Can't do the current tomography in 3D (at present).

For a rough idea of the inference capability - use Function Parameterisation in forward model.

Assume fixed/known pressure and coil currents and invert 40x30 polarisation angle map to  $j_\phi$ , assuming we can reconstruct to  $\pm 0.14^\circ$ .



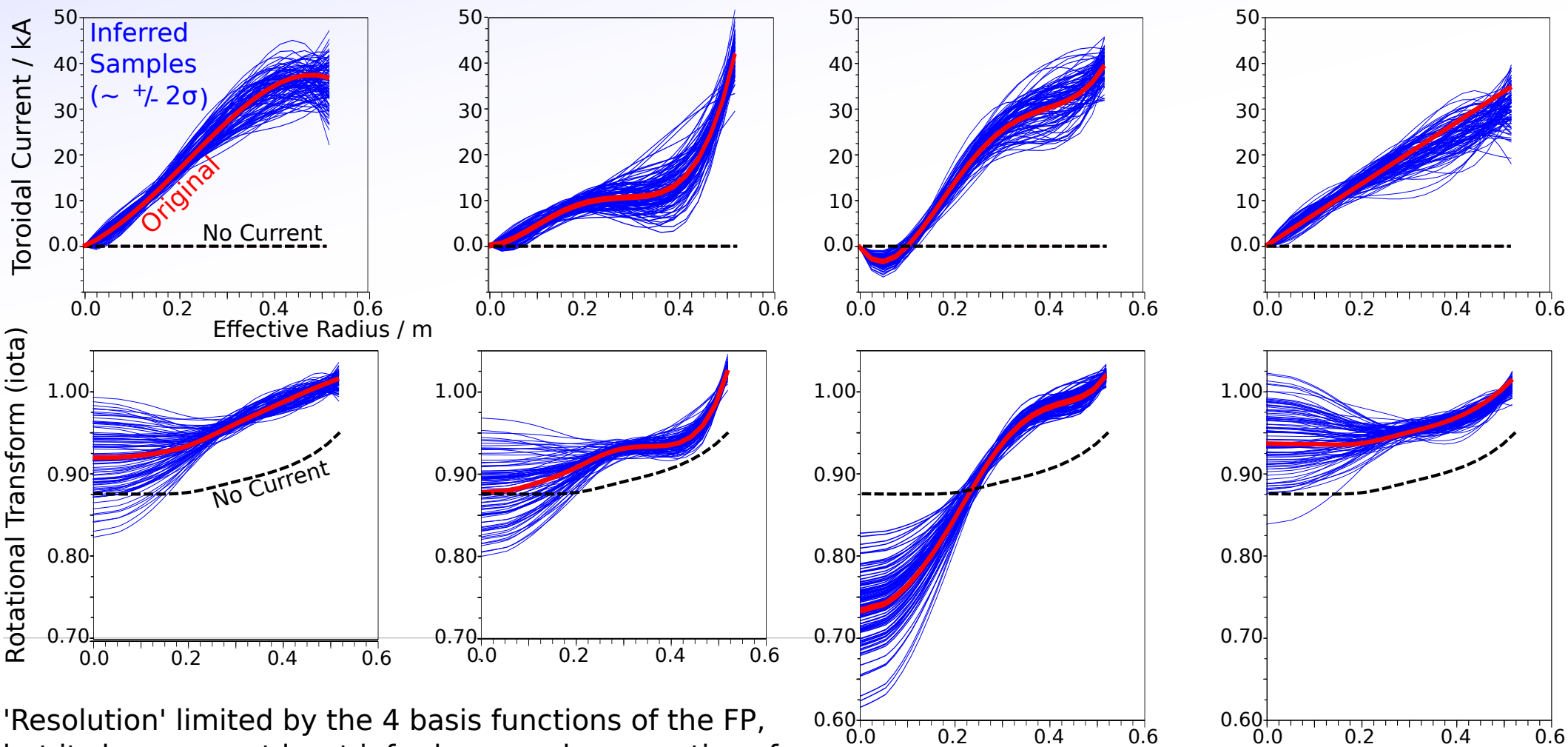


# Inference of $j_\phi$ (W7X)

Can't do the current tomography in 3D (at present).

For a rough idea of the inference capability - use Function Parameterisation in forward model.

Assume fixed/known pressure and coil currents and invert 40x30 polarisation angle map to  $j_\phi$ , assuming we can reconstruct to  $\pm 0.14^\circ$ .



'Resolution' limited by the 4 basis functions of the FP, but it shows can at least infer large scale properties of the bootstrap current profile.

Including other magnetic diagnostics should make it even better.



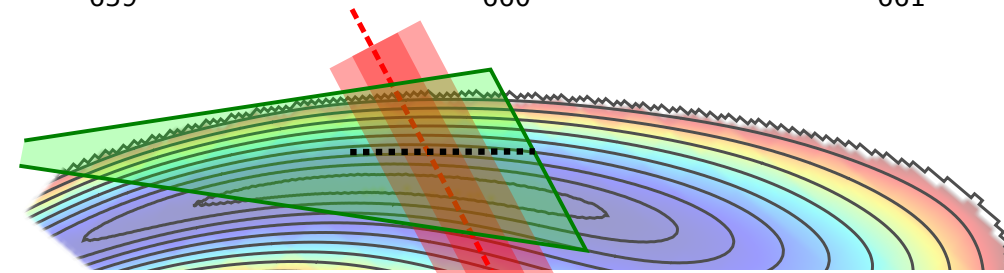
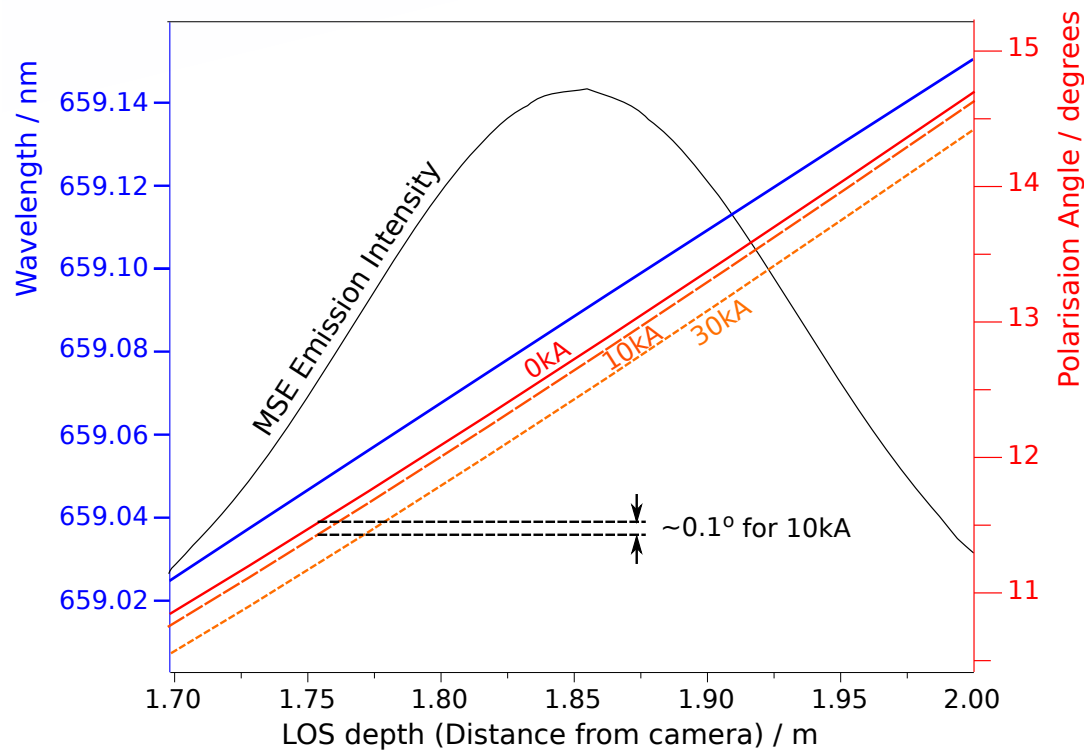
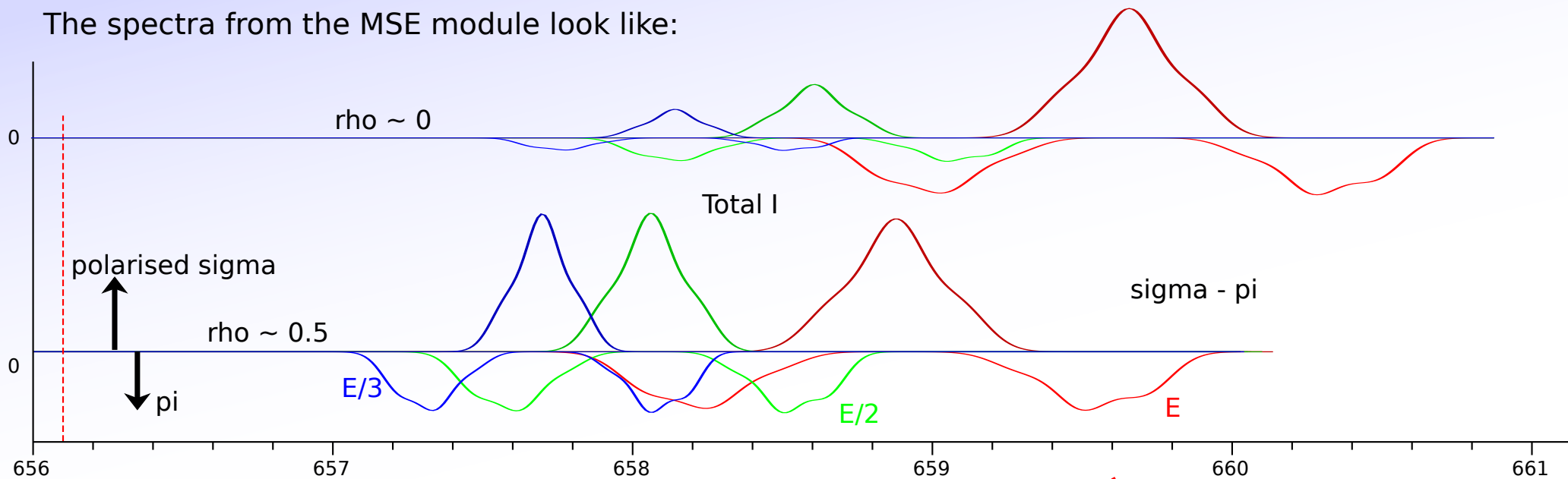
## Summary

- Developed detailed modular forward models for AUG + W7X magnetics, Neutral Beams, MSE and IMSE camera systems.
- Full modelling of the IMSE system under development for ASDEX Upgrade and its capability to infer pitch angle.
- Assessment of ability to directly calculate current in Axisymmetric systems from 2D IMSE measurements.
- Simulated Bayesian inference of plasma current from IMSE in ASDEX, without the assumptions associated with equilibrium codes, shows a significant improvement over equivalent 1D measurements.
  - It is relatively easy to also include equilibrium (axisym, isotropic, flow-free) within the Bayesian analysis.
- Modelling of IMSE system for W7X and initial assesment of local average polarisation/pitch angle measurement.
- Assesment of inference of broad information about induced plasma currents in W7X.



# Geometry (W7X)

The spectra from the MSE module look like:



For the Tokamak, pitch change is mostly due to cross-surface LOS integration  $\sim 0.6^\circ$ .

For W7X, pitch changes along  $\phi$  by  $>3^\circ$ .

A toroidal current of 10kA will give only  $\sim 0.08^\circ$  change, but is constant.

Need to be able to recover the *average*  $\theta$ .